PhD degree in Medical Nanotechnology

European School of Molecular Medicine (SEMM) and Italian Institute of Technology (IIT)

University of Milan

Faculty of Medicine

Settore disciplinare: BIO/10

Selection of epitope directed recombinant antibodies to inhibit mutated nucleophosmin activities

Chiara Martinelli

IFOM-IEO Campus, Milan

Matricola n. R07410

Supervisor: Prof. Pier Giuseppe Pelicci

IFOM-IEO Campus, Milan

Anno accademico 2009-2010

TABLE OF CONTENTS

REFERENCES

LIST OF ABBREVIATIONS

ABTS	2,2'-Azinobis [3-ethylbenzothiazoline-6-sulfonic acid]- diammonium salt
A. I.	Aggregation Index
ALCL	Anaplastic Large Cell Lymphoma
ALK	Anaplastic Lymphoma Kinase
AML	Acute Myeloid Leukemia
APC	Antigen Presenting Cells
APL	Acute Promyelocitic Leukemia
ATRA	All-*Trans* Retinoic Acid
BSA	Bovine Serum Albumin
CY3	CYanine 3
CY5	CYanine5
CDR	Complementarity Determining Region
DAPI	4',6-Diamidino-2-phenylindole
ELISA	Enzyme-Linked ImmoSorbent Assay
ER	Endoplasmic Reticulum
Fab	Fragment antigen binding
Fc	Fragment Crystallizable
FPLC	Fast Protein Liquid Chromatography
FLT3	Fms-like tyrosine kinase 3
FR	Framework Region
GFP	Green Fluorescent Protein
GST	Glutathione S-transferase
HA	Human influenza hemagglutinin
HBV	Hepatitis B Virus
HCAb	Heavy Chain Antibody

HD	Huntington's Disease
HIV	Human Immunodeficiency Virus
HPV	Human Papilloma Virus
HRP	HorseRadish Peroxidase
IG	InterGenic region
Ig	Immunoglobulin
IgNAR	Immunoglobulin of New Antigen Receptor
IMGT	international ImMunoGeneTics information system®
IPTG	Isopropyl-β-D-thiogalactopyranoside
ITD	Internal Tandem Repeat
KSHV	Kaposi Sarcoma-associated Herpes Virus
LB	Luria Bertani (medium)
mAb	monoclonal Antibody
MCS	Multi-Cloning Site
MEF	Mouse Embryonic Fibroblast
MHC	Major Histocompatibility Complex
MLF1	Myeloid Leukemia Factor 1
NES	Nuclear Export Signal
NLS	Nuclear Localization Signal
NuLS	Nucleolar Localization Signal
OD	Optical Density
PEG	PolyEthilenGlycol
PBS	Phosphate Buffered Saline
PBST	Phosphate Buffered Saline plus 0.1% Tween
PCR	Polymerase Chain Reaction
PTD	Protein Transduction Domain
RARα	Retinoic Acid Receptor α

RF	Replicative Form
SDS-PAGE	Sodium Dodecyl Sulphate - PolyAcrylamide Gel Electrophoresis
scFv	single-chain variable Fragment
Sf9	*Spodoptera frugiperda*
SV40 NLS	Simian Vacuolating Virus 40
TGN	*Trans*-Golgi Network
t. u.	transforming units
TY	Tryptone Yeast (medium)
US FDA	USA Food and Drug Administration
UV	UltraViolet
V-D-J	Variable-Diversity-Joining
VH	Variable (domain) of the Heavy chain
VHH	Variable Heavy chain (antibody)
VL	Variable (domain) of the Light chain
V-NAR	Variable (domain) of New Antigen Receptor
WHO	World Health Organization

FIGURES INDEX

ABSTRACT

Nucleophosmin (NPM1; also known as B23, NO38, or numatrin) is an abundant nuclear-cytoplasmic shuttling protein that is involved in different cellular processes such as centrosome duplication, cell cycle progression and stress response [1-4]. NPM1 physically interacts with several nuclear proteins, including nucleolin [5], p120 [6], p53 [7] and Mdm2 [8]. Recently, it has been demonstrated that NPM1 forms a stable complex with the tumor suppressor p19/Arf [9] and it is absolutely required for its correct localization and stabilization in the nucleolus [10, 11]. The observation of chromosomal translocations of the *NPM1* gene in human hematopoietic cancers has suggested that NPM1 contributes to tumor development by activating the oncogenic potential of the fused protein partners. Moreover, it has been found that about one-third of primary adult Acute Myeloid Leukemia (AML) patients bear mutations in the last exon of the NPM1 gene [12], leading to an aberrant cytoplasmic localization of the protein (NPMc+, [13]). Interestingly, the accumulation of NPMc+ in the cytoplasm appears responsible for the delocalization of proteins that, under normal conditions, interact with wild type NPM1 in the nucleus. In particular, NPMc+ binds, delocalizes and inactivates the p19/Arf tumor suppressor [14], as well as the Fbw7γ F-box protein that is involved in the proteasome-dependent degradation of the c-Myc oncoprotein [15]. These data prompted me to explore the possibility of blocking the aberrant activity of NPMc+ using NPMmutant-specific antibodies.
I report here the isolation, from the ETH2-Gold phage display library [16], of a recombinant antibody in scFv format specific for the NPMc+ protein. It univocally targets the mutated region at the C-terminal end of NPMc+. The specificity of this antibody was evaluated *in vitro* by performing western immuno-blot analyses, immunofluorescence and immunoprecipitation assays. I show that the scFv antibody performs as well as the mouse

monoclonal antibody specific for the same NPMc+ mutation and used as control. It is also able to immunoprecipitate the overexpressed and the endogenous NPMc+ proteins. Furthermore, I have found that the scFv can be efficiently expressed in mammalian cells as an intrabody, upon transfection of specific vectors that carry its cDNA sequence, and that it accumulates in the nucleus when fused to a nuclear localization signal (NLS). This evidence opened the opportunity to try the *in vivo* re-localization of NPMc+ from cytoplasm to the nucleus by using the recombinant antibody as a specific carrier. However, scFv-NLS fusions were unable to re-locate NPMc+ into the nucleus. The addition of multiple NLSs to the scFv did not modify the sub-cellular localization of NPMc+. In conclusion, I have been able to isolate a recombinant antibody that specifically targets NPMc+ protein. This antibody, directed against the C-terminal epitope of the mutated protein, has been biochemically and functionally characterized both *in vitro* and *in vivo*. The scFv successfully expresses as an intrabody in mammalian cells and specifically interacts with the native NPMc+ *in vivo*, thus giving the premises for its further development as a potential innovative therapeutic tool.

INTRODUCTION

CHAPTER 1

1. The immune system

The immune system is a complex network of chemical mediators, cellular components, specialized tissues and organs that has evolved to protect the integrity of the organism against any kind of pathogen, chemical substance and foreign agent that may penetrate the body and damage it. This is accomplished through the identification, neutralization and removal of the exogenous molecules, therefore, the immune system must be able to distinguish between what is part of the organism, such as its own healthy cells and tissues ("self"), and what could be potentially harmful ("not self"). This ability is mediated by different classes of receptors and proteins (Toll-like receptors, T-cell receptors, MHC complexes and immunoglobulins), which either expose on their surface or directly recognize specific elements of the infectious agents (antigens), eliciting an appropriate immune response. Immunity can be subdivided into innate and adaptive, depending on the types of recognition mechanisms involved and responses developed.

1.1 The innate immune system

The innate immune system is the first host defense against any foreign pathogen that enters the body; it acts in a non-specific manner and does not give a long-term immunity. The innate immune response is very rapid due to the fact that i) only few kinds of molecular profiles are recognized as "non self" and ii) all the immunological components involved are already predetermined at the genetic level and are able to carry out their functions without the need of any further maturation step. First responses to infections are mediated

by i) chemical molecules, responsible for the process of inflammation (cytokines), ii) physical barriers (epithelial cells of the skin, mucous membranes and secretions), iii) blood proteins (complement system factors), and iv) cellular components, predominantly members of the myeloid cell line (mast cells, granulocytes, macrophages, dendritic cells) and, in minor part, of the lymphoid one (natural killer cells, γδ T lymphocytes and B1 lymphocytes). These cells are characterized by the presence of specific membrane receptors responsible for antigen recognition and presentation (antigen presenting cells, APC); they are able to directly eliminate pathogens by phagocytosis and to induce inflammatory responses.

1.2 The adaptive immune system

Specific immunity is carried out by lymphoid B cells (humoral immunity) and T cells (cellular immunity) that work together with all the accessory cells, which are activated during the innate immune response. In mammals, B and T lymphocytes are produced in the bone marrow and mature in the bone marrow (B) and in the thymus (T), respectively (Figure 1A). After antigen exposure, T cells become activated, mature and differentiate in T helper cells, that coordinate the immune response by activating B lymphocytes and macrophages, and T cytotoxic cells, that are responsible for cell lysis. The complex mechanism carried out by the T helper cells relies on cell-cell interactions and on the release of soluble molecules (cytokines). In the presence of an antigen, B cells become activated, start proliferating (clonal expansion) and differentiating (primary response, Figure 1B). B cells differentiate into the germinal centers of the secondary lymphoid organs and develop into effector cells (plasma cells), that secrete immunoglobulins (Igs, named also antibodies) and memory B cells. Most likely, adaptive immunity has been selected because of its ability to adjust and change in a very specific way, each time an exogenous molecule comes in contact with one of its components. The large variability of

the molecular combinations represented by the antigens (it is estimated to be 10^7-10^9 different variants) is well balanced by the enormous number of different molecules responsible for their identification. The adaptive immune response has evolved two key functions: i) the ability to retain an immunological memory, by preserving the cells responsible for the successful recognition and neutralization of exogenous agents (secondary response) and ii) the capacity to train all its components to discriminate between "self" and "non self", in order to avoid autoimmunity (tolerance mechanism). The adaptive system acts through three consecutive steps: i) antigen recognition, ii) lymphocytes activation, iii) elimination of the antigen (effector phase). After these events have occurred, the adaptive system returns to homeostasis but preserving memory cells.

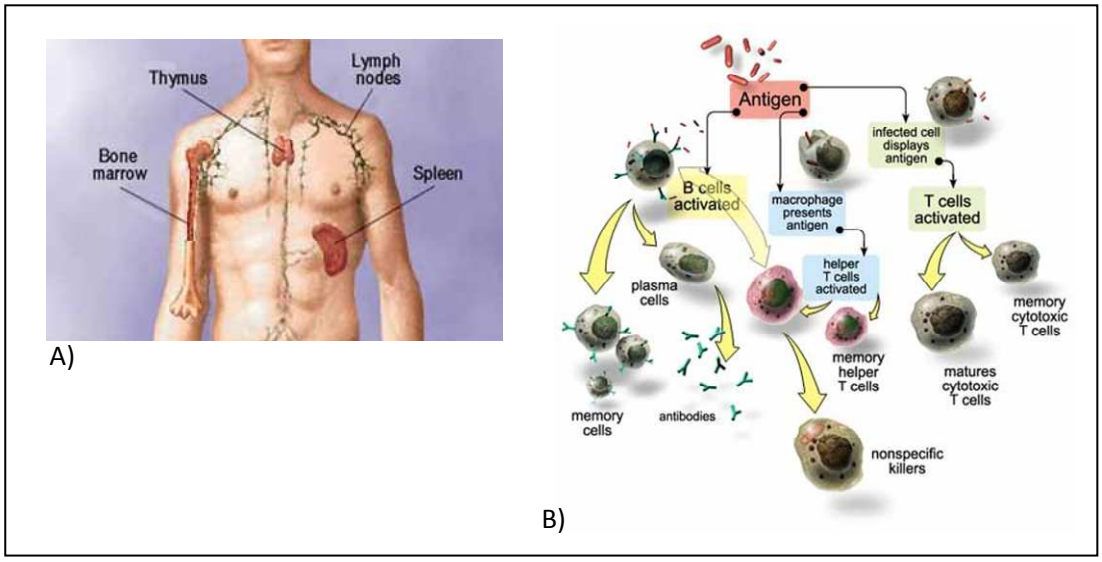

Figure 1. Human lymphoid organs and adaptive immune response. A) *Schematic representation of the human primary and secondary lymphoid organs (from "Mayo Foundation for Medical Education and Research", www.mayo.edu).* ***B)*** *Scheme of the main cellular components and events involved in the adaptive immune response (from "the Human Immune Response System", www.uta.edu/chagas/images/immunSys.jpg)*

2. Immunoglobulins: molecular structure and function

G. Edelman and R. Porter were the first to identify the structure of immunoglobulins, a discovery that was awarded by the Nobel Prize in 1972 [17, 18]. Igs are "Y" shaped glycoproteins circulating in the organism, able to neutralize pathogens by specifically recognizing their antigenic determinants (epitopes). Mature B cells express on their plasma membrane immunoglobulins that serve as antigen receptors (IgM) and, only after antigen exposure, differentiated B cells (plasma cells) start secreting immunoglobulins as soluble molecules (Figure 1B). IgGs are the most abundant class of immunoglobulins present in human blood (ca. 85% of serum Ig) and they are the most widely used for therapeutic and diagnostic applications [19]. They are organized into a tetrameric structure, formed by the interaction between four chains: two identical heavy chains (H, MW: 50-70 KDa) and two identical light chains (L, MW: 23 KDa), stabilized by hydrogen bonds and inter-/intra-chain disulfide bridges. Both types of chains present a series of repetitive units, called immunoglobulin domains. In a typical IgG it is possible to recognize two functional regions joined by a flexible stretch of polypeptide chain (hinge region): i) the constant region, responsible for mediating the interaction between the antibody and the complement components or the innate immunity cells (Fc, fragment crystallizable); ii) the variable region, where the antigen binding site is located (Fab, fragment antigen binding; Figure 2A). The portion of the antibody responsible for binding to the target epitope is called paratope and is constituted by the contribution of the variable domains of both light and heavy chains. Each variable domain contains three hypervariable complementarity determining regions (CDR1, CDR2, CDR3), that are responsible for the specificity of the antigen recognition. These regions form three flexible loops stabilized by the β-sheets of the framework regions (FR, Figure 2B and 2C). Among the six CDRs present in each antigen combining site, the two CDR3 sequences show the greatest variability, which is

generated by specific genetic and molecular mechanisms. Five different constant heavy chains (α, γ, δ, ε, μ) define five different functional classes (isotypes) of antibodies, named respectively IgA, IgG, IgD, IgE and IgM. Each of them presents specific effector functions and tissue distributions.

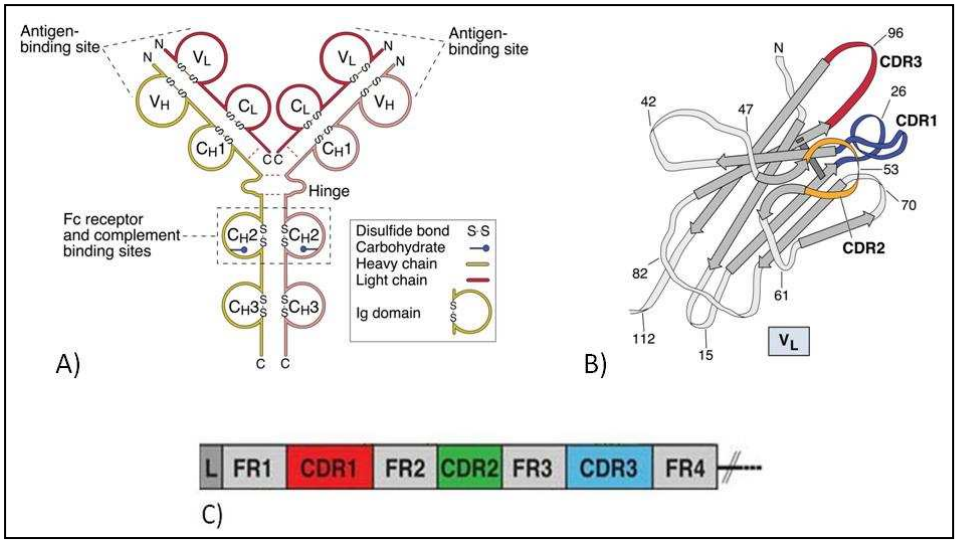

Figure 2. Molecular structure of immunoglobulins. A) *Scheme of an immunoglobulin showing the antigen binding site (Fab) and the Fc portion.* ***B)*** *Schematic representation of an immunoglobulin variable domain (VL). The three complementarity determining region (CDR) loops are coloured; β-sheets of the framework regions are in gray.* ***C)*** *Scheme of a typical variable domain structure showing the organization of the framework regions (FRs) and the complementarity determining regions (CDRs) (from "Cellular and molecular immunology", Abbas and Lichtman, 5th edition)*

2.1 The immunoglobulin genes

The large variability of the immunoglobulins associated to the membrane of B lymphocytes is generated in the bone marrow during B cells maturation. This process involves rearrangements into the germline antibody encoding genes. In fact, their transcription and translation starts after a series of random rearrangements (somatic/V(D)J recombination) has occurred. Each mature B cell exposes on its surface one specific immunoglobulin which recognizes only one antigenic epitope and which is encoded by a

single functional heavy chain gene and a single functional light chain gene. Immunoglobulin light chains (κ and λ) and heavy chains are encoded by different genetic *loci* constituted by distinct sequences, present in multiple copies (Figure 3). Some intronic regions, which contribute to the regulation of transcription and RNA splicing, are located between these genetic segments. The light chains (κ and λ) are encoded by the V and J (joining) genes, which rearrange giving the V_LJ_L segment (light chain variable domain), and by the C_L segment (light chain constant domain). The heavy chains are encoded by the V, D (diversity) and J genes, which rearrange giving the $V_HD_HJ_H$ segment (heavy chain variable domain), and by the C_H segment (heavy chain constant domain). The additional D (diversity) genetic region encodes for some of the heavy chain CDR3 residues.

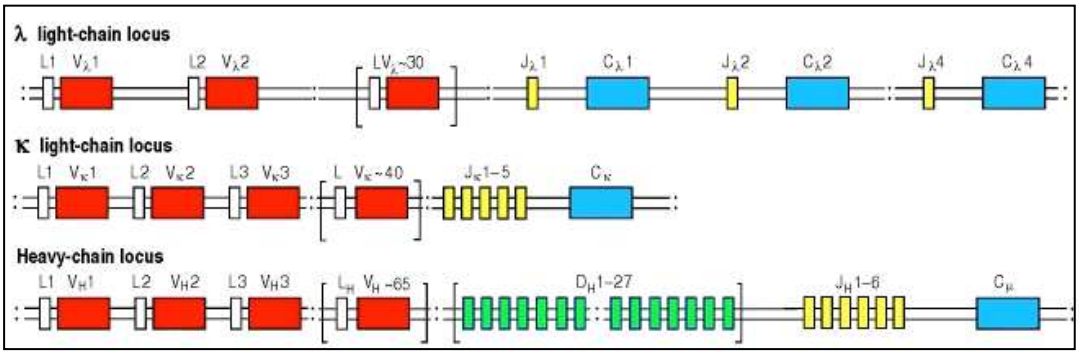

Figure 3. Genetic organization of the mouse immunoglobulin loci. *(from "Immunobiology", Janeway et al., 5th edition)*

2.2 The V(D)J recombination

The process of V(D)J recombination is site-specific and is mediated by a complex of specific enzymes (V(D)J recombinases). The random rearrangements that occur during B lymphocytes maturation are regulated by a precise cascade of events in each genetic *locus*. The heavy chain segments undergo a first rearrangement which creates a DJ junction, deleting the interposed region. Then, one V gene segment is bound to the DJ portion

creating the rearranged VDJ complex; therefore, the primary RNA transcript comprehends the VDJ complex together with the proximal C genes (both μ and δ). A second specific splicing event between the VDJ region and the Cμ gene creates the functional mRNA encoding for the μ heavy chain (Figure 4, upper part). A similar process of recombination occurs in the light chain encoding regions and creates a VJ complex which is then combined with the C region (κ or λ), leading to a functional mRNA encoding for the κ or λ light chains (Figure 4, lower part).

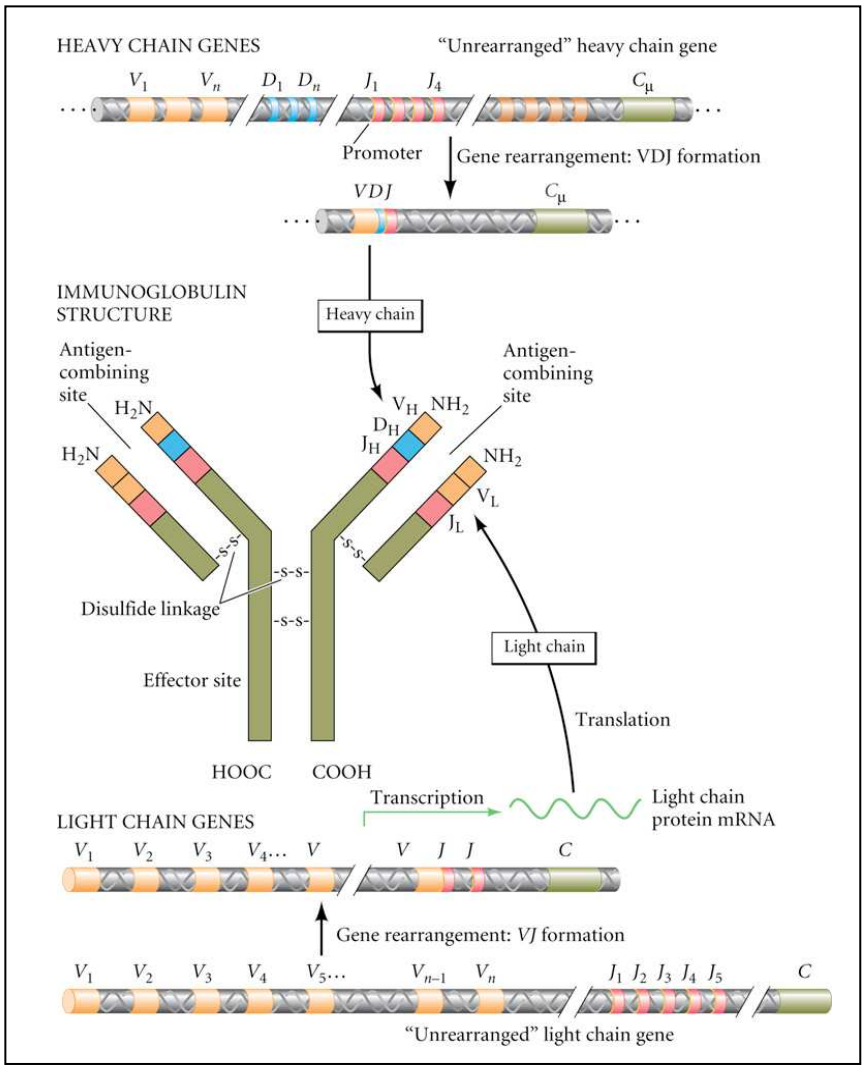

Figure 4. Gene rearrangement of the immunoglobulin heavy and light chains. *(from Gilbert S.F., "Developmental biology", 8th edition)*

In the endoplasmic reticulum, the two newly synthesized heavy and light chains are linked together and translated creating a functional IgM, which remains fused to the B cell plasma membrane. Although B lymphocytes are diploid cells, a fine regulatory mechanism which allows the expression of the rearranged genes encoded by one of the two chromosomes (allelic exclusion), ensures that each B cell will present one single specific immunoglobulin. The generation of the highly variable repertoire of immunoglobulins relies not only on the contribution of the combinatorial diversity, which takes place during somatic recombination of the different encoding genetic segments, but also of the junctional diversity, due to the introduction of DNA sequence variations (insertion and deletions of nucleotides) by a mechanism of improper joining of the gene segments.

2.3 B lymphocytes differentiation

Mature B cells leave the bone marrow expressing on their membrane IgM or IgD with a single antigenic specificity and circulate in the blood and lymph, which transport them to the secondary lymphoid organs. After antigen recognition, they start proliferating (clonal expansion), differentiating and creating a population of plasma cells, which secretes antibodies and memory B cells. In the germinal centers, actively proliferating B cells undergo a further process of immunoglobulin differentiation (somatic hypermutation) in the variable heavy and light chains, expecially in the residues located in the CDRs. Successively, new intrachromosomal recombination events in the heavy chain constant genes generate a change into the immunoglobulin class (class switching), while antigen specificity is preserved. Recently, it has been found that, although very different, these two molecular events are linked by the intervention of the AID (activation-induced deaminase) enzyme, which causes localized DNA deaminations. Based on the DNA damage repair pathway activated, cells undergo one of the two processes [20-22].

2.4 The antigen-antibody binding

The hypervariable regions of the heavy and light chains of immunoglobulins create a cleft where the antigenic determinants perfectly adapt in a sort of key-lock mechanism. The bonds that hold the antigen linked to the antibody are multiple and reversible, because of their non covalent nature. They consist of: hydrogen bonds, electrostatic bonds, Van der Waals forces and hydrophobic bonds. Some distinctive properties of the immunoglobulins have to be considered when analyzing antigen-antibody interactions:

- **Affinity:** antibody affinity defines the strength of the interaction between a single antigenic determinant (epitope) and a single combining site of the antibody. It is given by the sum of the attractive and repulsive forces at the antigen-antibody interface.
- **Valency:** antibody valency is the number of binding sites per antibody molecule. IgGs, for example, have two identical antigen binding sites (valency = 2).
- **Avidity:** antibody avidity is a measure of the overall strength of binding between an antigen and an antibody. For example, a multimeric antibody (like a pentameric IgM, which presents ten binding sites) may display a stronger avidity than that of a conventional IgG (which presents two binding sites) for the same polyvalent antigen.
- **Specificity:** antibody specificity refers to the ability of an individual antibody combining site or of a population of antibody molecules to react only with a distinct antigen or with a definite epitope on a macromolecular antigen. Antibodies can distinguish differences between i) the primary structure of an antigen, ii) the isomeric forms of an antigen and iii) the secondary and tertiary structures of an antigen.

- **Cross-reactivity:** antibody cross-reactivity refers to the ability of an individual antibody combining site to react with more than one antigenic determinant, or the ability of a population of antibody molecules to react with more than one antigen. Cross-reactions arise because the cross-reacting antigen shares an epitope with the immunizing antigen or because it presents an epitope which is structurally similar to one of the immunizing antigen (multispecificity).

3. The antibody-mediated immune response

The fraction of immunoglobulins present in a serum upon stimulation by an antigen is very heterogeneous due to the fact that, different plasma cells start to secrete different classes of antibodies, each recognizing specific epitopes present on the surface of the same antigen. This “polyclonal” response is primarily responsible for the protection of an organism against pathogens. Typically, it is possible to induce a polyclonal antibody response *in vivo* by immunizing an animal (usually a mouse) with the desired antigen. After the immune response has taken place and B lymphocytes have proliferated and differentiated, polyclonal IgGs can be separated from the animal serum by purification against their target. On the other hand, in order to obtain monospecific antibodies against a particular epitope, it is possible to select *in vitro* the single clone of plasma cells from which they are secreted: this is called “monoclonal” antibody (mAb) isolation.

3.1 Monoclonal antibodies and their therapeutic applications

Due to their unique properties, immunoglobulins have also been employed for many years now as valid tools in basic research, diagnostic and therapy. Therapeutic antibodies can be provided *in vivo* to i) specifically block the activity of a particular molecule, by binding its target (for example, they can prevent cell growth, by blocking specific cell surface receptors) or ii) they can be modified *in vitro* to obtain specialized carriers for the delivery

of radionuclides, toxins, drugs and enzymes. Monoclonal antibodies (mAbs) were firstly introduced to detect and purify their target antigen. In 1975, Kohler and Milstein ([23], Nobel Prize in 1984) revolutionized the field of immunology by providing the feasibility to fuse a myeloma cell line that had lost the ability to secrete antibodies, with healthy plasma cells obtained from spleens of immunized mice. This was the start of hybridoma fusion technology. The resulting hybridoma contains both the genes that control the specific antibody production, inherited from the spleen cells, and the genes that allow unlimited proliferation, inherited from the myeloma cells. Serial dilutions facilitate the separation of single clones secreting antibodies that can be grown in microtitre plates and screened by ELISA in order to select those suitable for large-scale production (Figure 5A). In a few years, the exciting possibility of raising unique antibodies against almost any epitope and, in particular, against tumor-specific antigens has led to the development of immunotherapy. Throughout the progression of monoclonal drug development, different formats of antibodies have been created: murine, chimeric, humanized and human (Figure 5B). Initially, therapeutic antibodies were murine, but their use was limited by many side-effects: i) short serum half-life *in vivo*, ii) limited penetration into tumor sites, iii) reduced stimulation of cytotoxicity, iv) induced immunogenicity with possible onset of allergic reactions in treated patients, v) unwanted Fc-induced effector functions (cytokine activation, receptor blockade [24]). To overcome some of these drawbacks, chimeric (murine variable regions fused with human constant regions [25, 26]) and humanized antibodies, obtained by grafting murine hypervariable domains into human antibodies, were developed [27]. However, it was observed that humanized antibodies bound the antigen with much lower affinities than their parent murine monoclonal antibody [28, 29]. Fully human antibodies were obtained after the introduction of large scale *E. coli* expression [30, 31] and phage display technology [32]. Currently, hundreds of monoclonal antibodies are employed in clinical trials and the U.S. FDA has approved many of them for

cancer treatment [33, 34], transplant rejection [35], reumathoid arthritis [36] and several other diseases (Table 1). Therapeutic application of monoclonal antibodies is defined as "passive immunotherapy" and relies on the repeated administration of antigen-specific antibodies obtained outside the body of the patients, in order to try to "immunize" them against a disease. In this case, the host's immune system is not directly stimulated to react. In contrast, the "active immunotherapy" approach aims at the long-term induction of a disease-specific immune response and tries to train up the host's immune system to recognize and destroy specific cells. This is achieved by administering i) vaccines created using malignant cells isolated from the patient, that have been presented to and cultured *in vitro* with the patient's own immune system cells or ii) vector-based vaccines, through which a virus or another vector is exploited to introduce disease specific proteins together with other molecules that can stimulate the patient's immune system to react specifically against them.

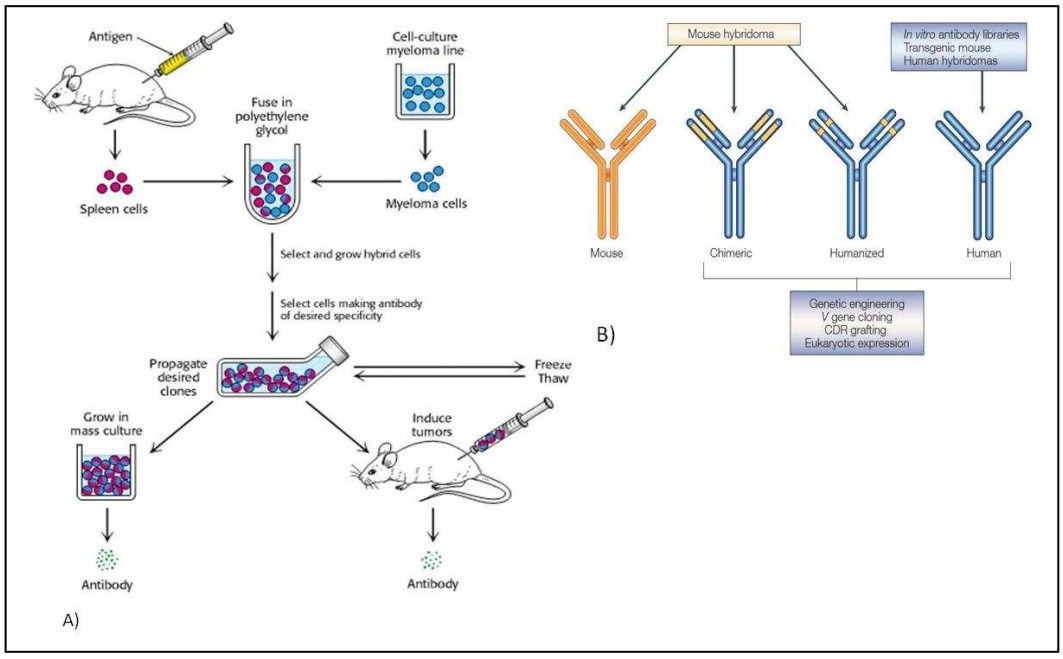

Figure 5. **Monoclonal antibodies and their formats.** ***A)*** *Simplified representation of the main steps necessary to obtain monoclonal antibodies by the hybridoma fusion technology (from "After C. Milstein. Monoclonal antibodies". Copyright © 1980 by Scientific American, Inc.).* ***B)*** *Different formats of monoclonal antibodies engineered for immunotherapeutic applications (from[37])*

4. Passive cancer immunotherapy

Nowadays, the most widely diffused cancer immunotherapy approach relies on the targeting by the antibody of a protein or receptor specifically expressed on transformed cells (targeted therapy), in order to try to induce tumor cells death. In fact, even though malignant cells are basically recognized by the immune system as the patient's own cells, in many cases they display particular antigens that are inappropriate for the cell type or the stage of development, or they overexpress surface receptors which are rare or absent in healthy cells. The biological effects upon clinical administration of antibodies are multiple and include neutralization of signaling proteins or specific blocking of receptor binding sites [38]. Typically, cancer cells growth can be inhibited employing mAbs which are able to prevent the interaction between growth factors and their receptors. mAbs can also mark tumor cells in order to elicit an immune response that can destroy them by antibody-mediated effector functions. Moreover, antibodies can also be used as carriers for the targeted delivery to the tumor sites of covalently linked cytotoxic agents. Even if passive cancer immunotherapy often requires high doses of tumor antigen specific mAbs and is of limited duration, antibody-based therapies have shown significant results in both the treatment of solid tumors and hematological malignancies. Nevertheless, this approach presents some limitations due to the complexity of a disorder such as cancer. In fact, therapy performed with mAbs has be proven to be not always successful because: i) antibodies are not used as a first-line therapy and often in patients already weakened and subjected to chemotherapy or surgery, ii) they are targeted against antigens that, even if present in a specific type of cancer, can vary between different individuals, iii) they can become ineffective due to the intrinsic high rate of mutations of tumor cells (tumor escape) and finally, iv) they can often show remarkable toxicity, especially when administered at high doses.

Trade name	Target	Source	Year	Indication
Orthoclone®	CD3	murine	1986	Transplant rejection
ReoPro™	CD41	chimeric	1994	Cardiovascular disease
Rituxan™	CD20	chimeric	1994	Non-Hodgkin's lymphoma
Zenapax®	CD25	humanized	1997	Transplant rejection
REMICADE®	TNF-α	chimeric	1998	Rheumatoid arthritis
Simulect®	CD25	chimeric	1998	Transplant rejection
Synagis™	RSV F-protein	chimeric	1998	RSV infection
Herceptin®	Her-2	humanized	1998	Breast cancer
Mylotarg™	CD33	humanized conjugated with ozogamicin	2000	Acute Myeloid Leukemia
Campath®	CD52	humanized	2001	Chronic lymphocytic leukemia
Zevalin®	CD20	murine conjugated with Yttrium- 90	2002	Non-Hodgkin's lymphoma
HUMIRA™	TNF-α	human	2003	Rheumatoid arthritis
Bexxar®	CD20	murine conjugated with Iodine 131	2003	Non-Hodgkin's lymphoma
Xolair®	IgE	humanized	2003	Severe (allergic) asthma
Erbitux™	EGFR	chimeric	2003	Colorectal cancer
TYSABRI®	VLA4	humanized	2004	Multiple Sclerosis
Avastin™	VEGF	humanized	2004	Metastatic colorectal cancer, non-small cell lung cancer
Vectibix™	EGFR	human	2006	Metastatic colorectal cancer
LUCENTIS™	VEGF-A	humanized	2006	Wet Macular Degeneration
Soliris®	CD59	humanized	2007	Paroxysomal nocturnal hemoglobinuria
CIMZIA®	TNF-α	PEGylated fragment	2008	Rheumatoid arthritis
Simponi™	TNFα	human	2009	Rheumatoid & psoriasic arthritis, active ankylosing spondylitis

Table 1. *List of the U.S. FDA approved mAbs for therapy in humans (updated from http://tbiweb.org/tbi/file_dir/TBI2008/TBI2008_2_24.pdf)*

CHAPTER 2

1. The phage display technology

Phage display was introduced in 1985 by George Smith, who created a vector for the expression of an exogenous peptide on the surface of filamentous phages [39]. Since then, different kinds of libraries exposing a large variety of peptides and proteins have been generated and, in the last decades, these tools have given important contributions to many scientific discoveries. The main advantage of the use of phage display libraries is that they comprehend billions of unique clones that can be simultaneously screened against almost any target of interest. The principle of phage display relies on the fact that the exposed molecules are genetically fused to a phage coat protein in a way that each phage expresses only one single clone. In this manner, a straight link is established between the displayed phenotype and the corresponding genotype carried by the bacteriophage [40].

1.1 Filamentous bacteriophages

Filamentous phages are the type of bacteriophages most commonly employed to expose biological molecules. They are single-stranded DNA (ssDNA) viruses that infect gram-negative bacteria. Their structure is similar to a filament, with a length of about 900 nm and a diameter of 6-10 nm. Filamentous phages are known as Ff and include strains M13, fl, Fd and ft. A shell (capsid) protects the ssDNA molecule that has a length of approximately 6400 bp. The capsid is constituted by several oligomeric coat proteins: pVIII, which is the most abundant and is present in about 2700 copies, pVII and pIX, present on one side of the phage in three to five copies, and pIII and pVI located on the

other side and present in three to five copies as well (Figure 6A and B). In most cases, pIII is the protein fused to the displayed polypeptide: it has a N-terminal domain, that binds the *E. coli* F pilus and a C-terminal domain, that is anchored inside the particle and is constitutive part of the capsid structure. Filamentous phages infect bacteria by exploiting as a receptor the F pilus present in "male" *E. coli* cells; they do not induce host cell lysis, but instead they induce them to produce and secrete new viruses. A viral life cycle (Figure 7) can be subdivided into three main steps: i) infection (attachment and penetration), ii) replication of the genome and iii) maturation (assembly and release) of the new phages. The process starts with the interaction between the pIII protein and the end of the *E. coli* F pilus: the pVIII protein undergoes a conformational change and shortens allowing the phage DNA to be exposed and then included into the host cell cytoplasm. Later, pVIII is stripped off and ends up in the inner cell membrane, where it may be stored and re-used to produce new particles. The circular single-stranded DNA (+ strand) is converted into a double-stranded replicative form (RF) and at this point, two proteins play a critical role: pII and pV. The first one, pII, nicks the double stranded form of the genome to initiate the rolling-circle replication of the + strand and the synthesis of a new helix together with the templates encoding for the pIII and pVIII proteins. The second, pV, competes with double stranded DNA formation by sequestering copies of the + strand DNA and creating a protein/DNA complex that can be packaged into new phages. The number of double stranded genomes in the bacterial host is regulated by pX. Assembly occurs at the inner cell membrane and new single-stranded DNA is packaged into protein coats and released through the bacterial membrane. It is thought that, before phage secretion starts, two of the minor phage coat proteins, pIX and pVII, interact with the pV/single-stranded DNA complex in a specific region called packaging sequence. Finally, the pV proteins covering the single-stranded DNA are replaced by the pVIII proteins embedded in the bacterial membrane and the growing phage filament is threaded through the membrane. Once the

phage DNA has been fully coated by pVIII, the release terminates by adding the pIII/pVI cap and the new particle can be finally released from the bacterial surface [41].

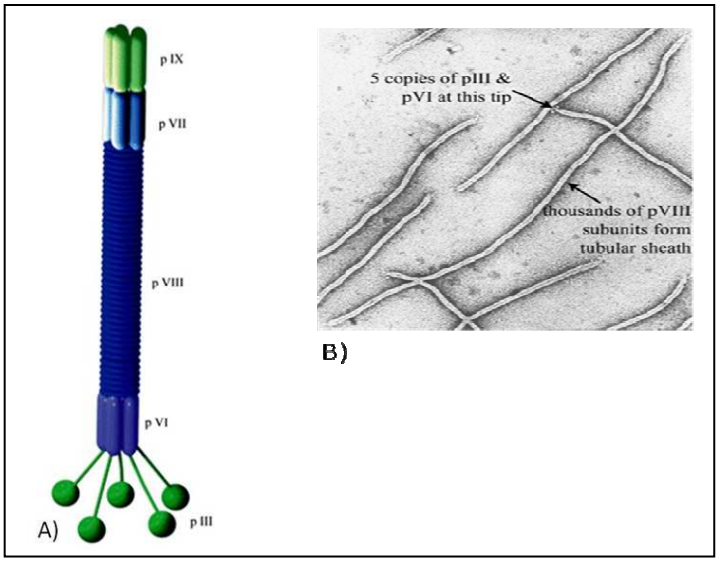

Figure 6. Structure of filamentous bacteriophages. A) *Representation of a typical bacteriophage: coat proteins are indicated (from http://www.scielo.br/pdf/gmb/v28n1/a01v28n1.pdf).* ***B)*** *Electron micrograph of the filamentous phage fd (from [42])*

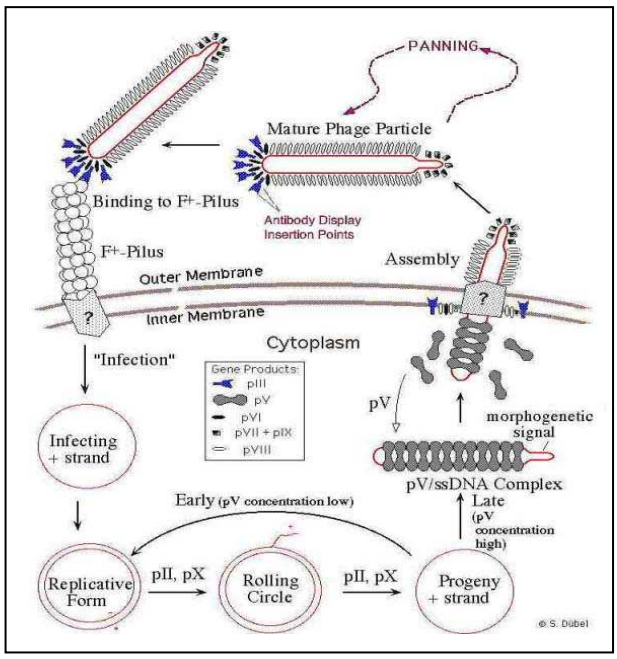

Figure 7. Life cycle of filamentous bacteriophages. *Scheme of the bacteriophage life cycle and the main steps of the replication process (graphics from S. Dübel)*

1.2 The antibody phage display

Antibody phage display relies on the principle that genes encoding for one or more variable domains of an immunoglobulin can be cloned in frame with the phage minor coat protein pIII into a selectable "phagemid" vector [43, 44]. A phagemid is a plasmid that presents both an *E.coli* and a phage derived (M13) replication origin, a signal sequence for the periplasmic secretion, the phage pIII gene and an antibiotic resistance marker, while it lacks the genes encoding for the phage structural proteins (Figure 8). Indeed, to assemble new phages and properly package the DNA, it is necessary to superinfect the cells containing the vector with a helper phage (M13K07), whose genome carries an autonomous replication origin, a kanamycin resistance, and encodes for all the capsid proteins. The system is very powerful because i) the M13K07 genome is designed with a modified intergenic region (that encompasses a packaging signal sequence and the origins of replication of the two strands, IG), which causes it to be replicated and packaged less easily than the phagemid vector (that carries a wild type IG) and ii) the wild type pIII protein (3-5 copies per phage), that competes with the pIII fused to the antibody (encoded by the phagemid) for the incorporation into the phage particle, is translated more efficiently from the phage genome and inserted into the new particles. At the end of the packaging process, most of the phages that expose an antibody show a monovalent display. This gives the chance to select and enrich antibodies with high affinity, since avidity effects, which would decrease the dissociation rate from the target antigen, are avoided. A phagemid vector allows both the antibody display on the phage particle and its soluble secretion in the periplasmic space. This is possible because of the presence of an Amber codon, that is located between the antibody gene and that of pIII protein. This codon functions as a transcription end point when using bacterial "non suppressor" strains (like HB2151), while it is not recognized by bacterial "suppressor strains" (like TG1). The

system allows to obtain respectively soluble antibodies or displayed antibodies fused to the phage surface (Fig. 8). The fusion protein expression is regulated by the lacZ promoter. Glucose in the growth medium represses the lacZ promoter preventing the production of the pIII-antibody fusion and favouring F pilus generation, which in turn enables helper phage infection. Once the helper phage genome is incorporated into the cell, then glucose is removed and phage-antibody expression starts.

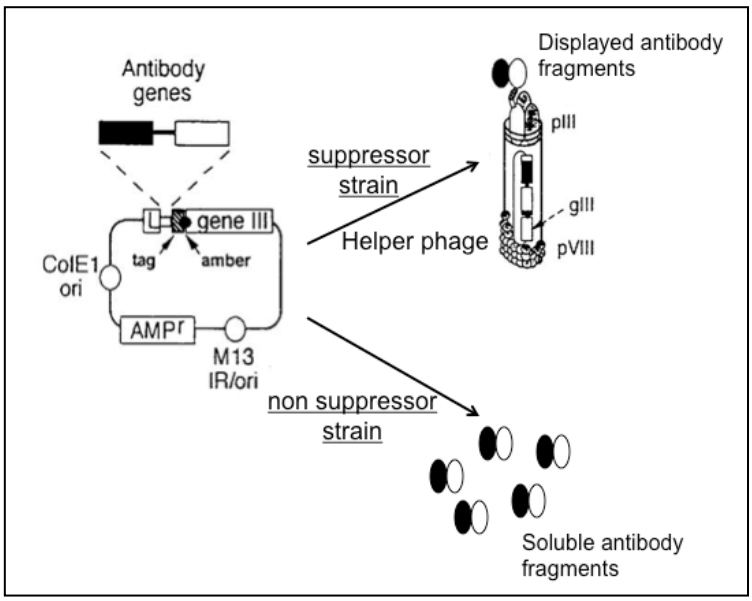

Figure 8. Schematic representation of displayed antibody expression (suppressor strain) or soluble antibody expression (non suppressor strain). *(adapted from [44])*

1.3 The (bio)-panning procedure

The phage selection procedure (bio-panning) can be subdivided into four main steps: i) exposure of the phage particles to the target antigen (immobilized protein, cell, tissue) in order to identify specific ligands, ii) removal of non specifically bound phages, iii) elution and recovery of the phages specifically bound to the antigen, iv) bacterial infection and amplification of the specific phages (Figure 9). Several rounds of selection and amplification, at different stringency conditions, are performed to enrich the population in

high affinity binders. The putative positive antibody clones are produced as soluble proteins from single colonies grown in microtitre plates and then tested by ELISA on their target. Each binder can be identified by DNA sequencing and unique sequences can be sub-cloned and produced in large scale for biochemical characterization.

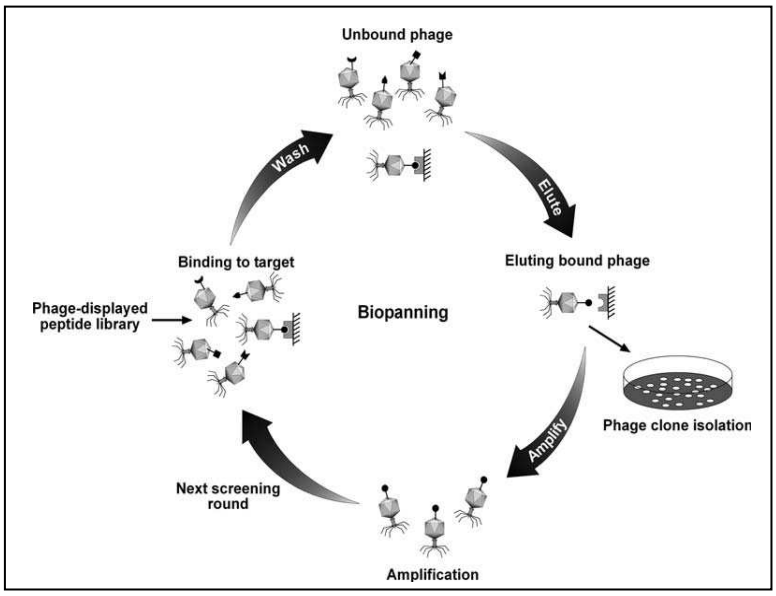

Figure 9. Antibody phage display. *Flowchart of the antibody selection procedure from phage display libraries (bio-panning), showing the enrichment of an antigen specific phage-antibody (circle) from a background of non specific phage-antibodies (from [45])*

2. Recombinant antibodies and their clinical applications

The first antibody fragments without Fc regions were generated by proteolytic treatment with papain or pepsin, that yield Fab and $(Fab)_2$ fragments, respectively (Figure 10, [46]). However, proteolysis is generally not absolutely specific and does not produce molecules smaller than Fab portions. In contrast, the process of *in vitro* selection using phage display libraries allows obtaining high affinity binders against almost any target antigen in a relatively easy way. Engineered recombinant antibodies have been successfully selected from immunized mice [47, 48], macaques [49], sheeps [50] and chickens [51], as well as from naïve phage display libraries [52-56]. Two kinds of antibody repertoires can be created *in vitro*: i) synthetic libraries comprehend collections of antibodies built by *in vitro*

assembly of VDJ gene segments [16, 57-60]; in this case, a predetermined level of randomization of the CDR regions can be introduced, during assembly, into the germline V gene segments [61, 62]; ii) semi-synthetic libraries present combinations of natural and synthetic diversity; they can be engineered by shuffling natural CDR regions [63] or by mixing naturally rearranged and highly functional CDR3 sequences with synthetic CDR1 and CDR2 diversity [64]. Recombinant antibody fragments present many advantages in respect to the conventional monoclonal antibodies: i) they can be selected in a shorter time ii) they can be *in vitro* manipulated to enhance their specificity and affinity properties (affinity maturation), and iii) they can be produced in large scale at relatively low costs. Depending on the purpose to be achieved, different molecular formats have been generated by engineering antibody sequences (Figure 10). The structure of recombinant antibodies has been modified in order to reduce the portion responsible for the effector functions, while retaining only one or two domains that are dedicated to antigen binding. The most diffused recombinant antibodies are Fab and single-chain variable fragment (scFv) formats. A scFv antibody is constituted by a single polypeptide chain encoding for the light-chain (VL) and heavy-chain variable (VH) domains covalently connected by a short flexible polypeptide [65-67]. This linker must not interfere with the tridimensional conformation of the antibody, it has to be resistant to proteolysis and it must not contain charged residues, in order to reduce unwanted interactions between the surfaces of the VH and VL regions [66], [68]. scFvs show a monovalent antigen binding affinity and can be easily manipulated and modified by conjugation to drugs, toxins, radionuclides, viruses, and enzymes both for diagnostic and therapeutic applications [24, 69, 70]. Multimeric scFv fragments such as diabodies, triabodies and similar molecules have been designed because of i) their multivalency, that should increase their avidity slowing their dissociation rates from the cell surface or multimeric antigens [71] and ii) their longer persistence *in vivo* [72, 73]. Moreover, combining two different scFvs, each with an antigenic specificity, it

has been possible to create bispecific antibodies that can direct effector functions towards two independent therapeutic targets and limit complement activation [74]. As an alternative, minibodies have been engineered by covalently linking bi/multivalent scFv fragments to other kinds of proteins that tend to self-associate, obtaining molecules with longer serum half-lives [75-77].

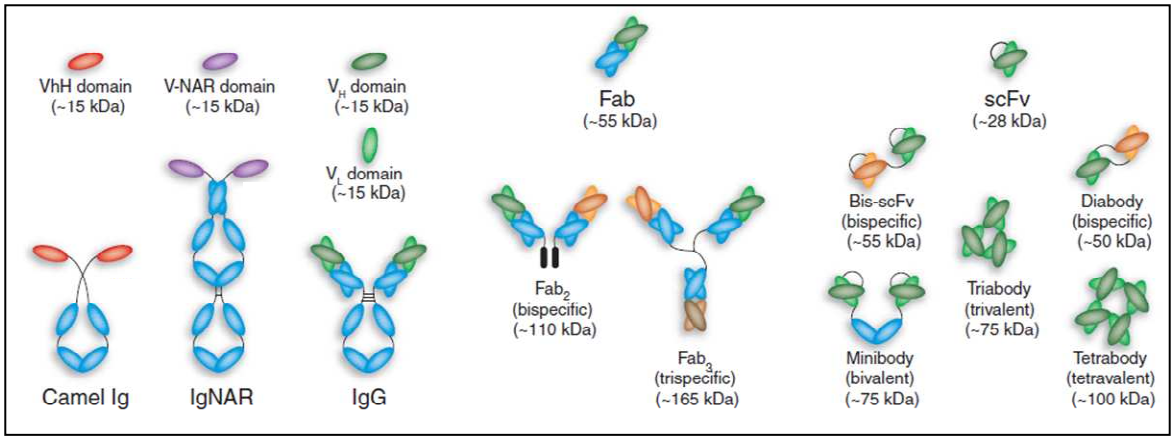

Figure 10. Molecular formats of recombinant antibodies. *Scheme of different recombinant antibody formats (from [24])*

Recently, the discovery of the presence in Camelids and sharks immune systems [78, 79] of heavy chain antibodies (HCAb) constituted by a single variable domain bound to a conventional constant domain, has led to the intriguing opportunity to exploit them for biotechnological applications. In fact, they show an elevated germline complexity [80, 81] and their variable domains (referred to as VHH in Camelids and V-NAR in sharks) are the smallest naturally occurring antigen-binding molecules known to date. VHHs show high stability and solubility and, due to their peculiar paratope conformation (a convex and protruding H3 loop, [82]), they preferentially bind hidden epitopes and clefts, like the active sites of enzymes [83, 84]. It has been demonstrated that isolated VHH domains exhibit a strong antigen binding activity, perfectly compensating the lack of the VL domains [85]. The increasing availability of recombinant antibodies has led to the

development of therapeutically relevant molecules, in particular for cancer treatment. In many cases, antibodies are responsible for the delivery of concentrated and specific "loads" to a desired tissue or cell type (targeted therapy, [86]). They can be employed as carriers for toxic cargoes [87-89] or as mediators to release enzyme prodrugs into tumor sites [90, 91]. This approach relies on pre-targeting a tumor with an antibody-coupled enzyme, then the antibody is removed and the enzyme converts an administered non toxic precursor into a drug that blocks cell growth. Furthermore, innovative affinity maturation methods have been developed in order to improve the binding properties of the selected binders [92-97]. Much work has been done in the diagnostic field, in particular in tumor imaging, by radiolabelling antibody molecules [98-101] and by creating fluorescent nanobodies [102].

3. The "intrabodies" (intracellular antibodies) and their applications

The term "intrabody" indicates an antibody molecule that is expressed intracellularly and directed to a defined subcellular compartment [103]. The potential of this technology relies on the fact that intrabodies can induce the phenotypic knockout of intracellular target molecules i) by directly blocking the antigen and its function, ii) by re-directing it to a specific intracellular location or iii) by inhibiting its translocation from the ER to the cell surface. Fusions with signal sequences allow for antibody localization in the nucleus, endoplasmic reticulum, Golgi apparatus, mitochondria or cell membrane, while their absence leads to its retention in the cell cytoplasm (Figure 11). The intrabodies' technology is a very promising therapeutic tool because it may help to solve some of the problems linked to current antibody treatments, like tumor penetration, short serum-half life and even poor specificity.

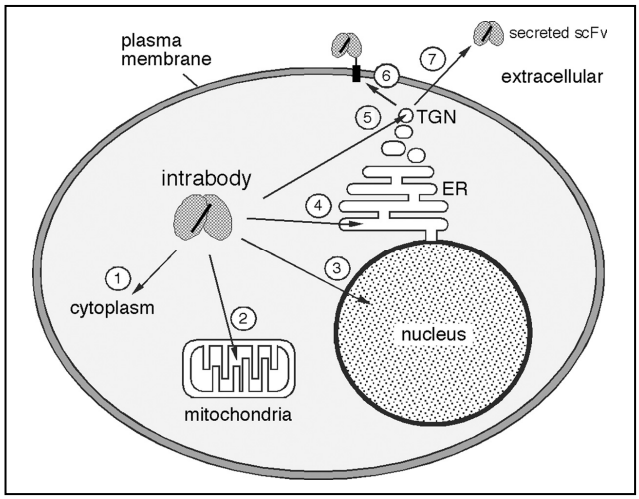

Figure 11. Intracellular antibodies and their localization. *Subcellular localization of intracellular antibodies. Intrabodies can be directed to the cytoplasm (1), mitochondria (2), nucleus (3), endoplasmic reticulum (ER) (4), trans-Golgi network (TGN) (5), plasma membrane (6) or secreted in the extracellular space (7), adapted from [104]*

The first successful application of intracellular antibodies to block a complex biological process in the cytosol of vertebrate cells was the expression of an scFv fragment directed against the GTPase p21Ras in the cytoplasm of *Xenopus laevis* oocytes that caused the inhibition of their insulin-induced meiotic maturation [105]. When the same antibody was expressed in mammalian cells cytoplasm, it was observed that p21Ras was sequestered into aggregates in an scFv-dependent manner leading to efficient inhibition of DNA synthesis [106]. Intrabodies have been used as means to inhibit tumor growth. Blocking VEGF-R2 and Tie2 pathways by using specific intra-diabodies, resulted in a 92% inhibition of tumor growth and angiogenesis in a human melanoma xenograft model [107]. *In situ* expression and secretion of a bispecific diabody *in vivo* reduced tumor growth by activating tumor-resident human T lymphocytes citotoxicity [108]. The use of lentiviral vectors for its expression was demonstrated to be feasible in human primary peripheral blood lymphocytes and has opened a promising avenue for gene therapy of human solid tumors [109]. Interesting results have been obtained in targeting receptor tyrosine kinases like EGFR or ErbB2, which are overexpressed in a variety of tumors including breast and

ovarian cancers. Intrabodies equipped with an ER localization signal, that specifically retains receptor molecules, generated a phenotypic knock out. Cells proliferation was inhibited *in vitro* and *in viv*o in ErbB2 overexpressing cancer cell lines, and human ovarian tumor cells underwent apoptosis [110-114]. Intrabodies have also been employed for the functional inhibition of some viral envelope proteins and host cells receptors. These viruses include human papilloma virus (HPV) [115], Kaposi Sarcoma-associated Herpesvirus (KSHV) [116], Human Immunodeficiency Virus (HIV) [117], and Hepatitis B Virus (HBV) [118]. Intrabodies targeting nuclear antigens have been shown to induce growth arrest and cell death. These targets include cell cycle regulators, transcription factors, viral and cellular oncogenic proteins and structural components of chromatin. Intracellular antibodies which are able to restore the DNA-binding and transcriptional activity of certain p53 mutants have been described [119]. Recently, researches have focused on neurodegenerative disorders like Huntington's (HD) [120], Parkinson's [121], Alzheimer's [122] and prion diseases [123], characterized by the accumulation of intracellular proteins. Intrabody-mediated *in vivo* suppression of the neuropathology using a *Drosophila* model of HD, resulted in an increase in the proportion of HD flies surviving to adulthood [120]. However, when trying to develop intrabody-based drugs, the main challenge is the delivery of their coding sequences to the specific target cells. Intrabodies need to be functional within the cell and, therefore, they require a vehicle which is able to deliver them inside target cell populations. A possible solution is to directly deliver the antibody cDNA through viruses (gene therapy) [124]. Retroviral and adenoviral gene transfer systems have been already developed to carry intrabody genes into target cells *ex vivo* or *in vivo* [125, 126]. In a Phase1 trial for the treatment of ovarian cancer, adenoviruses have been used to deliver an anti-ErbB2 retained antibody [127-129]. Nowadays, technical alternatives are in development in order to avoid the use of viral vector transduction technologies. One approach is to target molecules through liposomes or

encapsulating them with cationic lipids or peptides [130]. Another option would be to exploit peptide transduction domains (PTDs), which have the natural capacity to cross the cell membrane and can ferry linked polypeptides [131, 132].

4. The Cogentech1 VHH antibody phage display library

Most of the VHHs recovered so far have been isolated from immunized camels or llamas; in fact, recombinant VHH phage display libraries created from immunized animals have been the preferred tools for the isolation of high-affinity specific binders [84, 133, 134]. More recently, several synthetic and naïve VHH libraries have been constructed from llamas and sharks [54-56, 135-137], and the feasibility of selecting specific antibodies has been shown using a relatively small naïve shark library (10^7) [55]. Cogentech1 is a naïve VHH library prepared starting from 10^9 lymphocytes collected and isolated from one liter of blood of non-immunized llamas (*Llama glama*) [56]. The heavy chains of the immunoglobulins were first amplified from a retro-transcribed cDNA template, then VHHs were separated from VHs and reamplified using degenerate primers. VHHs were cloned into the phagemid vector pHEN4 (Figure 12, [133]). The total diversity of the library is in the order of $5x10^7$ different clones.

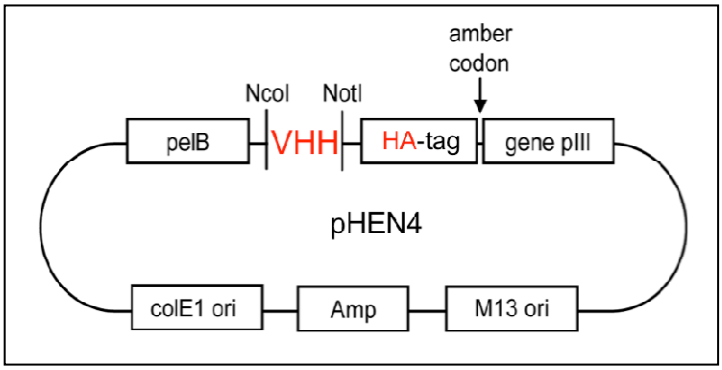

Figure 12. Schematic representation of the pHEN4 phagemid vector. *The pIII gene, the antibiotic resistance (ampicillin), the bacterial replication origin (colE1), the phage replication origin (M13 ori) and the pelB leader sequence (which directs the protein to the periplasmic space of E. coli) are indicated. VHHs were cloned between NcoI-NotI restriction sites as fusions with HA tag*

5. The ETH-2 Gold scFv antibody phage display library

The ETH-2 Gold library is a modified version of the synthetic antibody library of Pini et al., [57]. The library was improved by Viti et al., [58] and, finally, by Silacci et al., [16]. This phage display library of human recombinant antibodies in scFv format comprehends $3x10^9$ different clones. Human antibodies were assembled from approximately 50 different VH and 70 VL germline genes. The ETH-2Gold library was built using three antibody germline gene segments: DP-47 for the VH, DPK-22 and DPL-16 for the VL [138], and a large repertoire was created by appending short variable complementarity determining region 3 (CDR3). Sequence variability was introduced by PCR (using partially degenerate primers) into the CDR3 loops, which are known to largely contribute to antigen recognition, while the remaining parts of the antibody molecule were kept constant. A completely randomized sequence of four, five, or six amino acid residues was appended to the VH germline segment, thus forming short CDR3 loops, whereas a partially randomized sequence of six amino acid residues was appended in the VL (Figure 13A, [139]). After this amplification step, the resulting VH and VL segments were assembled by PCR and the library was cloned into the phagemid vector pHEN1 (Figure 13B, [140]).

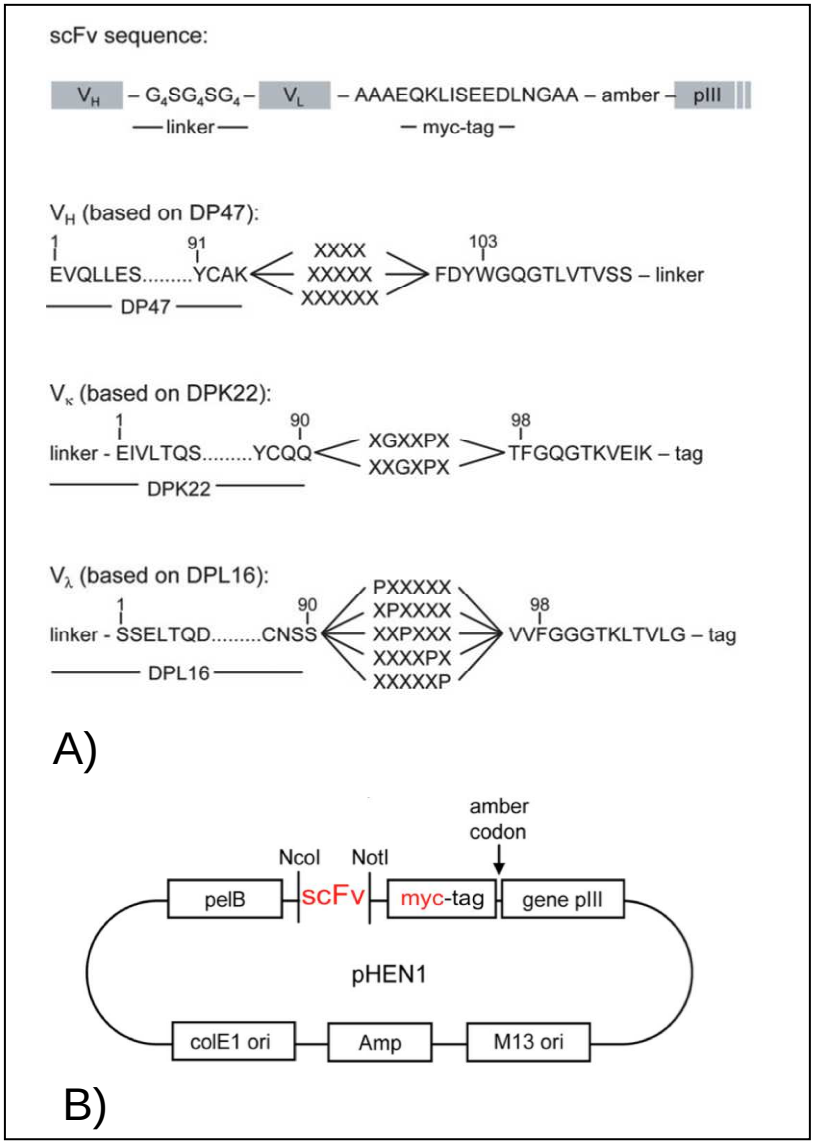

Figure 13. Design of the ETH-2 Gold antibody phage display library. A) *The sequence of the relevant amino acid residues of the variable heavy and light chains are represented together with the human antibody germline segments from which they were derived. Antibody residues are numbered according to [141].* ***B)*** *Schematic representation of the pHEN1 phagemid vector. The pIII gene, the antibiotic resistance (ampicillin), the bacterial replication origin (colE1), the phage replication origin (M13 ori) and the pelB leader sequence (which directs the protein to the periplasmic space of E. coli) are indicated. scFvs were cloned between NcoI-NotI restriction sites as fusions with myc tag (adapted from [16])*

CHAPTER THREE

1. Acute myeloid leukemia

Acute myeloid leukemia (AML) is a cancer of the myeloid cell line, characterized by rapid growth of abnormal white blood cells that accumulate in the bone marrow and interfere with the production of normal cells. AML is the most common acute leukemia affecting adults and its incidence increases with age. The symptoms of AML are caused by replacement of normal bone marrow with leukemic cells, which causes a drop in red blood cells, platelets, and normal white blood cells. Although several risk factors for AML have been identified, the specific cause of the disease remains unclear. As an acute leukemia, AML progresses rapidly and is typically fatal within weeks or months if left untreated. AML presents several subtypes, and treatment and prognosis differ among them. Five-year survival varies from 15% to 70% and relapse rate varies from 33% to 78% depending on the subgroup. Initially, AML is treated with chemotherapy to induce a remission; then patients may receive additional chemotherapy or a hematopoietic stem cell transplant. Recent research into the genetics of AML has succeeded in generating tests that can predict which drug or drugs may work better for a particular patient, as well as how long that patient is likely to survive. The single most important prognostic factor in AML is the cytogenetic status: different cytogenetic abnormalities are associated with different outcomes. For example, the t(15;17) translocation (PML/RARα, promyelocytic leukemia/retinoic acid receptor alpha) that is found in acute promyelocytic leukemia patients is associated with good prognosis, while a number of other genetic aberrations (e.g. *FLT3* internal tandem duplication, ITD) are related to poor prognosis and a high risk

of relapse after treatment [142-144]. The proteins involved in this translocation are PML, a matrix-associated nuclear phosphoprotein which regulates senescence and apoptosis and functions as a growth suppressor [145] and RARα, a nuclear receptor involved in retinoid signaling [146]. Many genes are under investigation as prognostic factors or as possible therapeutic targets, including *CEBPA* (CCAAT Enhancer Binding Protein Alpha), *BAALC* (Brain and Acute Leukemia, Cytoplasmic), *ERG* (ETS Related Gene) and *NPM1* (Nucleophosmin 1). *CEBPA* encodes for a bZIP transcription factor, which plays important roles in lineage determination and gene activation in a variety of cell types. In hematopoiesis, CEBPA is a key factor in driving the development of myeloid cells and mutations in CEBPA occur in approximately 10% of all acute myeloid leukemias (AMLs) [147]. *BAALC* is a highly conserved gene among mammals and it is implicated in acute myeloid leukemia. Its overexpression has been demonstrated to be strictly related to poor prognosis in AML patients [148]. ERG is a member of the ETS family of transcription factors; it is a transcriptional regulator expressed in early myeolcytes at higher levels than in mature lymphocytes and therefore, it may act as a regulator of differentiation of early hematopoietic cells [149]. Genetic abnormalities related to *NPM1* (see paragraph 2. for a detailed description of protein functions) have been described in different types of hematological malignancies [150] and three chromosomal translocations involving this gene have been identified so far. The t(2;5) translocation involves the N-terminal portion of *NPM1* and leads to a fusion with the catalytic domain of the membrane-associated receptor tyrosine kinase ALK (anaplastic lymphoma kinase), that renders it constitutively active. This aberration is present in about 30% of Anaplastic Large Cell Lymphomas (ALCL, [151]). The t(5;17) (q35;q21) is a rare variant found in some cases of Acute Promyelocitic Leukemias (APL, [152]). Also in this case, the N-terminal end of NPM1 is fused to the RARα C-terminal portion, leading to the recruitment of co-repressor proteins that interfere with RARα-dependent transcriptional activities [153]. As a consequence,

myeloid differentiation is stopped; patients that present this genetic abnormality can be treated with super-physiological doses of ATRA (all-*trans* retinoic acid) that release the block [154]. The third translocation t(3;5)(q25;q35) is found in less than 1% of AML cases [155]. In this case, *NPM1* is fused to *MLF1* (myelodisplasia/myeloid leukemia factor 1, a cytoplasmic protein that has a putative role in normal hematopoietic differentiation) and it has been shown to be able, together with the oncogene RASV12, of transforming Mouse Embryonic Fibroblasts (MEFs) [156]. Recently, *NPM1* mutations, which lead to the cytoplasmic delocalization of the protein (NPMc+), have been found in about 35% of acute myeloid leukemia patients that present a normal karyotype, suggesting a relevant role for *NPM1* in AML onset. AML with NPMc+ mutations probably represent a new distinct group of AML and it has been included as a provisional entity in the 2008 revision of the WHO classification of myeloid neoplasms and acute leukemia [157]. Due to the stability of this mutation, many different diagnostic techniques have been already developed for its identification and for the detection of NPMc+ localization [158-165]. Interestingly, some of the most recurrent AML genomic aberrations, like t(15;17), t(8;21) and inv(16) are mutually exclusive with *NPM1* mutations [166], while a significant correlation has been reported between *NPM1* mutation and mutations in *FLT3*-ITD [12]. NPMc+ AML that are *FLT3*-ITD negative have a general better prognosis, due to the higher remission rate after chemotherapy [12, 167-171]. Although the mechanism has not been completely elucidated, it was observed that NF-kB, that is involved in pharmacological resistance [172] and is frequently upregulated in AML patients [173], results delocalized and inactivated by NPMc+, therefore increasing cell chemosensitivity [174].

2. Nucleophosmin (NPM): a multifunctional protein

Nucleophosmin (NPM; also known as B23, NO38, or numatrin) is a nuclear-cytoplasmic shuttling protein that is involved in different cellular processes such as centrosome duplication, cell cycle progression and stress response [1-4]. NPM is present within the cell in two isoforms which are generated from a single gene *via* alternative splicing: the longer and most abundant B23.1 (294 residues), and the shorter and less abundant B23.2 (259 residues) [175]. NPM normally localizes in the nucleus and the B23.1 isoform accumulates in the granular region of the nucleolus. Most NPM published data regard the B23.1 longer isoform, normally referred to as NPM1. NPM1 contains distinct functional domains that are responsible for its multiple biochemical functions (Figure 14, [176]). NPM1 belongs to the family of nucleoplasmins proteins (Np) which share a conserved N-terminal acidic portion involved in oligomerization and chaperone activity. Nucleophosmin functions as a molecular chaperone for proteins: *in vitro* studies have demonstrated that it prevents protein aggregation and promotes renaturation of chemically denatured proteins [177]. Moreover, *in vitro* assays have shown that NPM1 favors replication from adenovirus chromatin [178] and behaves like a histone chaperone, able to assemble/disassemble histones and nucleosomes [179]. Moreover, NPM1 is able to enhance, at least *in vitro*, acetylation-dependent transcription [180]. The central portion of the protein is required for ribonuclease activity, together with the C-terminal domain, which contains basic clusters of amino acids involved in nucleic acid binding [176]. NPM1 associates both with DNA [181] and RNA [182] and it has been reported to have endoribonuclease activity on ribosomal RNA (rRNA, [183]). At the end of the NPM1 C-terminal portion, it is located an aromatic stretch that contains two tryptophan residues responsible for its nucleolar localization (NuLS, [184]). In addition, NPM1 includes a bipartite nuclear localization signal (NLS, [176]) and two nuclear export signals (NES, [185],[186]) which are essential

for its shuttling activity. Native NPM1 exists as an oligomer [187] and it has been shown that *Xenopus laevis* NO38, that is highly homologous to human nucleophosmin, can form pentamers and decamers [188]. The recent definition of the crystal structure of the human NPM1 core (amino acids 9-122) demonstrated that it forms decamers with structural plasticity at the pentamer-pentamer interface [189]. NPM1 physically interacts with many nuclear proteins, such as nucleolin [5], p120 [6], p53 [7] and Mdm2 [8]. Recently, it has been demonstrated that NPM1 forms a stable complex with the tumor suppressor p19/Arf [9, 11], and that it is absolutely required for its correct localization and stabilization in the nucleolus [10].

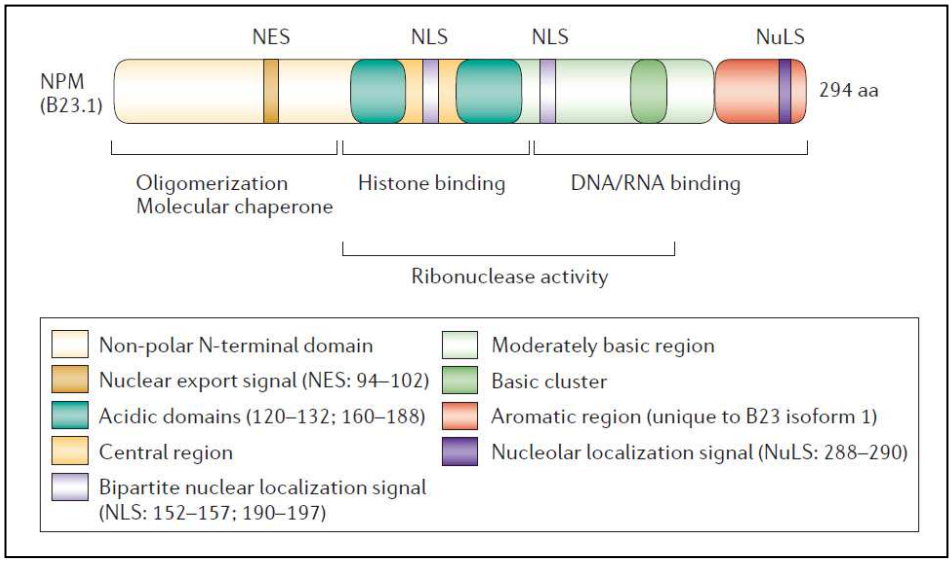

Figure 14. NPM1 protein structure. *NPM1 motifs and functional domains (from [190])*

2.1 Nucleophosmin and cancer

NPM1 is essential during mouse embryonic development. It has been demonstrated that inactivation of the *NPM1* locus in mice causes embryonic lethality at mid-gestation, and embryonic cells show unrestricted centrosome duplication and enhanced genomic instability [11, 191]. Mice heterozygous for *NPM1* inactivation ($NPM^{+/-}$) rapidly develop a hematologic syndrome similar to human myelodysplastic syndromes (MDS). Moreover, these mice frequently present hematologic tumors, with higher incidence of myeloid cancers [192]. Nucleophosmin is directly involved in the pathogenesis of different human malignancies. Overexpression of NPM1 has been reported in solid tumors of diverse cellular origin, including gastric [193], colon [194], prostate [195], bladder [196] and ovarian carcinomas [197], as well as during melanoma progression [198]. Chromosomal translocations of the *NPM1* gene have been observed in human hematopoietic cancers, and it has been suggested that NPM1 contributes to tumor development by activating the oncogenic potential of the fused protein partners. All *NPM1* translocations characterized so far involve the 5' region of the *NPM1* gene (oligomerization domain of NPM1), which is fused to three different partner genes: the anaplastic lymphoma kinase (*ALK*) [199], the retinoic acid receptor α (*RARα*) [152], and the myeloid leukemia factor 1 (*MLF1*) [155]. Recently, it has been demonstrated that about one-third of primary adult AML patients' cells with normal karyotype bear mutations in the last coding exon of the *NPM1* gene (exon 12, [12]). Mutations in the *NPM1* gene are heterozygous and are characterized by the insertion of short nucleotides stretches, leading to a reading frameshift and to a *de novo* formation of a CRM1/Exportin 1-dependent nuclear export signal (NES, [13]). More than 40 different mutations have been described: the most frequent one (mutation A) encompasses 75-80% of cases and consists of the duplication of the TCTG tetranucleotide (Figure 15, [200]). Loss of the two tryptophan residues (that are located in the C-terminal

portion of the protein and are necessary for nucleolar localization [201]) and the insertion of a new sequence of eleven amino acids contribute to the generation of a supplementary novel NES responsible for mutant NPM1 cytoplasmic delocalization (NPMc+) (Figure 15, [13, 201]). The abnormal accumulation of mutated NPM1 in the cytoplasm leads to the cytoplasmic delocalization of proteins that in normal conditions are localized to the nucleus and interact with NPM1 wild type protein. In particular, NPMc+ binds, delocalizes and inactivates, inducing their degradation, the tumor suppressor proteins p19/Arf and Fbw7γ. Fbw7γ is part of a E3 ubiquitin ligase complex involved in the degradation of c-Myc and, therefore, in cells expressing NPMc+ its inactivation causes increased levels of this oncogene [15]. In normal cells, c-Myc overexpression leads to p19/Arf upregulation, p53 stabilization and apoptosis. This is an important mechanism evolved to prevent c-Myc induced tumorigenesis [202]. However, in presence of NPMc+, p19/Arf is translocated to the cytoplasm too, it is rapidly degraded and, as a consequence, the p19/Arf-dependent p53 stabilization induced by c-Myc overexpression is lost [14]. Based on these data, NPMc+ is a *bona fide* oncogenic mutant that once expressed in a cell leads to c-myc oncogene activation and, at the same time, blocks the corresponding tumor suppressor mechanism deactivating p19/Arf. This strongly suggests that NPMc+ can contribute to the initiation and progression of leukemia. Thus, NPMc+ may represent an ideal molecular target for specific therapeutic intervention in these types of leukemia. One major problem is the high similarity between the NPMc+ and NPM1 wild type proteins; indeed, they differ only for the last C-terminal eleven amino acids and they are both present in leukemic cells, since *NPM1* mutations always occur only in one of the two *NPM1* alleles [12]. Interestingly, the tridimensional structure of the NPMc+ C-terminal region seems to be unfolded as compared to the wild type [203], although it is not yet clear if this region could influence the overall structure of NPM1, and in particular the interaction between NPMc+ and other proteins like p19/Arf.

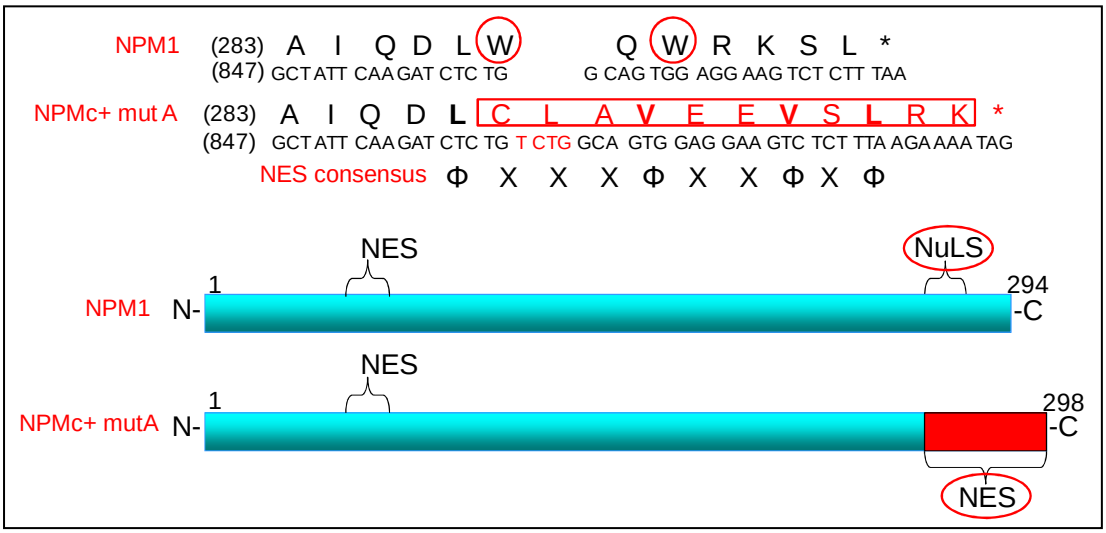

Figure 15. NPMc+ protein structure. *Amino acid sequence and schematic representation of the wild type NPM1 and NPMc+ mutation A proteins [200], showing the residues involved in the mutation and the novel nuclear export signal (NES, [13, 201]) created at the C-terminal end of the protein; (*) indicates stop codons. The NPMc+ amino acid residues that match the generic NES consensus (indicated below the alignment) are indicated in bold letters. X: any amino acid residue; Φ: Leucine, Valine, Isoleucine, Phenylalanine or Methionine residues*

RELEVANCE OF THE PROJECT

Nucleophosmin (NPM) is involved in human oncogenesis and, in particular, mutations in its coding sequence are the most frequent aberrations found in AML. About one-third of adult Acute Myeloid Leukaemia (AML) patients bear reading frameshift mutations occurring at the exon 12 of *NPM1*. As a consequence, the nucleolar localization signal (NuLS) present at the NPM1 C-terminal end is substituted by a *de novo* nuclear export signal (NES), which causes its cytoplasmic localization (NPMc+). Accumulation of mutated NPM1 is responsible for the delocalization of proteins that, in normal conditions, interact in the nucleus with wild type NPM1. Interestingly, it has been shown that NPMc+ binds, delocalizes and inactivates the tumor suppressor proteins p19/Arf and Fbw7γ, leading to the uncontrolled c-Myc overexpression. These data point out a central role of NPMc+ in leukemia pathogenesis and thus, it may represent an ideal molecular target for specific therapeutic intervention. In the last years, it has been already proven the possibility to raise antibodies that specifically recognize only the mutated form of NPM1, making the antibody-based therapy an appealing opportunity. I decided to perform a high-throughput selection, from non-immune phage display libraries, of recombinant antibodies directed against NPMc+ mutation A. This approach has many advantages: i) it could provide suitable tools able to act *in vivo* as competitors of the natural NPM1 interactors (as p19/Arf and Fbw7γ), due to steric hindrance, ii) the specific antibody sequences could be cloned into appropriate vectors to allow their expression as intrabodies, in order to investigate their biological effects *in vivo* and iii) the specific binders could be modified *in vitro* by fusing them to nuclear localization signals (NLSs), with the purpose to obtain molecules able to re-localize NPMc+ to the nucleus.

MATERIALS AND METHODS

1. Recombinant proteins: expression, purification and biophysical characterization

1.1 Expression and purification of recombinant NPMc+ and wild type NPM1

Recombinant NPMc+, wild type NPM1 proteins and wild type NPM1 fragments 1-117, 1-186, 186-294 were produced as GST fusions from pGEX4T vector (Amersham, Figure 16) using BL21 competent cells (Novagen). Cultures were grown at 37°C up to an OD600 of 0.4 in LB medium supplemented with 0.1 mg/mL ampicillin, induced with 0.1mM IPTG and incubated overnight at 20°C, 220rpm. Next day, cells were centrifuged, washed in PBS and subjected to total cell lysis [204]. Purification was performed by affinity chromatography on GSTrap FF column (5 mL, GE Healthcare) using ÄKTA FPLC Explorer. Eluted samples were dialyzed against PBS and protein purity was evaluated by colloidal blue (Instant Blue, Novexin) stained 12% SDS-PAGE gels. Yields were calculated by measuring the absorbance at 280 nm and applying the protein extinction coefficients.

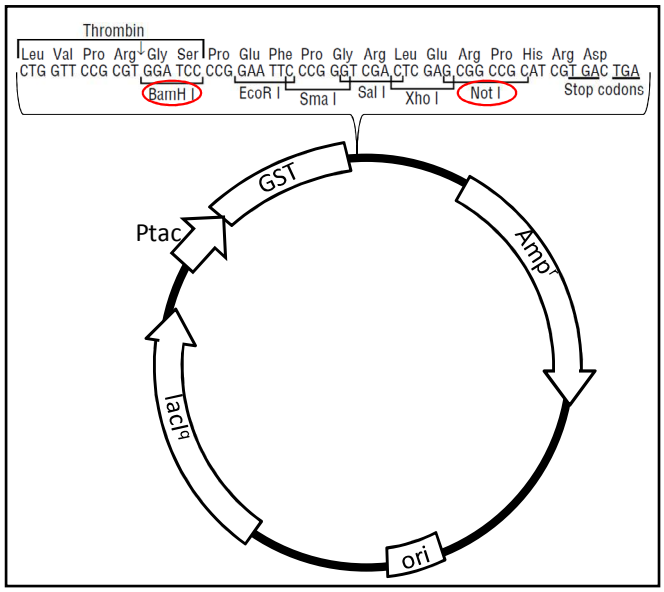

Figure 16. Map of the pGEX4T vector. *Sequence of the multi-cloning site (MCS) is reported in detail; red circles indicate the restriction sites used for cloning. The thrombin protease cleavage site, the ampicillin resistance (Amp^r), the origin of replication (ori), the lacI^q repressor gene, the Ptac promoter and the GST protein are indicated (Amersham).*

1.2 Determination of the aggregation rate

The presence of aggregates in the purified and dyalized NPMc+-GST were evaluated by measuring intrinsic fluorescence using a spectropolarimeter Jasco J-810 (JASCO). Samples at a concentration of about 250 µg/mL were excited by a monochromatic light (280 nm). An emission spectrum was recorded in the range 265 nm - 410 nm under the following conditions: 5 nm bandwidth, 2 nm datapitch and 1 accumulation. A spectrum recorded for the buffer alone (PBS) served as a subtraction baseline for all samples measured. A first maximum intensity at 280 nm (scattered light) and a second maximum intensity at 340 nm (the fluorescence signal from the protein) were recorded. From these two values an "Aggregation Index" [205] was calculated using the equation: A.I.= I 280/I 340, where I 280 and I 340 represent the intensity of emitted light at 280 nm and 340 nm, respectively.

1.3 FAR-UV CD (peptide bond circular dichroism) spectra measurement

Protein secondary structure was investigated by FAR-UV (200 nm – 250 nm) CD spectroscopy. 150 µg/mL of protein dialyzed against PBS, was measured using a cuvette with optical path 1 mm (HELLMA). CD spectra were recorded with a JASCO J-810 spectropolarimeter (JASCO) under the following conditions: 20 nm/min scan speed, 5 nm bandwidth, 0.2 nm datapitch and 1 accumulation.

1.4 Generation, expression and purification of recombinant NPMc+ fragment C-terminal

NPMc+ fragment C-terminal was designed as a 45 amino acids long peptide (NPMc+ amino acids from 255 to 298). It was synthesized by PCR amplification using primers NPMc+Forward: 5'-TAATGCCATGGATATAGAAAAAGGTG-3' and NPMc+Reverse: 5'-GTCTCTTTAAGAAAATAGGCGGCCGCTAAGAAT-3' using NPMc+ cDNA (cloned in pcDNA3) as a template. PCR reaction was performed following this protocol:

94°C-6 min; (94°C-40 sec, 55°C-40 sec, 72°C-50 sec) for 30 cycles; 72°C-10 min; 4°C. Insert was digested with NcoI-NotI restriction enzymes, cloned in pETM44 vector (Figure 17, [206] as MBP (Maltose Binding Protein)-6xHis tag fusion and transformed in BL21(DE3) competent cells (Novagen), following standard methods for bacterial transformation. Cultures were grown at 37°C up to an OD600 of 0.4 in ZYP-5052 medium, supplemented with 0.05 mg/mL kanamycin and then they were incubated overnight at 20°C, 220rpm. ZYP-5052 is a specific medium developed to allow for auto-induction of the expression as the culture approaches saturation [207]. Next day, cells were centrifuged, washed in PBS and subjected to total cell lysis. Purification was performed by affinity chromatography on HisTrap HP column (1 mL, GE Healthcare) using ÄKTA FPLC Explorer. Eluted samples were dialyzed against PBS and protein purity was evaluated by colloidal blue staining (Instant Blue, Novexin) of pre-casted 12% NuPAGE® Novex® Bis-Tris Gels (Invitrogen). Yields were calculated by measuring the absorbance at 280 nm and applying the protein extinction coefficient. Identity of the purified scFv-MutMyc was assessed by western immuno-blot analysis incubating the membranes with the mouse monoclonal antibody anti-Myc 9E10 (5 ug/mL) for 2 hours. After three washes in PBST (PBS added with 0.1% Tween-20), anti-mouse HRP conjugated (Bio-Rad) was added for 40 min at room temperature. Finally, membranes were washed three times in PBST and peroxidase activity was detected with a light sensitive film using an ECL Plus kit (Pierce) by mixing equal amounts of reagent 1 with reagent 2.

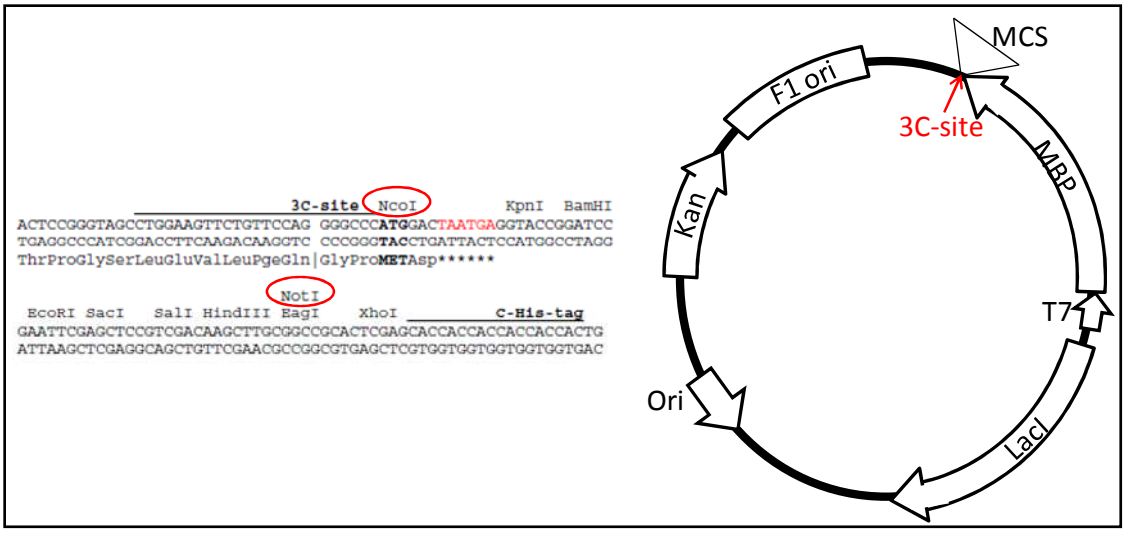

Figure 17. Map of the pETM44 vector. *Sequence of the multi-cloning site (MCS) is reported in detail on the left; red circles indicate the restriction sites used for cloning. The 3C protease cleavage site, the MBP protein, the T7 promoter, the lacI repressor gene, the origin of replication (ori) and the kanamycin resistance (Kan) are indicated [206]*

2. Selection and production of phage displayed recombinant antibodies

2.1 Selection of phage displayed VHHs

An aliquot of $5x10^{10}$ bacterial cells, harbouring phagemid vector pHEN4 [145], was grown in 2xTY medium [208] containing 0.1 mg/mL ampicillin and 1% glucose at 37°C up to an OD600 of 0.4 and infected with 20-fold excess of KM13 helper phage for 30 min at 37°C. Infected cells were harvested by centrifugation, resuspended in 2xTY 0.1 mg/mL ampicillin, 0.05 mg/mL kanamycin and 0.1% glucose and incubated overnight at 30°C, 150 rpm. Phage particles were precipitated from culture supernatant with 4% PEG 6000, 0.5 M NaCl, resuspended in sterile PBS, titrated and used for panning against the purified soluble NPMc+ protein. Phage library aliquots used for panning fusion protein were previously depleted from binders recognizing the fusion tag, by pre-panning them against GST coated on 4 mL Nunc-Immuno™ Maxisorp™ tubes (100 µg/mL). Unbound phages after the pre-panning incubation step (30 min rocking and 90 min standing upright at room

temperature) were recovered. NPMc+ was directly coated overnight at 4°C on the surface of 4 mL immunotubes at a concentration of 100 µg/mL using 50 mM sodium carbonate buffer, pH 9.6 [209]. Tubes were blocked with 3% BSA in PBST at room temperature for 2 hours, washed three times with PBS before the addition of $3x10^{15}$ phages for the first round of panning. After 30 min rocking and 90 min standing upright at room temperature, tubes were washed 10 times with PBST and 10 times with PBS, bound phages were eluted with 0.1M triethylamine, pH 11.0. Eluted phages were titrated, used to infect TG1 cells (Stratagene) and plated on 2xTY ampicillin, glucose large square plates. Colonies were scraped, infected with 10^{10} KM13 helper phages, grown overnight and phage particles precipitated from culture supernatant with 4% PEG 6000, 0.5M NaCl. The new sublibrary of phages was resuspended in sterile PBS, titrated, depleted against fusion tag (GST) and used in the second round of panning. The same complete procedure was repeated for the third round of panning alternating 3% BSA in PBST and 2% skimmed Milk in PBS as blocking agents.

2.2 Screening and production of VHHs

Ninety-six single colonies from the third round of panning were grown at 37°C in 2xTY supplemented with 0.1 mg/mL ampicillin, 0.1% glucose for 3-4 hours, induced with 1mM IPTG and incubated overnight at 28°C. Cultures were harvested, washed in PBS and subjected to three cycles of rapid freeze/thaw. Cultures were then centrifuged and the periplasmic extracts (supernatants) containing soluble HA-tagged VHHs were diluted 1:3 and incubated with the mouse monoclonal antibody anti-HA 12CA5 (10 µg/mL) for being used in ELISA. Maxisorp 96-well plates (Nunc) were coated with either the fusion protein alone or the fusion tag in 50 mM sodium carbonate buffer, pH 9,6 overnight at 4°C. NPMc+ was coated at a concentration of 1 µg/mL. Plates were blocked with 2% BSA for 2 hours, washed three times with PBS and incubated 1 hour with periplasmic extracts. Plates

were washed three times with PBS plus 0.1% Tween and incubated with anti-mouse HRP conjugated (Bio-Rad) for 1 hour at room temperature. Finally, plates were washed three times with PBST and the reaction was developed by adding ABTS. The absorbance at 405 nm was measured after 30 min incubation. Clones with an absorbance value higher than 0.25 and that recognized exclusively the recombinant protein and not the fusion tag were considered positives. Their cDNAs were sequenced using the primers: M13Forward 5'-CAGGAAACAGCTATGACC-3', pHEN4reverse 5'-CAACTTTCAACAGTCTATGC-3' and then analyzed to identify unique binders.

2.3 Epitope mapping of the selected VHHs

Maxisorp 96-well plates (Nunc) were coated with either the fusion proteins NPMc+, wild type NPM1 and NPM1 fragments 1-117, 1-186, 186-294 or the fusion tag (GST) in 50mM sodium carbonate buffer, pH 9.6 overnight at 4°C. All antigens were coated at a concentration of 1 µg/mL. Periplasmic extracts of the selected five different VHH clones were obtained and a standard ELISA procedure was followed as in **2.2**.

2.4 Selection of phage displayed scFvs

The ETH-2 Gold phage display library was purchased from Philotec s.r.l. (Siena). The general procedure of antibody selection was performed following the ETH-2 Gold phage display library manual (September 2005 version). A bacterial colony (*E. coli* TG1) was transferred from a minimal plate (M9) into 5 mL of 2xTY medium and grown overnight at 37°C at 200 rpm. Next day, it was subcultured by diluting 1:100 (OD600 of 0.1) into fresh 2xTY medium, grown until OD600 of 0.4 and then infected with 10^{12} KM13 helper phages for 40 min at 37°C. Infected cells were harvested by centrifugation, resuspended in 2xTY 0.1 mg/mL ampicillin, 0.05 mg/mL kanamycin and 0.1% glucose and incubated overnight at 30°C, 150 rpm. Phage particles were precipitated from culture supernatant with 4% PEG

6000, 0.5M NaCl, resuspended in sterile PBS, titrated and used for panning against the purified soluble antigen NPMc+ fragment C-terminal. Phage library aliquots used for panning fusion proteins were previously depleted from binders recognizing the fusion tag, by panning them against MBP coated on 4 mL immunotubes at a concentration of 100 µg/mL. 10^{13} t.u. phage library (mixing the 4 phage library sub-aliquots) in 1 mL PBS were added to immunotubes containing 2 mL of 4% skimmed Milk in PBS (to give a final concentration of 2% MPBS) and put 30 min rocking and 90 min standing upright at room temperature. After the pre-panning incubation step, unbound phages were recovered and left at 4°C to be used the next day for the panning procedure. NPMc+ fragment C-terminal was directly coated on the surface of 4 mL immunotubes (overnight at 4°C) at a concentration of 25 µg/mL in 50 mM sodium carbonate buffer, pH 9.6. Tubes were rinsed 3 times with PBS and then blocked with 2% skimmed Milk in PBS at room temperature for 2 hours. After three washes in PBS 10^{13} t.u. phages were added for the first round of panning. After 30 min rocking and 90 min standing upright at room temperature, tubes were rinsed 10 times with PBST and 10 times with PBS, bound phages were eluted with 0.1M triethylamine, pH 11.0 for 5 min rocking. Eluted phages were poured in a microfuge tube with 50mM TrisHCl ph7.4 + 1mM $CaCl_2$ and vortexed. Trypsin (Sigma) at a concentration of 10 mg/mL was added in order to eliminate the background given by helper phages and samples were left in rotation for 15 min. Phages were titrated, used to infect TG1 cells and plated on 2xTY 0.1 mg/mL ampicillin and 1% glucose large square plates at 30°C. Colonies were scraped, infected with 10^{12} KM13 helper phages and grown overnight at 30°C, 150rpm. Phage particles were then precipitated from culture supernatant with 4% PEG 6000, 0.5M NaCl. The new sublibrary of phages was resuspended in sterile PBS, titrated, depleted against fusion tag (MBP) and used in the second round of panning. The same complete procedure was repeated for the third round of panning.

2.5 Screening, production and purification of scFvs

Ninety-six single colonies from the third panning of each antigen were grown at 37°C in 2xTY supplemented with 0.1 mg/mL ampicillin, 0.1% glucose for 3-4 hours, induced with 1mM IPTG and incubated overnight at 30°C. Cultures were harvested, supernatants containing soluble Myc-tagged scFvs were filtered through disposable 0.45 µm filters and added with 0.02% Sodium Azide with Complete Protease Inhibitor Cocktail (Roche). Supernatants were diluted 1:3 and incubated with the mouse monoclonal antibody anti-Myc 9E10 (8 µg/mL) for being used in ELISA. Maxisorp 96-well plates (Nunc) were coated with either the fusion protein alone or the fusion tag in 50mM sodium carbonate buffer, pH 9.6 (overnight at 4°C). NPMc+ fragment C-terminal was coated at a concentration of 1 µg/mL. Plates were blocked with 2% BSA 2 hours, washed three times with PBS and incubated 1 hour with the supernatants. Plates were washed three times with PBST and incubated with anti-mouse HRP conjugated (Bio-Rad) for 1 hour at room temperature. Plates were washed three times with PBST, the reaction was developed by adding ABTS and the absorbance at 40 nm was measured after 30 min incubation. Clones with an absorbance value higher than 0.49 and that recognized exclusively the recombinant protein and not the fusion tag were considered positives. Their cDNAs were sequenced using the primers: Fdseq1 5'-GAATTTTCTGTATGAGG-3' and PelbBack 5'-AGCCGCTGGATTGTTATTAC-3' and then analyzed to identify unique binders. Clones with unique sequence were chosen to be produced in large scale. Antibody fragments were purified from culture supernatant by affinity chromatography on HiTrap MabSelect SuRE (5 mL) Protein A-derived ligand column (GE Healthcare) using ÄKTA FPLC Explorer. Protein A-Sepharose is normally used to purify antibodies encoded by VH segments from the VH3 family [62]. Size-exclusion chromatography of the purified samples was performed on HiLoad 16/60 Superdex 200 (GE Healthcare). Protein purity was evaluated

by colloidal blue (Instant Blue, Novexin) stained 12% SDS-PAGE gels and the correspondence of the identified bands to scFv proteins was verified by western immuno-blot analysis using the mouse monoclonal antibody anti-Myc 9E10 (5 µg/mL) as primary antibody. Yields were calculated by measuring the absorbance at 280 nm and applying the protein extinction coefficient.

3. Cloning of the scFv-Mut antibody in mammalian expression vectors

The selected scFv-Mut was cloned in pEGFP-C1 (Clontech, Figure 18A) as a GFP fusion. Its cDNA was amplified by PCR using the following primers:

- FW: 5'-CCAAGCTTCCATAGAGGTGCAG-3'
- REV: 5'-GGGGCCGCATAGTCTAGACTAGAT-3';

scFv-Mut was cloned in pcDNA3.1 (Invitrogen, Figure 18B) as a Flag fusion. Its cDNA was amplified by PCR using the following primers:

- FW: 5'-CCAAGCTTCCATGGAGGTGCAGCTGTTGGAGTCTGGG-3'
- REV: 5'-CTGACCGTCCTAGGCGCGGCCGCAGACTACAAGGACGACGATGACAAG-3';

scFv-Mut was cloned in pcDNA3.1 (Invitrogen) as a SV40 NLS-HA fusion. Its cDNA was amplified by PCR using the following primers:

- FW: 5'-CCAAGCTTCCATGGAGGTGCAGCTGTTGGAGTCTGGG-3'
- REV: 5'CTAGGCGCGGCCGCATACCCCTACGACGTGCCCGACTACCCCAAAAAGAAACGAAAAGTATAGTCTAGACTAG-3';

The same primers were used to amplify by PCR the cDNA of an unrelated scFv antibody. scFv-Mut was cloned in pcDNA3.1 (Invitrogen) as a SV40 4xNLS-HA fusion. Its cDNA was amplified by PCR using the following primers:

- FW:
  5’CCAAGCTTCCATGCCCAAAAAGAAACGAAAAGTACCCAAAAAGAAAC GAAAAGTAATGGAGGTGCAGCTGT-3’

- REV:
  5’CGACGTGCCCGACTACCCCAAAAAGAAACGAAAAGTACCCAAAAAG AAACGAAAAGTATAGTCTAGACTAG-3’

All inserts were cloned using HindIII-XbaI restriction sites. Positive clones were verified by colony PCR, analytical digestion and DNA sequencing.

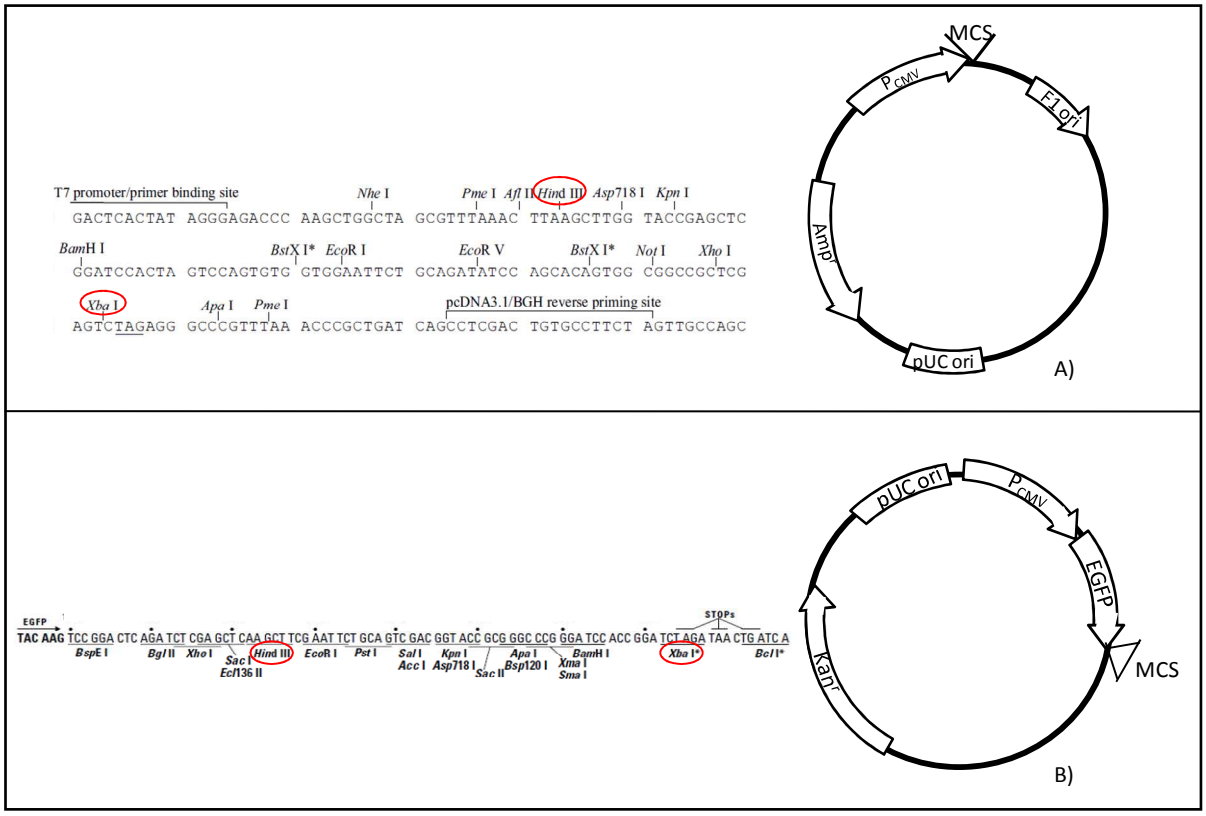

Figure 18. Maps of the pcDNA3.1 and the pEGFP-C1 vectors. A) *Sequence of the multi-cloning site (MCS) is reported in detail on the left; red circles indicate the restriction sites used for cloning (Invitrogen). The Pcmv promoter, the neomycin resistance, the ampicillin resistance (Amp^r) and the origin of replication (pUC ori) are indicated.* ***B)*** *Sequence of the multi-cloning site (MCS) is reported in detail on the left; red circles indicate the restriction sites used for cloning (Clontech). The Pcmv promoter, the EGFP protein, the kanamycin/neomycin resistance (Kan^r/Neo^r) and the origin of replication (pUC ori) are indicated*

4. Cell lines: culture conditions, transfections and infections

4.1 Sf9 insect cells: culture conditions

Sf9 insect cells were cultured at 27°C in Sf 900 II SMF medium (Gibco).

4.2 Sf9 insect cells: transfection, infection and protein production

Sf9 (*Spodoptera frugiperda*) insect cells were transfected with the pFastBacDual plasmids (Invitrogen) expressing either wild type NPM1 or NPMc+. This vector displays two expression cassettes: one, where the gene of interest is cloned and the other, where the GFP gene is cloned. Each cassette is controlled by an independent promoter. For Sf9 cells transfection, 2 mL of cells at a density of $0.5x10^6$ cells/mL were seeded in a 6-wells plate. Plates were gently rocked and cells were let attach for 15-30 min. The transfection mix was prepared by adding the following reagents in the indicated order: 10µl sterile water, 6µg PCR-verified bacmide and 18µl transfection reagent (Insectogene T030-1.0, Biontex). The solution was mixed, left at room temperature for 10 min and then added to the cells. After 24 hours, the medium was replaced with fresh medium and cells were incubated at 27°C for 96 hours. Then, 100µl of the baculoviral supernatant were harvested and used for infection of 5 mL cells, seeded at a density of $0.8x10^6$ cells/mL. GFP fluorescence was monitored at the microscope. When 80-90% of cells resulted GFP positive, 100 µl of their baculoviral supernatant were harvested and used to infect new cells. Two cycles of the infection procedure were performed. For protein expression, 5 mL of cells at a density of $1.2x10^6$ cells/mL were infected with 500µl of baculoviral supernatant obtained as described before. After incubation at 27°C for 96 hours, cells were harvested, washed and subjected to three cycles of sonication. Then centrifuged and resuspended in 500µl of 2xPBS.

4.3 Mammalian cell lines: culture conditions

HeLa, OCI-AML2 and OCI-AML3, MEFs NPM1$^{-/-}$p53$^{-/-}$ cells were cultured at 37°C, 5% CO_2 and 20% O_2. HeLa cells were grown in Dulbecco's modified Eagle Medium (DMEM-BioWhittaker, Lonza) supplemented with 10% of fetal bovine serum of Southern American origin, L-glutamine (2 mM), penicillin (100 U/mL), streptomycin (100 mg/mL). OCI-AML2 and OCI-AML3 cell lines were grown in MEM Alpha + GlutaMAX^{TM}-I medium (Gibco) supplemented with 20% of fetal bovine serum of Southern American origin, glutamine and antibiotics. MEFs NPM1$^{-/-}$p53$^{-/-}$ were grown in DMEM supplemented with 10% of fetal bovine serum of Northern American origin, glutamine and antibiotics.

4.4 Mammalian cell lines: transfection

HeLa and MEFs NPM1$^{-/-}$p53$^{-/-}$ cells were transfected using Lipofectamine^{TM} 2000 (Invitrogen). For transfection of 10cm plates, 24µg of DNA were diluted in 1.5 mL OptiMEM® medium (Invitrogen). In a separate tube, 60µl of Lipofectamine^{TM} 2000 reagent were mixed with 1.5 mL of OptiMEM® medium (Invitrogen). Each tube was incubated 5 min at room temperature and then the two solutions were mixed and incubated together 15 min at room temperature, in order to allow liposome-DNA complexes to form. Lipofectamine-DNA mixture was directly added to the plates that were incubated at 37°C, 5%CO_2 and 20% O_2. For transfections in smaller or bigger plates, scaling-down or scaling-up of doses was done. Expression of the transfected construct was detectable after 24-48 hours post-transfection. For co-transfection, a sequential procedure using the same Lipofectamine^{TM} 2000 (Invitrogen) method was set up: first, the scFv-Mut plasmid was transfected then, after 24 hours, the plasmid encoding for NPMc+ was added with a second transfection. In this way, I reasoned that the scFv-Mut would have had the time to produce and fold before NPMc+ and therefore it would have been able to bind it as soon as it was synthesized in the cells.

5. Biochemical methods

5.1 Western immuno-blot analysis

For western immuno-blot analysis, total cell lysates were clarified by centrifugation and quantified using the Bio-Rad protein assay (BIO-RAD), according to the manifacturer's instructions. Recombinant purified proteins and cell lysates (1-50µg per gel lane) in 2xSDS Laemmli buffer were boiled 5 min at 95°C and separated on a SDS-PAGE gel, using an appropriate acrylamide concentration (stock 40%, 37:1 mix of acrylamide:bisacrylamide) to resolve the molecular weight of the targeted proteins. Proteins were transferred onto a nitrocellulose membrane (0.45µm pore; Whatman Group). After blocking with 5% skimmed Milk in PBST for 2hours at room temperature, proteins of interest were detected by specific antibodies at the optimal dilution in 5% skimmed Milk in PBST (overnight, at 4°C). After three washes in PBST, appropriate HRP conjugated secondary antibodies (Bio-Rad) were added (40 min at room temperature). Finally, membranes were washed three times in PBST and peroxidase activity was detected with a light sensitive film using an ECL Plus kit (Pierce) by mixing equal amounts of reagent 1 with reagent 2.

5.2 Immunoprecipitation assay

HeLa cells were seeded in 10 cm^2 plates and cultured in standard culture medium, before being transiently transfected using Lipofectamine^{TM} 2000 (Invitrogen), as described in **4.4**. After 24 hours, transfected HeLa cells were washed and lysed in Mild Lysis Buffer (50mM TrisHCl at pH 8, 150mM NaCl, 0.5% NP40 added with protease inhibitors) on ice. Lysates concentrations were determined using the Bio-Rad Protein Assay (BIO-RAD), according to the manifacturer's instructions. For immunoprecipitations, 100µg of HeLa cell lysates transiently transfected with NPMc+-GFP and NPMc+ expression vectors or 300µg of OCI-AML2 and OCI-AML3 patients' cell lysates were incubated with the scFv-MutMyc (10µg)

in rotation overnight at 4°C. Samples were extensively washed with ice-cold lysis buffer and finally, precipitated proteins were detached from protein A-sepharose (GE Healthcare) by dissolving the pellet in 2xSDS Laemmli buffer, denatured by boiling and run onto a 10% SDS-PAGE gel. The T26 home-made mouse monoclonal antibody anti-NPMc+ [217], was used to detect the immunoprecipitated NPMc+ by western immuno-blot analysis as described in **5.1**.

5.3 Co-immunoprecipitation assay

For immunoprecipitations on HeLa cell lysates transiently co-transfected (as in **4.4**) with scFv-MutFlag and NPMc+-GFP expressing vectors, 400µg of total lysate (obtained as described in **5.2**) were incubated with mouse M2 anti-Flag agarose beads from mouse (Sigma) and with mouse IgG agarose beads as control (Sigma) in rotation overnight at 4°C. Samples were extensively washed with ice-cold lysis buffer and finally, precipitated proteins were detached from the beads by dissolving the pellet in 2x SDS Laemmli buffer, denatured by boiling and run onto a 10% SDS-PAGE gel. The T26 home-made mouse monoclonal antibody anti-NPMc+ [217] was used to detect the immunoprecipitated NPMc+ and mouse M2 anti-Flag antibody (Sigma) was used to detect the presence of the scFv-MutFlag by western immuno-blot analysis as described in **5.1**.

5.4 Immunofluorescence assay

HeLa cells were grown on 0.2% gelatin-coated coverslips and transiently transfected using Lipofectamine^{TM} 2000. After 24 hours, transfected Hela cells were rinsed twice with PBS and fixed in 4% Paraformaldehyde in PBS at room temperature for 10 min. After two washes in PBS, cells were permeabilized 5 min with 0.2% Triton X-100, washed in PBS and blocked in BSA 2% in PBS for 30 min at room temperature. Then, the blocking solution was removed and the slides were stained with primary antibodies diluted at the

appropriate concentrations in blocking solution, for 1hour at room temperature. After two washes in PBS, secondary antibodies were added and the slides incubated for 30 min at room temperature. The secondary antibodies were CY3-labeled donkey anti-mouse, or CY5-labeled goat anti-rabbit IgG (Jackson Immuno Research Laboratoires), diluted in blocking solution as following: CY3-labelled antibodies 1:400, CY5-labelled antibodies 1:50. After two washes in PBS slides were counterstained with DAPI for 5 min, rinsed in distilled water, to eliminate salts and mounted with mounting solution (Mowiol). Stained cells were assessed by fluorescence microscopy at the DAPI, GFP, CY3 and CY5 channels. Images were acquired using an Olympus AX70 microscope equipped with a CoolSNAP *EZ* Turbo 1394 (Photometrics®) camera, and the MetaMorph® software (Molecular Devices inc.) was used. Images were then processed using ImageJ 1.43 software, freely available at http://rsbweb.nih.gov/ij/index.html.

6. Antibodies used in this study

- Anti-Myc 9E10. Mouse monoclonal antibody home-made. Used 5 µg/mL in western immuno-blot, 8 µg/mL in ELISA, 2 µg/mL in immunofluorescence

- Anti-HA 12CA5. Mouse monoclonal antibody home-made. Used 10 µg/mL in ELISA

- Anti-HA (HA.11, Covance). Mouse monoclonal antibody. Used 1:200 in immunofluorescence

- Anti-Flag M2 (Sigma). Mouse monoclonal antibody. Used 1:6000 in western immuno-blot

- Anti-NPMc+ T26. Mouse monoclonal antibody home-made. Used 1:1000 in western immuno-blot, 1:100 in immunofluorescence, 10 µg in immunoprecipitation

- Anti-NPM1 clone 338. Mouse monoclonal antibody home-made. It recognizes the C-terminal end of NPM1. Used 1:5 in western immuno-blot

- Anti-NPM clone 376. Mouse monoclonal antibody home made. It recognizes the N-terminal end of NPM protein. Used 1:10 in western immuno-blot

- Anti-NPM1 (Zymed). Mouse monoclonal antibody. Used 1:1000 in western immuno-blot

- Anti-nucleolin (Abcam, ab50279). Rabbit polyclonal antibody. Used 1:800 in immunofluorescence

- scFv-MutMyc. Human recombinant antibody isolated in this study from the ETH2-Gold library (Silacci et al., 2005). Used 1:3 as supernatant (in combination with mouse monoclonal antibody α-Myc 9E10) in western immuno-blot, 2 µg/mL in immunofluorescence, 10 µg in immunoprecipitation

RESULTS

1. Expression and purification of recombinant mutated NPMc+ protein and of recombinant wild type NPM1 fragments

My first step was to produce all the reagents necessary for the isolation of the antibodies. Among the different NPM1 mutations, I decided to focus on mutation A ([200], Figure 15) since it is the most frequent (80% of the NPMc+ AML cases display this variant). Recombinant NPMc+ full length fused to Glutathione S-transferase (GST) tag (NPMc+-GST) was produced in *E. coli* and the total cell lysate was purified by affinity chromatography (Figure 19A). The fraction containing eluted NPMc+-GST was dialyzed against PBS and run on a 12% SDS-PAGE gel to evaluate protein purity. Upon colloidal blue staining (Instant Blue, Novexin), some bands were visible, which ran at lower molecular weight than the fusion protein, indicating a slight protein degradation (Figure 19B, lane 3). The presence of aggregates was assessed by measuring the intrinsic fluorescence of the protein (Aggregation Index, A.I. [205]). The A.I. was calculated using the following equation (λexc 280 nm): **I 280 nm** (scattered light) **/ I 340 nm** (max. emitted light), and the sample showed a value of 1.7, indicating a significant degree of aggregation (Figure 20A). The GST tag promotes protein dimerization and can contribute to bind together partially misfolded monomers of nucleophosmin, a protein that forms oligomers in its native conformation [189]. Consequently, even a limited percentage of misfolded proteins can contribute to the accumulation of large aggregates. The secondary structure composition of NPMc+-GST was analyzed by Circular Dicroism in the Far-UV region: the purified protein showed a spectrum compatible with the expected one, namely mainly composed by α-helices (GST tag component) and β-sheets (nucleophosmin component, Figure 20C, [210]). In parallel, a set of partially overlapping recombinant NPM1 fragments was designed that covered the entire wild type protein sequence. Such fragments were produced as GST fusions and purified by affinity chromatography. The quality of the eluted samples was evaluated after protein separation on 12% SDS-PAGE gels and

successive staining with colloidal blue (Instant Blue, Novexin): some bands were visible, which ran at lower molecular weight than the fusion proteins, indicating a slight protein degradation (Figure 21A and B). This strategy was conceived for identifying which regions of the wild type NPM1 in common with the NPMc+ were recognized by the selected antibodies.

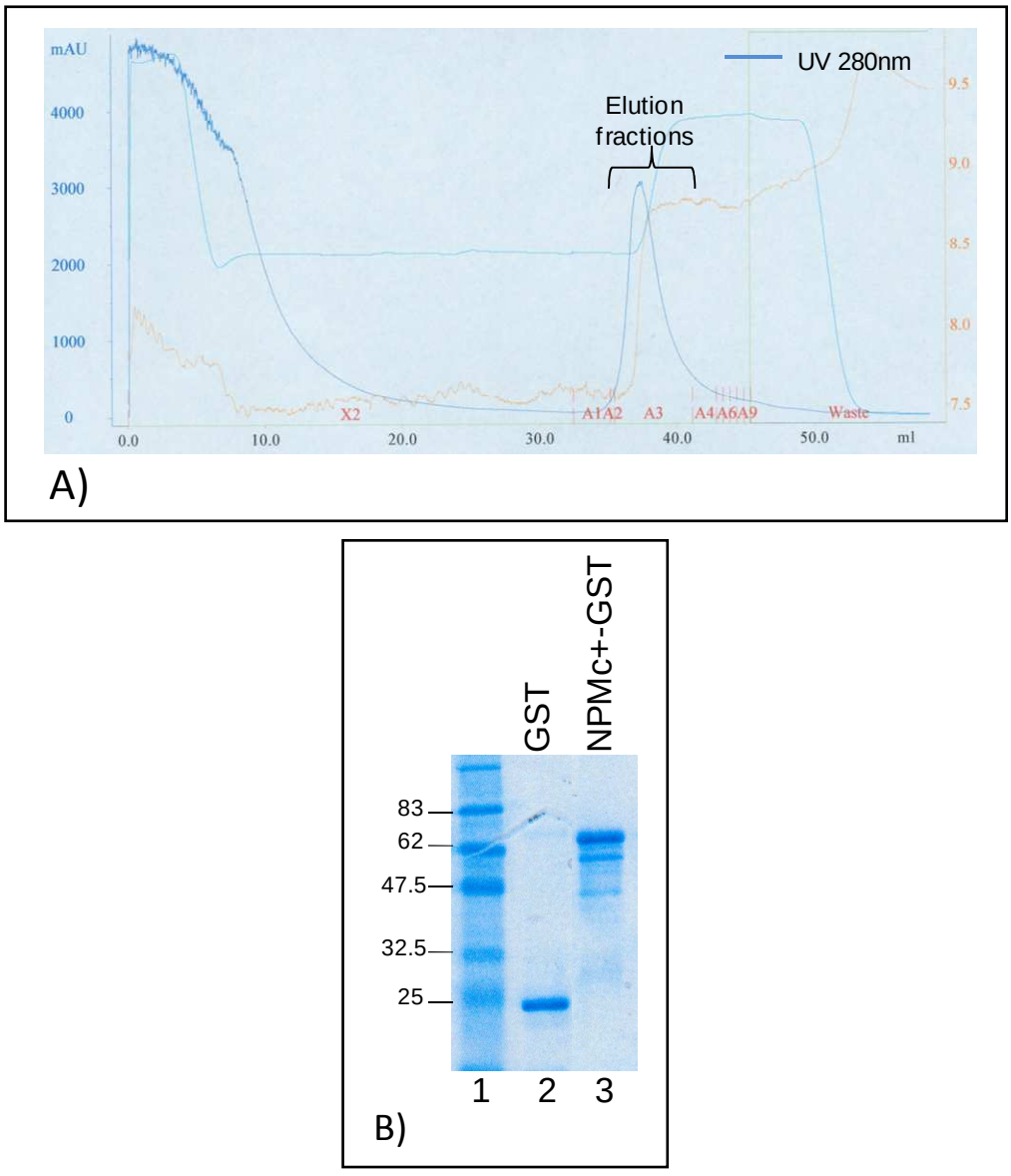

Figure 19. Purification of recombinant NPMc+-GST protein. A) *Affinity purification chromatogram of the recombinant NPMc+-GST protein. The elution peak is indicated by a blue line (UV absorbance at 280 nm).* ***B)*** *Colloidal Blue stained 12% SDS-PAGE gel loaded with 3 µg of the purified recombinant GST (lane 2) and NPMc+-GST (lane 3) samples. Protein molecular weight (lane 1) is indicated in KDa (Prestained Protein Marker, Cell Signaling)*

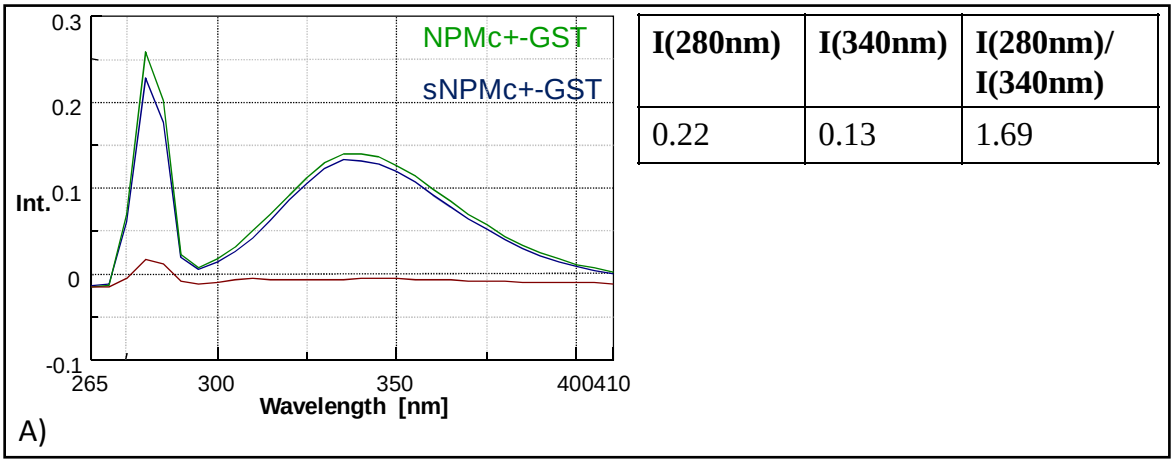

I(280nm)	I(340nm)	I(280nm)/ I(340nm)
0.22	0.13	1.69

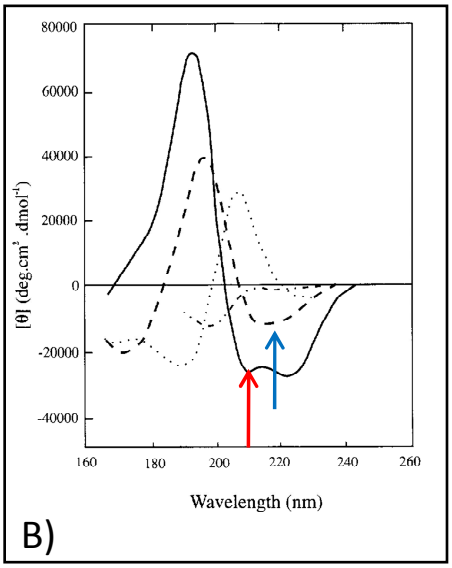

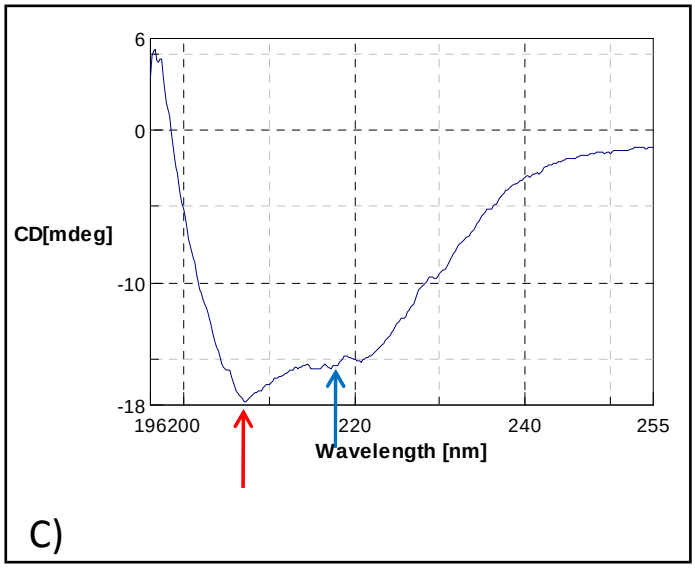

Figure 20. Biophysical characterization of the purified recombinant NPMc+-GST protein. A) *Emission spectrum of the purified recombinant NPMc+-GST protein in PBS (green line) excited at λ=280 nm. The spectrum obtained after buffer (red line) subtraction (sNPMc+) corresponds to the blue line.* ***B)*** *Far-UV CD spectra associated with different types of secondary structures: solid curve, α-helix; long dashes, anti-parallel β-sheet; dots, type 1 β turn; dots and short dashes, irregular structure [211].* ***C)*** *Far-UV CD spectrum of the purified recombinant NPMc+-GST protein. The red arrow indicates the typical minimum of α-helices, while the blue arrow indicates the minimum of β-sheets*

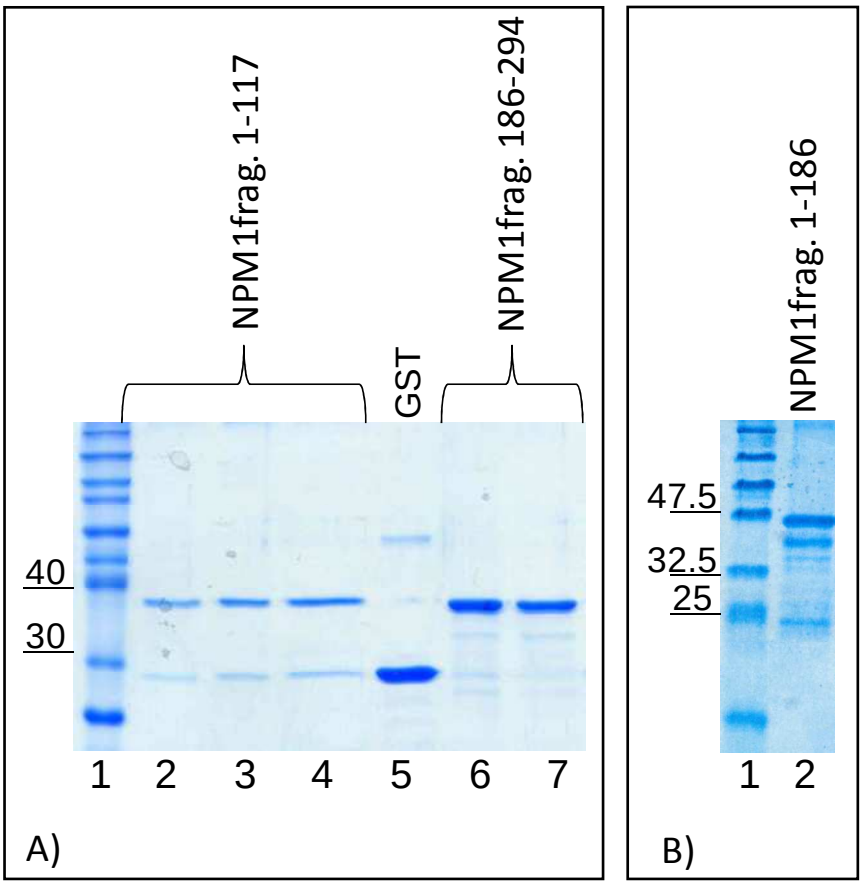

Figure 21. Purification of recombinant wild type NPM1 fragments. A) *Colloidal Blue stained 12% SDS-PAGE gel loaded with 500 ng-1 µg of the purified recombinant NPM1 fragment 1-117 fused to GST (lanes 2-4), 5 µg of the GST protein (lane 5) and 2-3 µg of the NPM1 fragment 186-294 fused to GST (lanes 6-7). Protein molecular weight (lane 1) is indicated in KDa (Novex® Sharp Protein Standard, Invitrogen).* ***B)*** *Colloidal Blue stained 12% SDS-PAGE gel loaded with 3 µg of the purified recombinant NPM1 fragment 1-186 fused to GST (lane 2). Protein molecular weight (lane 1) is indicated in KDa (Prestained Protein Marker, Cell Signaling)*

2. Selection of phage displayed VHHs, production and epitope mapping

I recovered a first panel of antibodies from a llama naïve phage display library created in our laboratory (Cogentech 1, [56]). In the framework of the library validation, I used the soluble purified recombinant NPMc+-GST full length protein as target for the isolation of specific binders. Panning procedure was optimized introducing a pre-panning step, in order to eliminate binders that specifically recognized the GST tag fused to the target protein. Three rounds of selection and amplification were carried out and, after the third one, periplasmic extracts recovered from 96 induced single colonies expressing HA-tagged VHHs, were tested by ELISA on the recombinant NPMc+-GST and GST proteins (Figure 22A and B). 33 clones specifically recognizing only the target antigen (the percentage of positive binders on the total binders screened was 34%), were obtained; the number of diverse VHHs selected was successively determined by DNA sequencing and resulted in five different clones. Protein sequences, aligned using the AlignX software program (VectorNTI Advance 9, Invitrogen), are reported in Figure 22C. In order to check if the selected antibodies specifically recognized the C-terminal epitope of the NPMc+ protein, I performed an epitope mapping by ELISA test using the bacterial periplasmic extracts of the five positive VHHs. A first ELISA test on the purified NPMc+-GST and wild type NPM1-GST full length proteins showed that the binders gave positive signals on both proteins, indicating that the binders recognized common epitopes. A second ELISA test carried out on the three NPM1 fragments (1-117, 1-186 and 186-294 fused to GST) that covered the entire wild type NPM1 sequence, revealed that the VHH clones bound to the N-terminal portion of nucleophosmin (Figure 23A). In particular, the mapped minimal interaction region corresponded to the first 117 amino acids (Figure 23B).

NPMc+-GST

0.930	0.620	0.010	0.000	0.490	0.030	0.780	0.750	0.780	0.760	0.420	0.530
0.640	0.000	0.860	0.000	0.880	0.890	0.640	0.050	0.440	0.810	0.580	0.710
0.670	0.000	0.660	0.020	0.450	0.520	0.880	0,020	0.000	0.000	0.690	0.030
0.080	0.790	0.720	0.930	0.700	-0.020	0.780	0.590	0.620	0.000	0.620	0.150
0.020	0.680	0.760	0.980	0.000	0.000	0.520	0.970	0.000	0.000	0.000	0.770
0.060	0.730	0.660	0.360	0.000	0.840	0.000	-0.010	0.120	0.830	0.620	0.460
0.500	0.000	0.790	0.720	0.840	0.950	0.830	0.730	-0.010	0.000	0.010	0.000
0.510	0.020	0.790	0.000	0.660	0.830	0.670	0.090	0.500	0.600	0.070	0.040

A)

GST

0.030	0.760	0.000	0.000	0.010	0.000	0.170	0.060	0.100	0.130	0.000	0.280
0.650	0.020	0.000	-0.010	0.300	0.410	0.420	0.010	0.180	0.000	0.000	0.360
1.010	0.010	0.370	0.000	0.110	0.000	0.370	-0.010	0.000	0.000	0.000	-0.010
0.020	0.450	0.000	0.440	0.000	0.000	0.210	0.390	0.160	0.000	0.390	-0.020
0.030	0.350	0.290	0.190	0.000	0.010	0.300	0.370	0.000	0.000	0.000	0.020
0.790	0.460	0.540	0.040	0.010	0.010	-0.010	0.010	0.010	0.000	0.460	0.200
0.790	0.010	0.000	0.000	0.220	0.070	0.170	0.010	0.000	-0.010	0.000	0.000
0.810	0.050	0.000	0.020	0.000	0.480	0.340	0.020	0.020	0.520	0.010	0.120

B)

```
                                                                                                                                        CDR3
CLONE 21A   MADVQLQASGGGLVQPGGSLRLSCAAS GFTFSIYT MSWVRQAPGKGLEWVSI INSSGGTT RYADSVKGRFTISRDNAKNTLYLHMNSLKPEDTAVYYC KIGRPNEN—-G-----L QGQGT QVTVSSGRYPYDVPDYGSGRA*
CLONE 210F  MADVQLQASGGGLVQAGGSLRLSCAAS GRTFSSYT MGWFRQAPGEEREFVAA ISWSGGKT YYADSVKGRFTISRDNANNTVYLQMNSLKPEDTAVYYC AATKRGSGRFG---VDY WGQGT LVTVSSGRYPYDVPDYGSGRA*
CLONE 13B   MADVQLQASGGGLVQTGGSLRLSCAAS GSTFSINV MGWYRQTPGKERELVAS ITG-RGIT NYADSVRGRFTISRDNAKNTVYLQMNSLKPEDTAVYYC NADMSTTG-WGKSFYRF WGQGT QVTVSSGRYPYDVPDYGSGRA*
CLONE 17H   MAEVQLQASGGGLVQPGGSLRLSCAAS GSIFSINA MGWYRQAPGKQRELVAA ITS-GGST NYADSVKGRFTISRDNAKNTVYLQMNSLKPEDTAVYYC NAQLRVDHPPGYYEYNY WGQGT LVTVSSGRYPYDVPDYGSGRA*
CLONE 23H   MADVQLQASGGGLVKAGGSLRLSCAAS GSGGSINR MGWYRQAPGKQRELVAT ITG-GGST NYADSAKGRFTISRDNAKSTVYLQMNSLKPEDTAVYYC NADLSSGR-YG--TYRY WGQGT LVTVSSGRYPYDVPDYGSGRA*
```

C)

Figure 22. Selection, production and sequence analysis of phage displayed VHHs. A) *Absorbance values at 405 nm from the ELISA test performed on the recombinant NPMc+-GST protein, using bacterial periplasmic extracts containing VHHs selected after the third round of panning. Clones with an absorbance value higher than 0.25, and that recognized exclusively the recombinant protein and not the fusion tag, were considered positive and are colored in blue.* ***B)*** *Absorbance values at 405 nm from the ELISA test performed on the recombinant GST protein, using bacterial periplasmic extracts containing VHHs selected after the third round of panning; values corresponding to those also positive on the NPMc+-GST protein are colored in yellow.* ***C)*** *Protein sequence alignment of the selected five different VHH clones obtained using the AlignX software program (VectorNTI Advance 9, Invitrogen); dashes indicate gaps introduced in order to optimize sequence alignment. CDR3 residues are indicated (as determined by IMGT annotation [212], www.imgt.org), (*) indicates stop codons*

GST	1-117	1-186	186-294	BLANK	
0.058	1.032	0.381	0.063	0.051	clone 17H
0.057	0.912	0.512	0.069	0.051	clone 13B
0.082	0.745	0.330	0.086	0.051	clone210F
0.071	0.940	0.429	0.079	0.051	clone 21A
0.062	0.619	0.319	0.059	0.051	clone 23H

A)

GST	1-117	1-186	186-294	
-	+	+	-	clone 17H
-	+	+	-	clone 13B
-	+	+	-	clone 210F
-	+	+	-	clone 21A
-	+	+	-	clone 23H

B)

Figure 23. Epitope mapping of the selected VHHs by ELISA test. A) *Absorbance values at 405 nm from the ELISA test performed on the purified recombinant NPM1 fragments 1-117, 1-186, 186-294 fused to GST and on the purified recombinant GST protein, using bacterial periplasmic extracts containing the five selected VHH clones.* ***B)*** *Summary of the results obtained from the ELISA test in Figure 23A*

3. Generation, expression and purification of the recombinant NPMc+ fragment C-terminal

A recent finding showed that the NPMc+ C-terminal region lacks a secondary structure and this results in a completely unfolded domain [203]. The results obtained by panning the VHH library suggested me that the poorly structured NPMc+ C-terminal end, could represent an epitope scarcely recognizable by the peculiar extruding VHH paratope (Figure 24A). Therefore, I decided to address the problem by using the ETH2-Gold scFv library and perform a new selection of binders. scFv paratopes are constituted by two flexible variable domains, which preferentially recognize protruding and planar epitopes (Figure 24B). A peptide covering the last 45 amino acids of the NPMc+ protein (amino acids 255-298), where mutation A is located, was synthesized by PCR (Figure 25A) and expressed in bacteria as a fusion with the Maltose Binding Protein (MBP), a conventional stabilizing tag. The construct was purified by affinity chromatography (Figure 25B) and dialyzed against PBS. Protein purity was evaluated after having separated the protein sample in a pre-casted 12% NuPAGE® Novex® Bis-Tris Gel (Invitrogen), that allows for optimal band resolution (Figure 25C).

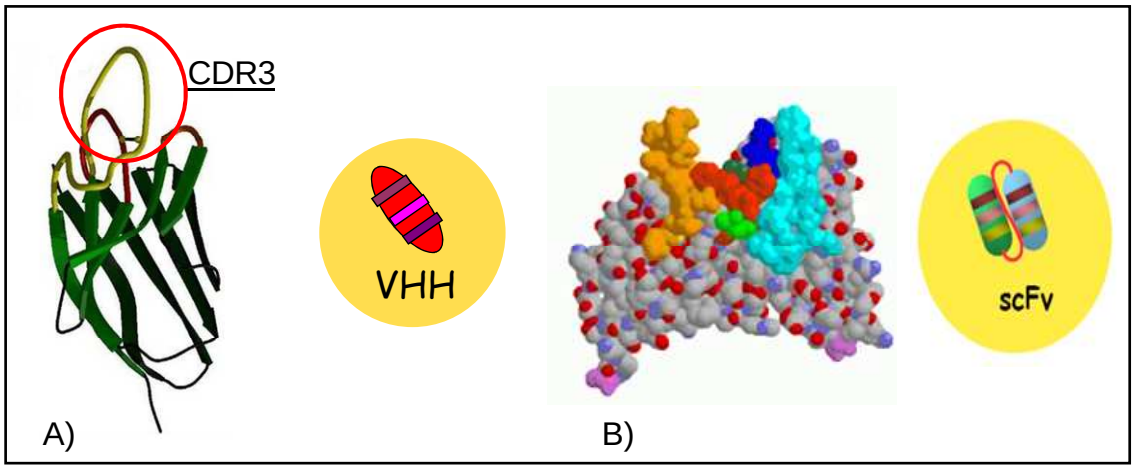

Figure 24. VHH and scFv antigen binding domains. A) *Tridimensional structure of a VHH antibody; the red circle indicates the extruding CDR3 domain (modified from [83]).* ***B)*** *Tridimensional structure of a scFv antibody (graphics from S. Dübel)*

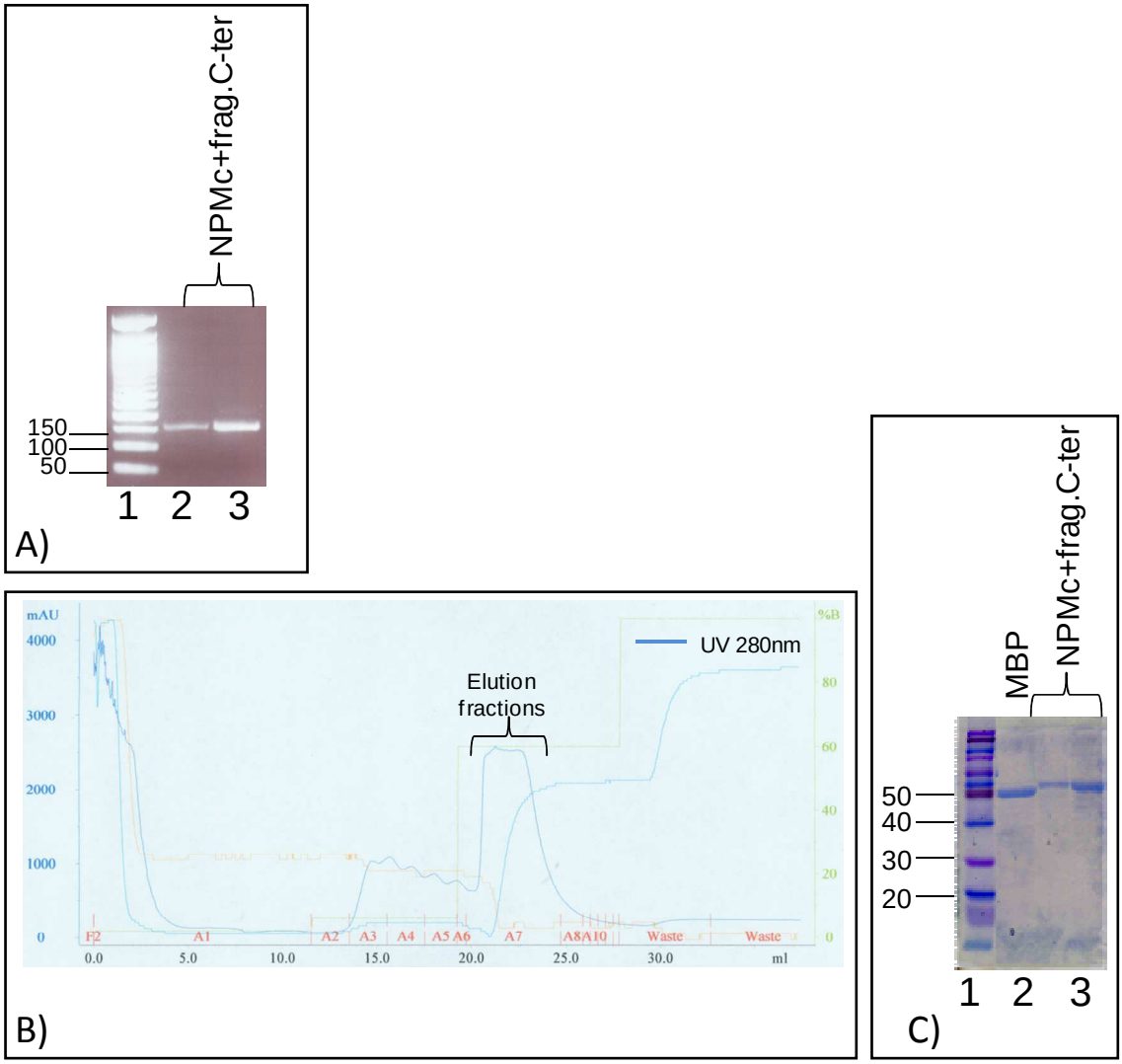

Figure 25. Generation, expression and purification of the recombinant NPMc+ fragment C-terminal. A) *50 ng (lane 2) - 100 ng (lane 3) of PCR product corresponding to the 5'-term NPMc+ fragment separated by electrophoresis on a 1% agarose gel. DNA molecular weight was determined by running, in parallel with the samples, a 50 base pairs DNA ladder (lane1, NEB).* ***B)*** *Affinity purification chromatogram of the recombinant NPMc+ fragment fused at the C-terminal of the MBP tag. The elution peak is indicated by a blue line (UV absorbance at 280 nm).* ***C)*** *Colloidal Blue stained 12% NuPAGE® Novex® Bis-Tris Gel loaded with 5 µg of the purified recombinant MBP protein (lane 1) and 1-5 µg of NPMc+ fragment C-terminal-MBP (lane 2-3). Protein molecular weight (lane 1) is indicated in KDa (Novex® Sharp Protein Standard, Invitrogen)*

4. Selection of phage displayed scFvs, production and purification

Three rounds of panning using the ETH2-Gold library against the NPMc+ fragment C-terminal were performed at high-stringency conditions, after a pre-panning step carried out against the fused tag (MBP). This procedure caused an almost complete depletion of the aspecific phages that recognized only MBP. Supernatants containing soluble recombinant Myc-tagged scFvs produced from 96 induced single colonies, were tested by ELISA on the recombinant NPMc+ fragment C-terminal in parallel with the MBP protein (Figure 26A and B). Six clones specifically recognized the target antigen and DNA sequencing indicated that all the six clones shared the same sequence, suggesting a high selective pressure toward this specific binder (Figure 26C). The scFv selected (thereafter indicated as scFv-MutMyc) was then produced in large scale and purified from culture supernatant by affinity chromatography. Protein purity was evaluated by separating the sample on a 12% SDS-PAGE gel stained with colloidal blue (Instant Blue, Novexin; Figure 27A). The identification of the band corresponding to the scFv was verified by western immuno-blot analysis using an antibody specific for the Myc tag (Figure 27B).

NPMc+ fragment											
0.179	0.249	0.246	0.421	0.417	0.352	0.252	0.314	0.429	0.490	0.448	0.320
0.120	0.467	0.490	0.291	0.504	0.341	0.394	0.631	0.279	0.414	0.329	0.329
0.141	0.190	0.227	0.245	0.425	0.259	0.430	0.471	0.484	0.456	0.449	0.290
0.100	0.292	0.290	0.668	0.365	0.342	0.301	0.456	0.366	0.378	0.454	0.326
0.161	0.095	0.353	0.499	0.254	0.131	0.339	0.348	0.381	0.205	0.349	0.366
0.101	0.318	0.329	0.342	0.301	0.338	0.369	0.387	0.472	0.401	0.328	0.344
0.079	0.364	0.283	0.349	0.310	0.348	0.323	0.321	0.365	0.310	0.329	-0.025
0.226	0.210	0.278	0.284	0.334	0.404	0.300	0.461	0.471	0.350	0.311	0.000

A)

MBP											
-0.047	-0.040	-0.040	-0.036	-0.035	-0.047	-0.038	0.100	-0.029	-0.029	-0.029	-0.033
-0.045	-0.039	-0.039	-0.044	-0.028	-0.036	-0.042	-0.035	-0.034	-0.034	-0.034	-0.040
-0.035	-0.036	0.013	-0.041	-0.035	-0.036	-0.028	-0.011	-0.032	-0.035	-0.032	-0.029
-0.041	-0.039	-0.026	-0.022	-0.032	-0.018	-0.032	-0.020	-0.035	-0.032	-0.032	-0.033
-0.034	0.018	-0.026	-0.031	-0.029	0.013	-0.030	0.145	-0.029	0.031	-0.012	-0.022
-0.033	-0.030	-0.029	-0.025	-0.018	-0.020	-0.013	-0.014	-0.022	-0.008	-0.017	-0.014
-0.045	-0.022	-0.033	-0.036	-0.036	-0.034	-0.032	0.090	-0.030	-0.028	-0.017	-0.037
-0.023	-0.014	-0.015	-0.018	-0.015	-0.011	0.065	-0.014	-0.013	0.087	0.003	0.000

B)

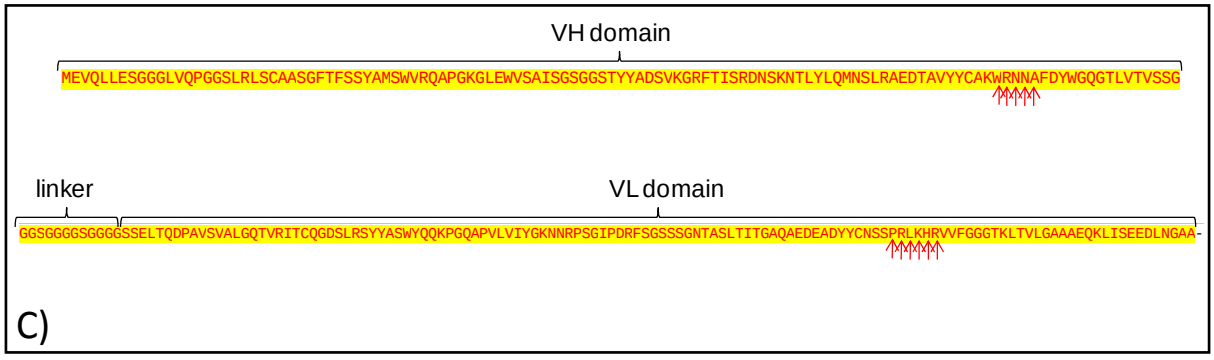

Figure 26. Selection, production and sequence analysis of phage displayed scFvs. A) *Absorbance values at 405 nm from the ELISA test performed using coated NPMc+-MBP fusion fragment and bacterial supernatants produced by clones expressing scFvs selected after three rounds of panning. Clones with an absorbance value higher than 0.49, and that recognized the recombinant protein but not the fusion tag, were considered positive and are colored in blue.* ***B)*** *Absorbance values at 405 nm from the ELISA test performed using coated MBP protein and bacterial supernatants produced by clones expressing scFvs selected after three rounds of panning. The wells corresponding to those positive for the fusion protein are colored in yellow.* ***C)*** *Sequence of the VH and VL domains of the selected scFv-Mut antibody; red arrows indicate VH and VL CDR3 amino acid residues subjected to random mutations during library construction [16].*

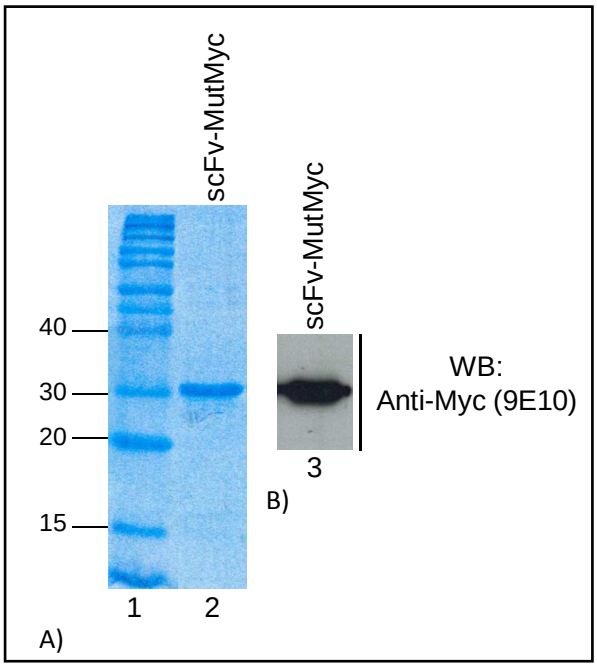

Figure 27. Purification of the selected scFv-MutMyc. A) *Colloidal Blue stained 12% SDS-PAGE gel loaded with 3 µg of purified recombinant scFv-MutMyc (lane 2). Protein molecular weight (lane 1) is indicated in KDa (Novex® Sharp Protein Standard, Invitrogen).* ***B)*** *Western immuno-blot analysis on purified recombinant scFv-MutMyc (lane 3) was performed using 9E10 mouse anti-Myc antibody (5 µg/mL)*

5. In vitro biochemical characterization of the scFv-MutMyc antibody selected against the NPMc+ fragment C-terminal

After the expression and purification of the anti-NPMc+ scFv-MutMyc, I began its functional characterization *in vitro*. In particular, I wished to confirm that scFv-MutMyc could univocally recognize the mutated region specific of NPMc+. To address this question, I performed different analyses: i) western immuno-blot analysis on purified recombinant NPMc+-GST and on NPMc+ fragment C-terminal; ii) western immuno-blot analysis on insect cell lysates overexpressing wild type NPM1 and NPMc+; iii) immunoprecipitation assay on transiently transfected HeLa cells overexpressing NPMc+; iv) immunoprecipitation assay on AML patients' cell lines that express endogenous NPMc+; v) immunofluorescence analysis on transiently transfected HeLa cells overexpressing NPMc+.

5.1 Western immuno-blot analysis

The western immuno-blot analysis was performed on both affinity purified recombinant proteins and insect cell lysates expressing either NPMc+ or wild type NPM1. As shown in Figure 28A, the scFv-MutMyc antibody specifically recognized only the mutated NPMc+, without reacting with the wild type NPM1 protein, neither with the purified recombinant MBP and GST tags nor an endogenous insect cell lysate, used as negative control. As a further control, two immuno-blot analyses were performed on wild type NPM1 and NPMc+ insect cell lysates, using either a mouse monoclonal antibody specific for the wild type NPM1 C-terminal end (Figure 28B) or a mouse monoclonal antibody that recognizes the N-terminal portion common to both proteins (Figure 28C, both antibodies are home-made).

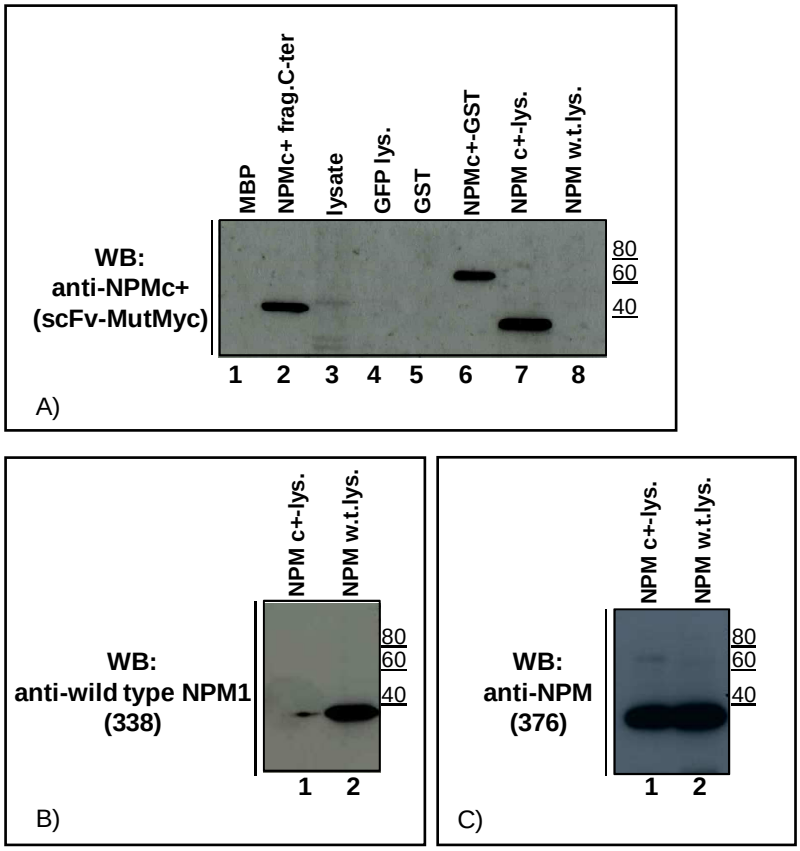

Figure 28. Western immuno-blot analysis on purified recombinant proteins and on insect cell lysates. A) *1 µg of NPMc+-GST and C-terminal NPMc+ fragment (lanes 6 and 2) were run on a 12% SDS-PAGE gel in parallel with 50 µg of insect cell lysates overexpressing NPMc+ (lane 7), wild-type NPM1 (lane 8) and GFP (lane 4). The membrane was incubated with scFvMut-Myc supernatant diluted 1:3 together with the mouse anti-Myc antibody 9E10 (5 µg/mL) that recognizes the Myc tag fused to the scFv. 1 µg of GST (lane 5) and MBP (lane 1) and 50 µg of an irrelevant insect cell lysate (lane 3) were used as controls.* ***B)*** *50 µg of insect cell lysates overexpressing either NPMc+ (lane 1) or wild type NPM1 (lane 2) were run on a 12% SDS-PAGE gel. The membrane was incubated with a mouse monoclonal antibody supernatant specific for the C-terminal end of the wild type NPM1 (clone 338, diluted 1:5).* ***C)*** *50 µg of insect cell lysates overexpressing NPMc+ (lane 1) and wild type NPM1 (lane 2) were run on a 12% SDS-PAGE gel. The membrane was incubated with a mouse monoclonal antibody specific for the N-terminal region of NPM, which is common to NPMc+ and wild type NPM1 proteins (clone 376, diluted 1:10)*

5.2 Immunoprecipitation and immunofluorescence assays

In order to understand wether the scFv-MutMyc antibody was able to bind the native protein expressed in mammalian cells, I performed immunoprecipitation experiments using cellular lysates obtained from HeLa cells transiently transfected with a plasmid (pEGFP-C1, Clontech) expressing the NPMc+-GFP fusion protein. As shown in Figure 29A (lanes 3 and 6), scFv-MutMyc immunoprecipitated NPMc+ with the same efficiency as the home-made anti-NPMc+ mouse monoclonal antibody used as control (clone T26, [213]); a band was visible, which ran at lower molecular weight than the NPMc+-GFP, indicating the presence of a protein degradation product. Similar results were observed using cell lysates obtained from HeLa cells transiently transfected with a plasmid (pcDNA5/FRT/TO, Invitrogen) expressing not tagged NPMc+ (Figure 29B). I then asked if our antibody could also recognize the endogenous NPMc+ and I performed an immunoprecipitation assay on cell lines derived from AML patients and either expressing (OCI-AML3) or not expressing (OCI-AML2) the NPMc+ allele [214]. As shown in Figure 30, the endogenous mutated NPMc+ present in the OCI-AML3 cell line was specifically immunoprecipitated by scFv-MutMyc. For unknown reasons, the binding efficiency was not as elevated as in the case of the overexpressed NPMc+-GFP and NPMc+ proteins. Immunofluorescence experiments were then performed on HeLa cells transiently transfected with a NPMc+-FlagHA expression vector. As shown in Figure 31A, the scFv-MutMyc antibody specifically recognized NPMc+ in the cytoplasm. The signal was similar to the one I obtained in the same cells with the mouse monoclonal antibody T26 used as control. The two antibodies did not give any aspecific signal on not transfected Hela cells (Figure 31B). As expected, immunofluorescence on HeLa cells transiently expressing NPMc+-GFP showed overlapping of the GFP signal with that of scFv-MutMyc in the cell cytoplasm (Figure 32A). The mouse monoclonal antibody T26 was used as control. As shown in Figure 32B,

the two antibodies did not give any aspecific signal on HeLa cells transiently expressing wild type NPM1-GFP protein (that localized in the nucleoli). Moreover, the scFv-MutMyc did not aspecifically recognize the EGFP protein, which showed a diffused staining in transiently expressing HeLa cells (Figure 32C).

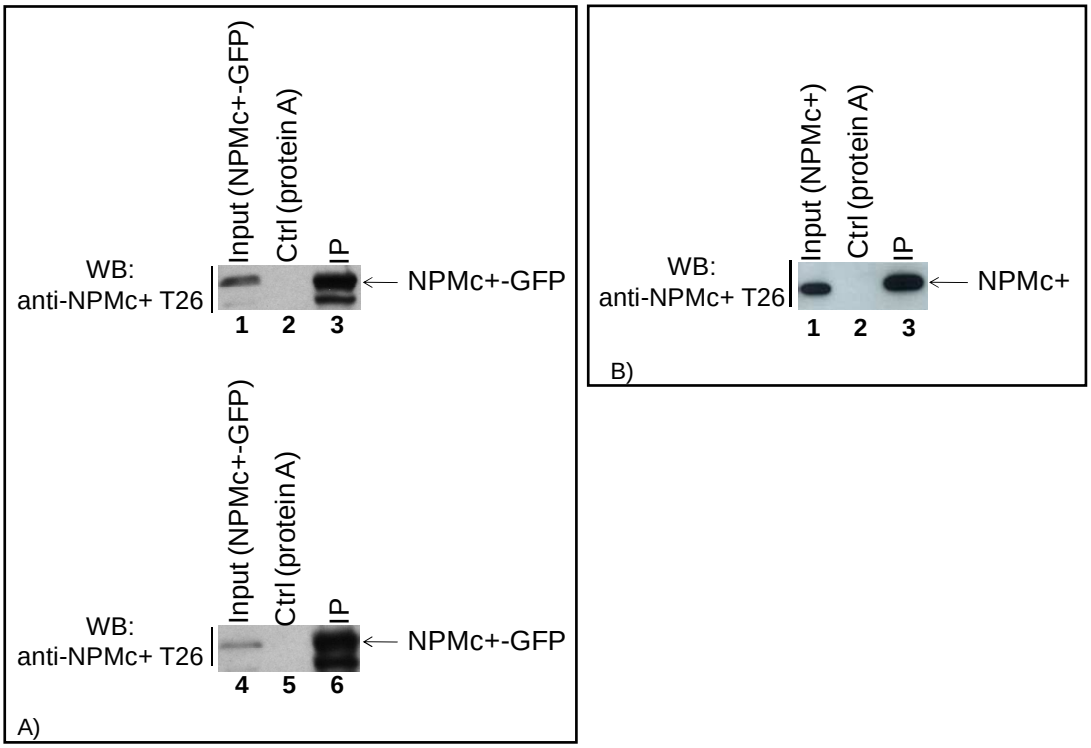

Figure 29. scFv-MutMyc immunoprecipitates the transiently transfected NPMc+ protein. A) *100 µg of immunoprecipitated HeLa cell lysate transiently expressing NPMc+-GFP was run on a 10% SDS-PAGE gel (lanes 3 and 6). The experiment was performed in parallel with 10 µg of scFv-MutMyc (lanes 1-3) and 10 µg of anti-NPMc+ mouse monoclonal antibody T26 (lanes 4-6). Lanes 2 and 5: control experiment performed with protein A-sepharose (GE Healthcare). The input is 10% of the total immunoprecipitated lysate (lanes 1-4). Membranes were probed with the mouse monoclonal antibody T26, diluted 1:1000.* ***B)*** *100 µg of immunoprecipitated HeLa cell lysate transiently expressing not tagged NPMc+ was run on a 10% SDS-PAGE gel (lane 3). The experiment was performed with 10 µg of the scFv-MutMyc. Lane 2: control experiment performed with protein A-sepharose (GE Healthcare). The input is 10% of the total immunoprecipitated lysate (lane 1). Membranes were probed with the mouse monoclonal antibody T26, diluted 1:1000*

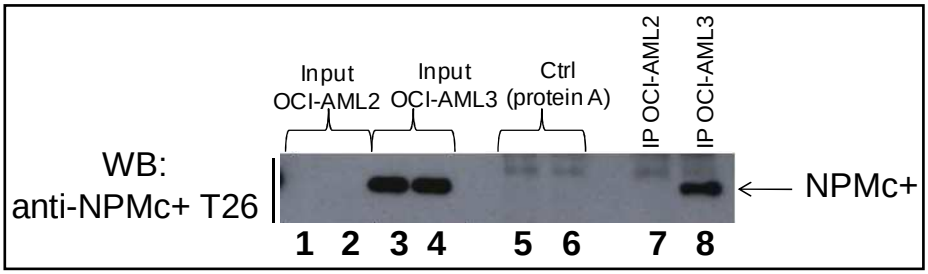

Figure 30. scFv-MutMyc immunoprecipitates the endogenous NPMc+ protein. *The immunoprecipitation performed with 10 µg of scFv-MutMyc on 300 µg of OCI-AML3 cell lysate expressing NPMc+ was run on a 10% SDS-PAGE gel (lane 8). A parallel experiment was performed on 300µg of OCI-AML2 cell lysate, which do not express NPMc+ (lane 7). Lanes 5-6: control experiment performed with protein A-sepharose (GE Healthcare) both on OCI-AML2 (lane 5) and OCI-AML3 cell lysate (lane 6). Inputs are 10% of the total immunoprecipitated lysates (lanes 1-2, OCI-AML2 cell lysate, and lanes 3-4, OCI-AML 3 cell lysate). The membrane was probed with the mouse monoclonal antibody T26 diluted 1:1000*

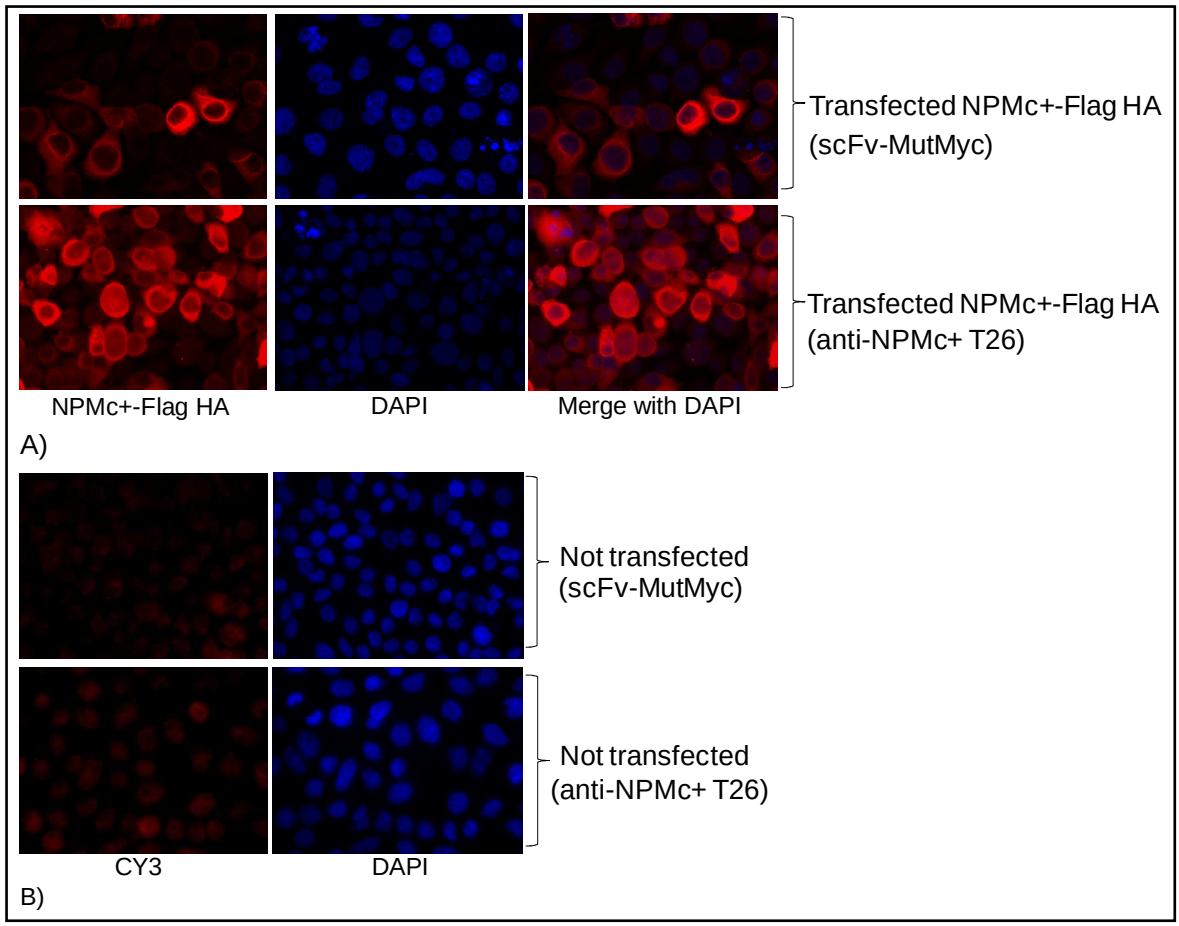

Figure 31. ScFv-MutMyc recognizes the NPMc+ protein in transiently transfected HeLa cells. ***A)*** *Immunofluorescence analysis on HeLa cells transiently expressing NPMc+-FlagHA was performed in parallel using purified scFv-MutMyc (2 µg/mL) detected with the mouse anti-Myc antibody 9E10 (2 µg/mL) or the mouse monoclonal antibody T26 diluted 1:100. Signals were detected by a cy3 conjugated anti-mouse secondary antibody.* ***B)*** *Immunofluorescence analysis on not transfected HeLa cells performed in parallel using purified scFv-MutMyc (2µg/mL) detected with the mouse anti-Myc antibody 9E10 (2 µg/mL) or the mouse monoclonal antibody T26 diluted 1:100. Signals were detected by a cy3 conjugated anti-mouse secondary antibody*

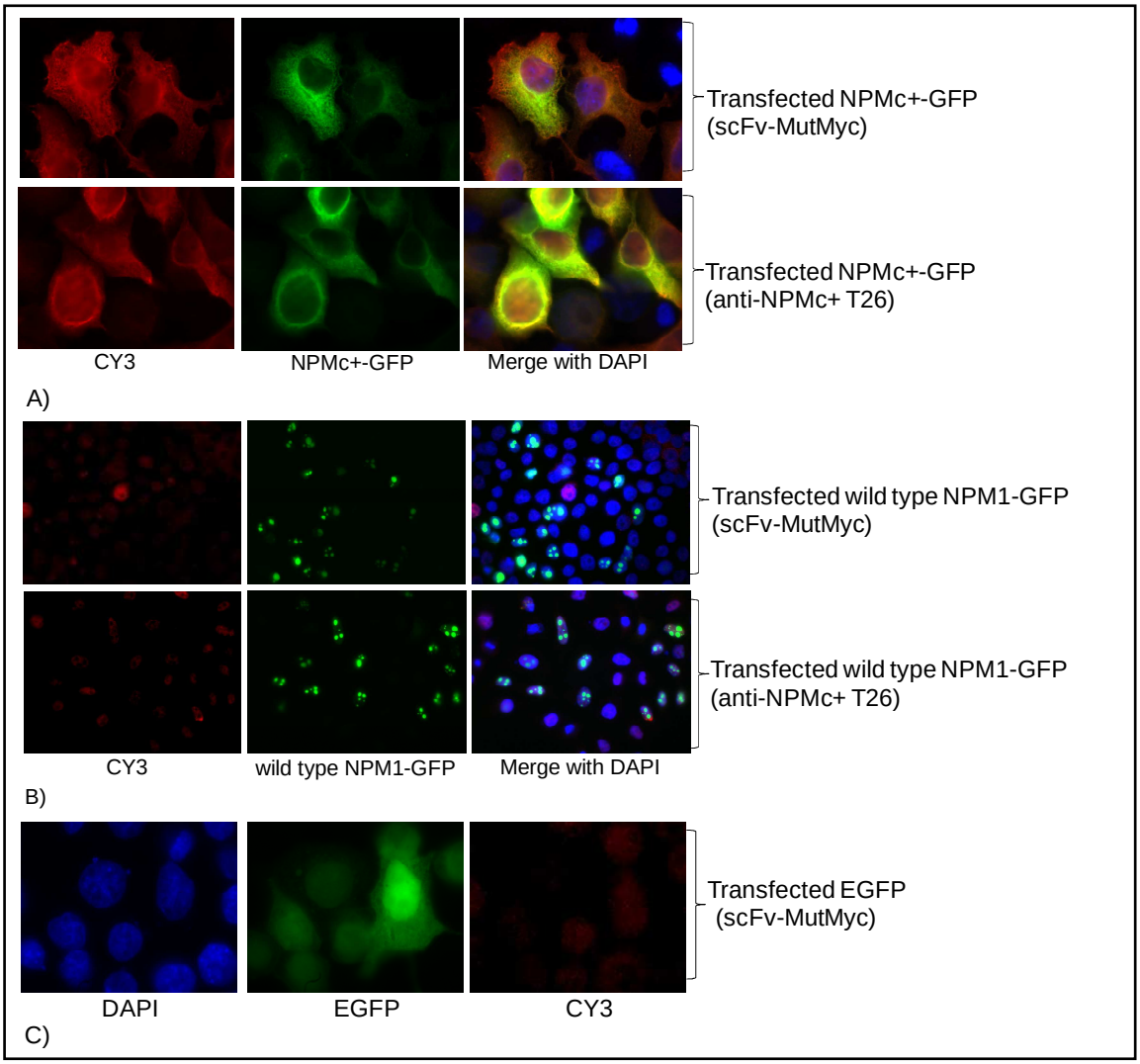

Figure 32. ScFv-MutMyc recognizes the NPMc+-GFP protein in transiently transfected HeLa cells. A) *Immunofluorescence analysis on HeLa cells transiently expressing NPMc+-GFP. The experiments were performed in parallel using purified scFv-MutMyc (2 µg/mL) detected with the mouse anti-Myc antibody 9E10 (2 µg/mL) or the mouse monoclonal antibody T26 diluted 1:100. Signals were detected by a cy3 conjugated anti-mouse secondary antibody.* ***B)*** *Immunofluorescence analysis on HeLa cells transiently expressing wild type NPM1-GFP. The experiments were performed in parallel using purified scFv-MutMyc (2 µg/mL) detected with the mouse anti-Myc antibody 9E10 (2 µg/mL) or the mouse monoclonal antibody T26 diluted 1:100. Signals were detected by a cy3 conjugated anti-mouse secondary antibody.* ***C)*** *Immunofluorescence analysis on HeLa cells transiently expressing EGFP. The experiment was performed using purified scFv-MutMyc (2 µg/mL) detected with mouse anti-Myc antibody 9E10 (2 µg /mL). Signals were detected by cy3 conjugated anti-mouse secondary antibody*

6. *In vivo* biochemical characterization of the scFv-Mut antibody selected against the NPMc+ fragment C-terminal

The *in vitro* biochemical characterization of scFv-MutMyc allowed us to conclude that the purified antibody recognized, specifically and efficiently, both the bacteria and insect cells derived recombinant NPMc+ protein. Furthermore, scFv-MutMyc bound to and immunoprecipitated NPMc+ as transiently expressed in Hela cells and as native protein present in a primary cell line derived from AML patients. Given these findings, I decided to try to express the scFv-Mut antibody directly inside the cells as an intrabody. Although this approach is very challenging due to the difficulties related to the cytoplasmic environment that is extremely unfavorable to the scFv-Mut proper folding, if successful, I reckoned I could obtain a cellular system where to study any biological effect related to the presence of the antibody *in vivo*.

6.1 Expression of the scFv-Mut as an intracellular antibody: immunofluorescence

The scFv cDNA was fused either with GFP or Flag tag in mammalian expression vectors. The antibody was efficiently produced in the intracellular environment of HeLa cells transiently transfected with the scFv-MutGFP expression plasmid. The cells showed a diffused staining and, in some cases, accumulation of the antibody in dense aggregates was visible (white arrows, Figure 33). This is compatible with the fact that the eukaryotic cell cytoplasm prevents the antibody from folding correctly and promotes its oligomerization. Moreover, the extremely crowded intracellular environment and an unfavorable redox potential contributes to the formation of detergent-insoluble aggregates [215, 216].

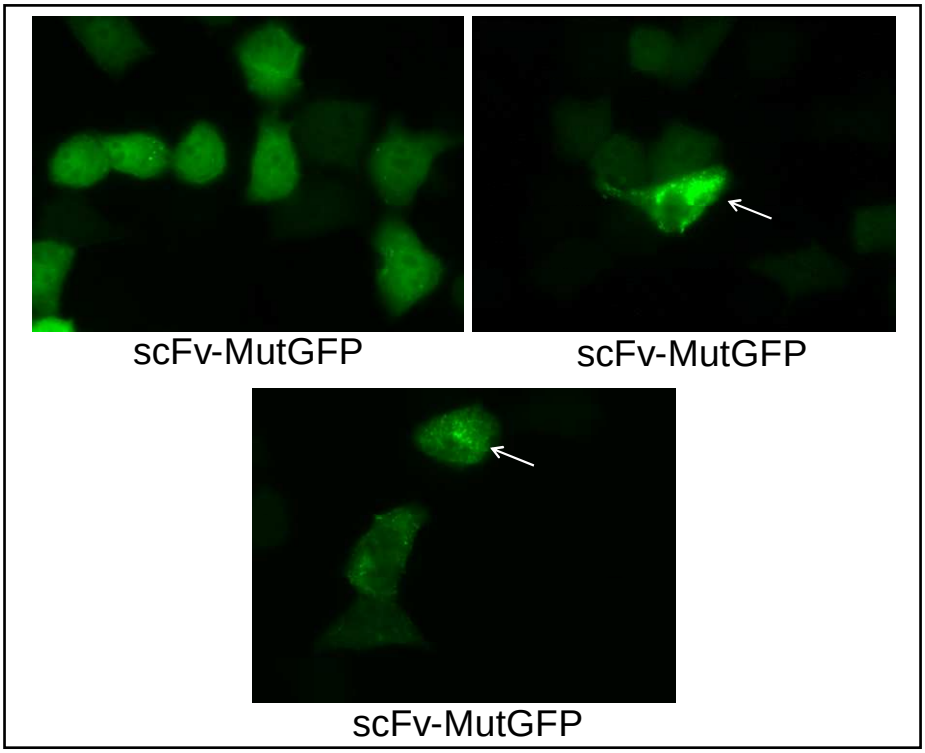

Figure 33. scFv-MutGFP expresses as an intracellular antibody in transiently transfected HeLa cells. *HeLa cells transiently transfected with the scFv-MutGFP expression vector*

Immunofluorescence on HeLa cells transiently co-transfected with both scFv-MutGFP and NPMc+ expression vectors showed that the two proteins localized in the same cell compartment (Figure 34, panel a). As shown in Figure 34 panel b, T26 antibody, specific for NPMc+ (Figure 34 panel c), did not recognize aspecifically scFv-MutGFP in transiently expressing Hela cells.

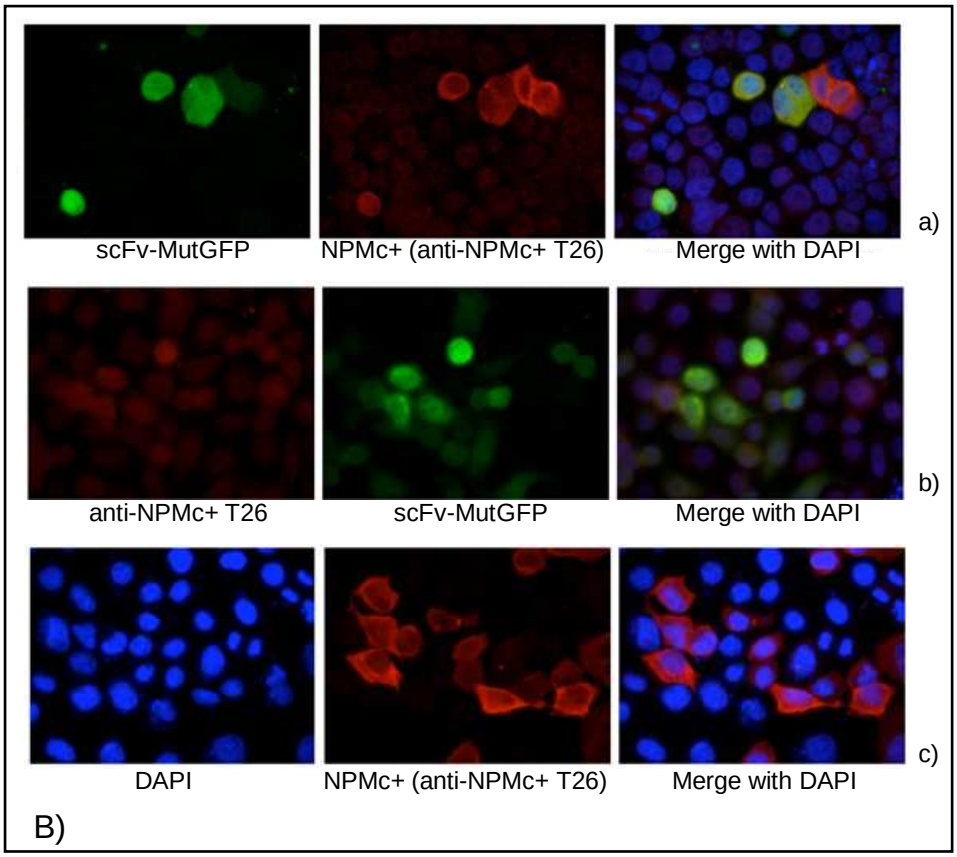

Figure 34. scFv-MutGFP and NPMc+ localize in the same cell compartment upon co-transfection in HeLa cells. Panel a) *Immunofluorescence on HeLa cells transiently co-transfected with scFv-MutGFP and NPMc+ expression vectors at a stoichiometric ratio of 1:1. The expression of NPMc+ was detected by the mouse monoclonal antibody T26, diluted 1:100. Signals were detected by an anti-mouse cy3 conjugated secondary antibody.* ***Panel b)*** *Immunofluorescence on HeLa cells transiently transfected with the scFv-MutGFP expression vector. Cells were stained with the mouse monoclonal antibody T26, diluted 1:100. Signals were detected by an anti-mouse cy3 conjugated secondary antibody.* ***Panel c)*** *Immunofluorescence on HeLa cells transiently transfected with NPMc+ detected by the mouse monoclonal antibody T26, diluted 1:100, followed by an anti-mouse cy3 conjugated secondary antibody*

6.2 Expression of the scFv-Mut as an intracellular antibody: co-immunoprecipitation assay

In order to investigate if the antibody was properly folded in the cells and it was able to recognize and bind NPMc+ in the cytoplasm, I conducted an immunoprecipitation experiment on lysates obtained from HeLa cells transiently co-transfected with scFv-MutFlag and NPMc+-GFP expression vectors. As shown in Figure 35A, the antibody was able to immunoprecipitate NPMc+-GFP, even though the binding efficiency was not elevated. The bands visible at a lower molecular weight than the immunoprecipitated NPMc+-GFP (lanes 5-8) corresponded to the immunoglobulins' heavy chains. As negative control, the same experiment was performed using unconjugated mouse IgG-agarose beads (Figure 35B); the bands corresponding to the immunoglobulins' heavy and light chains were visible (lanes 5-8). The results confirmed that, at least to some extent, scFv-MutFlag was functionally folded, and that the two proteins interacted in the intracellular milieu upon co-expression. Co-immunoprecipitation experiments performed on lysates obtained from HeLa cells transiently co-transfected with plasmids expressing scFv-MutFlag and wild type NPM1-GFP, and, in parallel, on anti-Flag M2 agarose beads (Figure 36A) and on mouse IgG-agarose beads (Figure 36B), further demonstrated that scFv-MutFlag bound specifically and exclusively to the mutant NPMc+ protein in the cells; the bands corresponding to the immunoglobulins' heavy and light chains were visible (lanes 4-6).

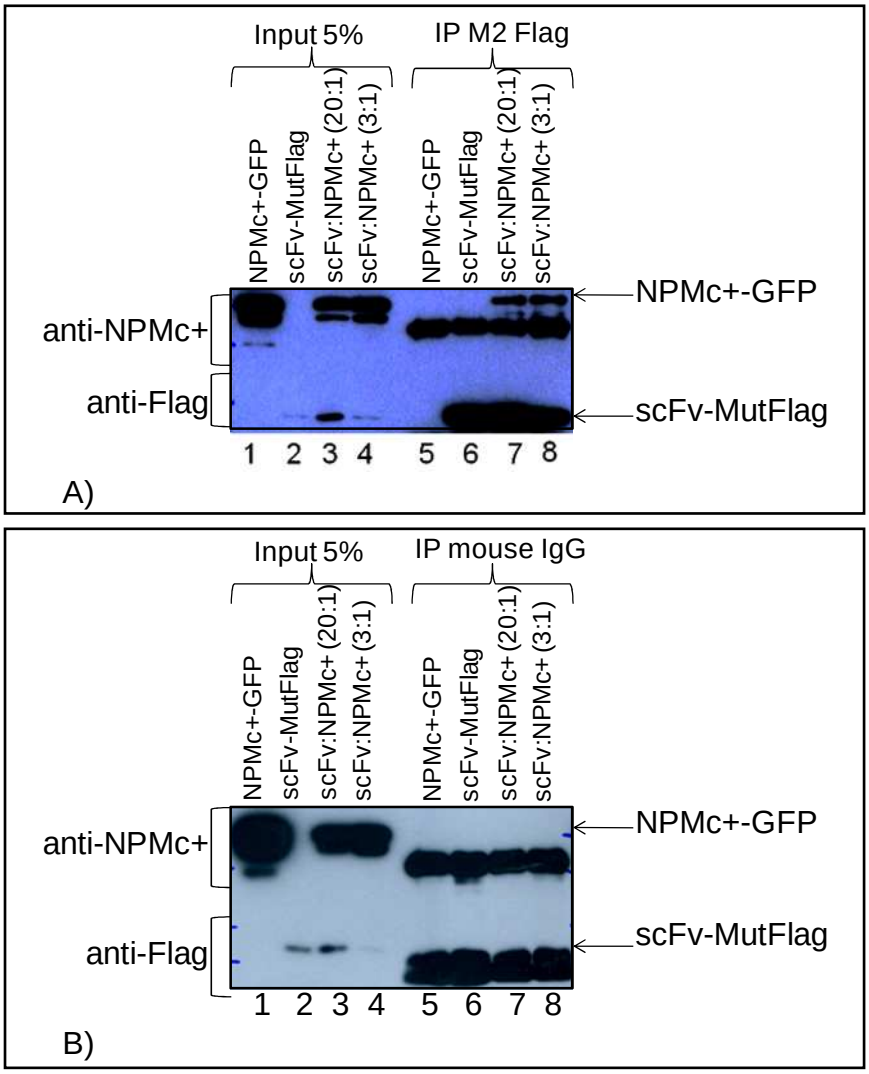

Figure 35. scFv-MutFlag co-immunoprecipitates with the NPMc+-GFP in transiently co-transfected HeLa cells. *Immunoprecipitation assay was performed using 400 µg of HeLa cell lysates transiently co-transfected with scFv-MutFlag and NPMc+-GFP expression vectors. The immunoprecipitated material was analyzed by western mmune-blotting. The experiment was performed using anti-Flag M2 agarose beads (Panel A) in parallel with mouse IgG-agarose beads as negative control (Panel B). Membranes were probed with the mouse monoclonal antibody T26, diluted 1:1000, and a mouse anti-Flag M2 antibody (diluted 1:6000, Sigma). Lanes 1-2: inputs of HeLa cells transiently transfected with NPMc+-GFP (lane 1) or scFv-MutFlag (lane 2). Lanes 3-4: inputs of HeLa cells transiently co-transfected with scFv-MutFlag and NPMc+-GFP at different stoichiometric ratios [lane 3, 20:1 (scFv-MutFlag : NPMc+-GFP); lane 4, 3:1 (scFv-MutFlag: NPMc+-GFP)]. Lanes 5-8: corresponding immunoprecipitations*

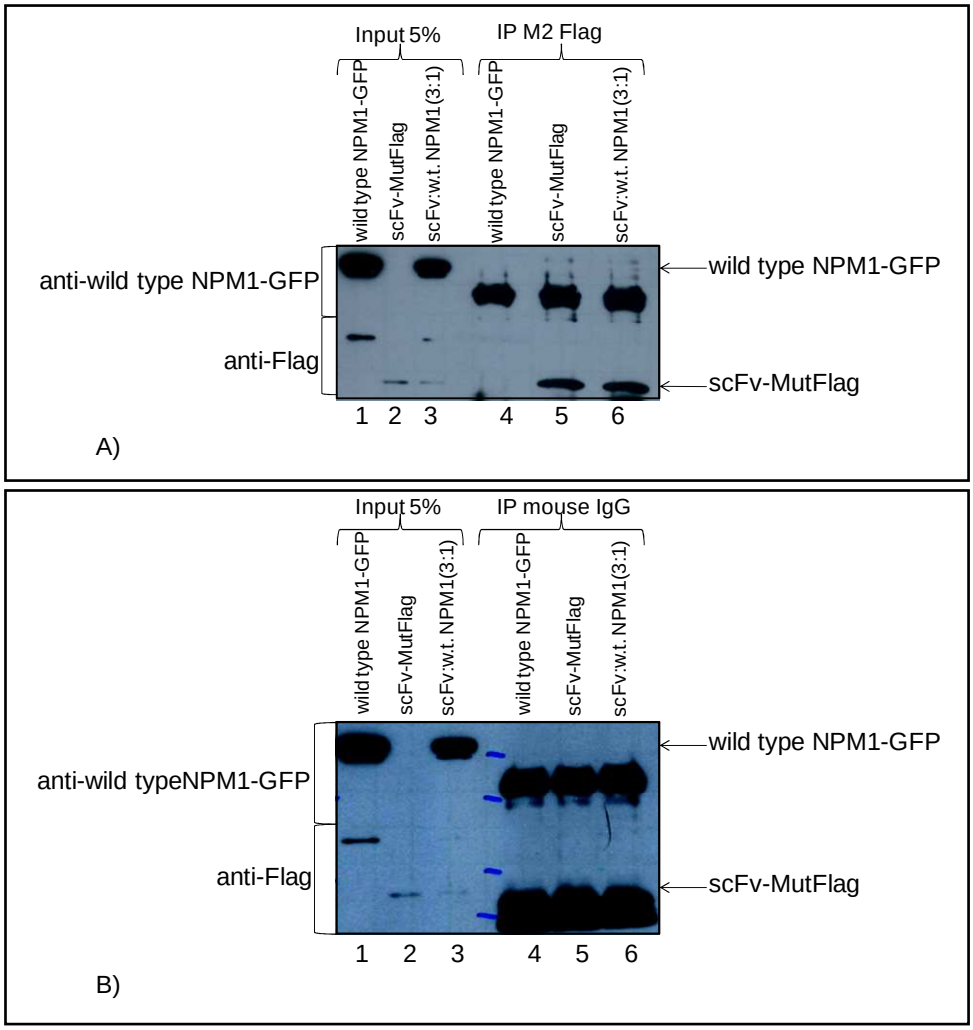

Figure 36. scFv-MutFlag does not co-immunoprecipitate with the wild type NPM1-GFP in transiently co-transfected HeLa cells. *Immunoprecipitation assay was performed using 400 µg of cell lysates from HeLa cells transiently co-transfected with scFv-MutFlag and wild type NPM1-GFP expression vectors. The immunoprecipitated material was analyzed by western mmune-blotting. The experiment was performed using anti-Flag M2 agarose beads (Panel A) in parallel with mouse IgG-agarose beads as negative control (Panel B). Membranes were probed with mouse monoclonal antibody anti-wild type NPM1, (diluted 1:1000, Zymed) and a mouse anti-Flag M2 antibody (diluted 1:6000, Sigma). Lanes 1-2: inputs of HeLa cells transiently transfected with wild type NPM1-GFP (lane 1) or scFv-MutFlag (lane 2). Lane 3: inputs of HeLa cells transiently co-transfected with scFv-MutFlag and wild type NPM1-GFP (at the stoichiometric ratio of 3:1). Lanes 4-6: corresponding immunoprecipitations*

7. Expression of scFv-Mut as an intracellular antibody fused to a nuclear localization signal (NLS)

Considering the capability of the intrabodies to interact with NPMc+, I then decided to explore the possibility to relocate NPMc+ to the nucleus by means of expressing the scFv-Mut intrabody fused to a nuclear localization signal [217, 218]. I subcloned the scFv cDNA fused to the simian virus (SV) 40 large T-antigen NLS [219] in tandem with the hemagglutinin epitope sequence (HA tag) in a mammalian expression vector. Immunofluorescence on HeLa cells transiently transfected with the plasmid expressing scFv-MutNLS showed a clear accumulation of the intrabody in the nucleus (Figure 37, panel a). However, when I conducted the same immunofluorescence experiment on HeLa cells transiently co-expressing both the scFv-MutNLS and NPMc+-GFP, I observed their almost complete co-localization in the cytoplasm (Figure 37, panel c), where NPMc+-GFP normally localizes (Figure 37, panel b), strongly suggesting that the majority of the antibody expressed in the cells was functional and efficiently bound to NPMc+. This observation could be explained by the strength of the additional NES present in the NPMc+: recent findings have demonstrated that such NES motif is more efficient in mediating nuclear export compared to other physiological NES [220]. The specificity of the binding between scFv-MutNLS and NPMc+ was further supported by immunofluorescence experiments performed on HeLa cells transiently co-expressing the antibody and wild type NPM1-GFP. As expected, scFv-MutNLS localized to the nucleus, but did not co-localize with the wild type NPM1-GFP nucleolar staining (Figure 37, panel d).

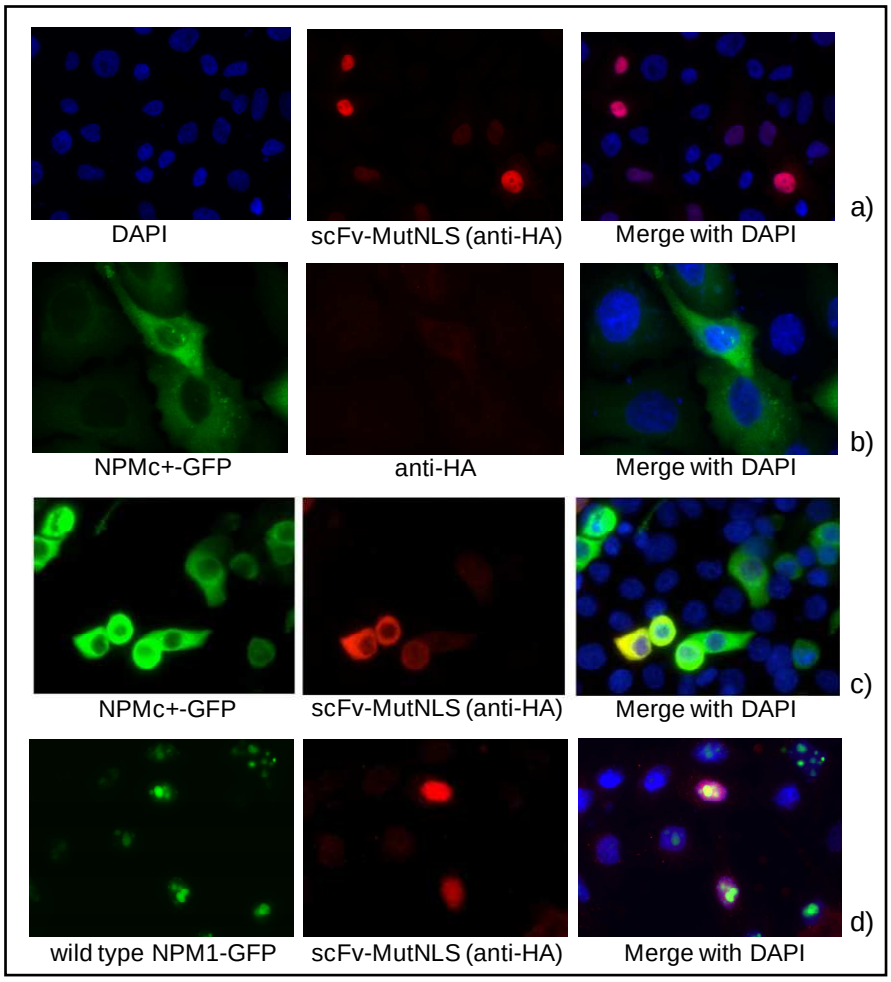

Figure 37. scFv-MutNLS co-localizes with NPMc+-GFP in the cytoplasm of transiently co-transfected HeLa cells. Panel a) *Immunofluorescence on HeLa cells transiently transfected with the scFv-MutNLS expression vector. Cells were stained with a mouse monoclonal antibody anti-HA (diluted 1:200, Covance), followed by an anti-mouse cy3 conjugated secondary antibody.* ***Panel b)*** *Immunofluorescence on HeLa cells transiently transfected with the NPMc+-GFP expression vector. Cells were stained with a mouse monoclonal antibody anti-HA (diluted 1:200, Covance), followed by an anti-mouse cy3 conjugated secondary antibody.* ***Panel c)*** *Immunofluorescence on HeLa cells transiently co-transfected with scFv-MutNLS and NPMc+-GFP expression vectors at a stoichiometric ratio of 1:1. The expression of scFv-MutNLS was detected by a mouse antibody anti-HA (diluted 1:200, Covance), followed by an anti-mouse cy3 conjugated secondary antibody.* ***Panel d)*** *Immunofluorescence on HeLa cells transiently co-transfected with scFv-MutNLS and wild type NPM1-GFP expression vectors at a stoichiometric ratio of 1:1. The expression of scFv-MutNLS was detected by a mouse antibody anti-HA (diluted 1:200, Covance), followed by an anti-mouse cy3 conjugated secondary antibody*

Finally, a mammalian vector expressing an unrelated scFv cDNA fused to a nuclear localization signal (NLS) in tandem with the hemagglutinin epitope (HA tag) was transiently transfected in HeLa cells. Immunofluorescence experiments showed that the antibody accumulated in the nucleus (Figure 38, panel a) and its localization remained unaltered also in the presence of NPMc+-GFP (Figure 38, panel b).

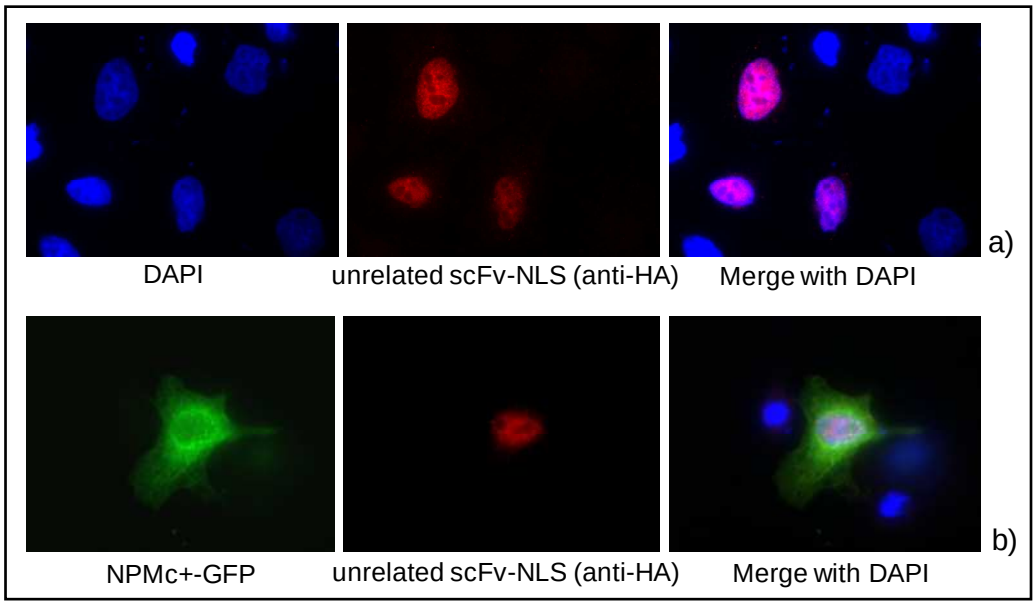

Figure 38. An unrelated scFv-NLS does not co-localize with NPMc+-GFP in the cytoplasm of transiently co-transfected Hela cells. Panel a) *Immunofluorescence on HeLa cells transiently transfected with an unrelated scFv-NLS expression vector. Cells were stained with a mouse monoclonal antibody anti-HA (diluted 1:200, Covance), followed by an anti-mouse cy3 conjugated secondary antibody.* ***Panel b)*** *Immunofluorescence on HeLa cells transiently co-transfected with an unrelated scFv-NLS and NPMc+-GFP expression vectors at a stoichiometric ratio of 1:1. The expression of scFv-NLS was detected by a mouse antibody anti-HA (diluted 1:200, Covance), followed by an anti-mouse cy3 conjugated secondary antibody*

Based on these data, I speculated that adding multiple NLS sequences to the scFv-Mut antibody could counteract the effects of the aberrant export signal that is present in the mutated NPMc+. I created a new cassette constituted by two NLSs at the N-terminus end and two NLSs plus an HA tag at the C-terminus end: between them, I inserted the scFv-Mut cDNA (scFv-Mut4xNLS, Figure 39, panel a). Immunofluorescence performed on HeLa cells transiently transfected with the plasmid expressing scFv-Mut4xNLS showed that it accumulated in the nucleus, as expected (Figure 39, panel b) and in some cases in the nucleolus as well (yellow arrows, Figure 39, panel c). This result might indicate that this antibody cross-reacted with wild type NPM1, which normally localizes in the nucleolus and interacts with NPMc+ through their homodimerization interface, contributing to its partial localization into the nucleus [201, 220]. In order to understand whether this was the case, I transiently expressed the antibody in Mouse Embryonic Fibroblasts (MEF) knockout for both NPM1 and p53 [11]. As shown in Figure 40, panels a-b, immunofluorescence on these cells confirmed the nucleolar staining, excluding the previous hypothesis. Then I tried to co-express the antibody and NPMc+ in HeLa cells in order to evaluate its ability to re-locate NPMc+ to the nucleus. Unfortunately, using transient transfection, I routinely obtained a very low efficiency of co-expression (Figure 42). Moreover, although the staining was mainly nuclear, when cells expressed only the scFv-Mut (Figure 39) and cytoplasmic, when cells expressed only the NPMc+ (Figure 41), in the rare co-transfected cells it was very heterogeneous both for localization and expression levels (Figure 42). In particular, in Figure 42 panel d, the scFv-Mut4xNLS (yellow arrows) was predominantly nuclear and only partially delocalized to the cytoplasm, where most of NPMc+-GFP (panel a, white arrows) localized. In Figure 42 panel b, NPMc+ partially localized in the nucleus (red and white arrows) also in the absence of the scFv-Mut4xNLS expression (panel e, red arrow) or when the scFv was partially delocalized to the cytoplasm (panel e, yellow arrow), maybe indicating that only

when the expression levels of the antibody were very high, it was possible to observe a partial re-localizing effect on NPMc+. In other cells, NPMc+-GFP was predominantly cytoplasmic (panel b, blue arrow and panel c, white arrow) even though the antibody was clearly nuclear (panel e, pink arrow and panel f, yellow arrow). In conclusion, these results made it difficult to understand whether the antibody had had any clear effect on NPMc+ localization. Further experiments are now in progress in order to obtain retrovirally infected AML cell lines (derived from patients and that express endogenous NPMc+) stably expressing the scFv-Mut4xNLS, to test whether it has any effect on NPMc+ cellular localization or whether it contributes to p19/Arf relocalization, by interfering with the binding between NPMc+ and p19/Arf. In both cases, it will be investigated whether the antibody has any direct influence on cell growth and viability.

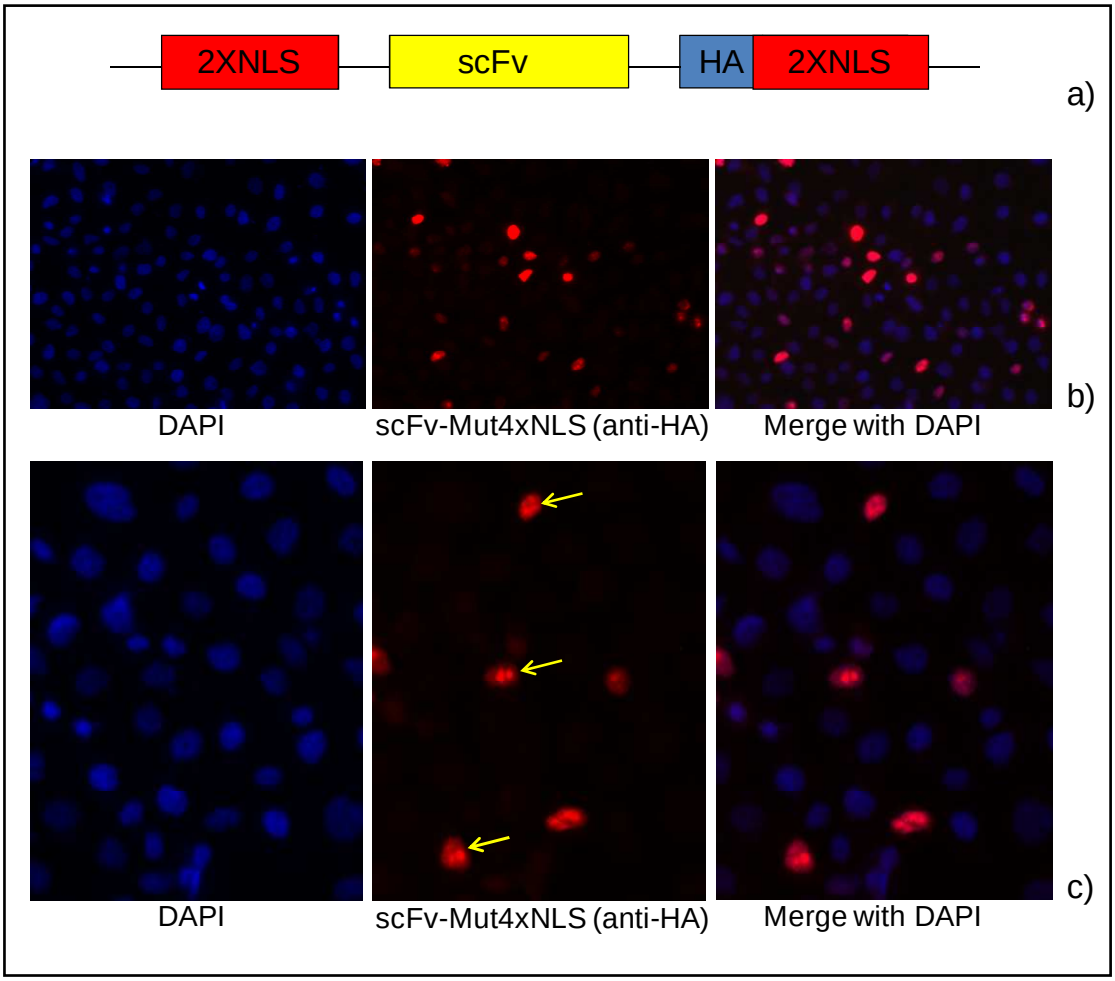

Figure 39. scFv-Mut4xNLS localizes to the nucleus in transiently transfected HeLa cells. ***Panel a)*** *Scheme of the cassette created for the expression of the scFv-Mut4xNLS.* ***Panel b) and Panel c)*** *Immunofluorescence on HeLa cells transiently transfected with the plasmid expressing scFv-Mut4xNLS. Cells were stained with a mouse monoclonal antibody anti-HA (diluted 1:200, Covance), followed by an anti-mouse cy3 conjugated secondary antibody. Yellow arrows indicate scFv-Mut4xNLS nucleolar staining*

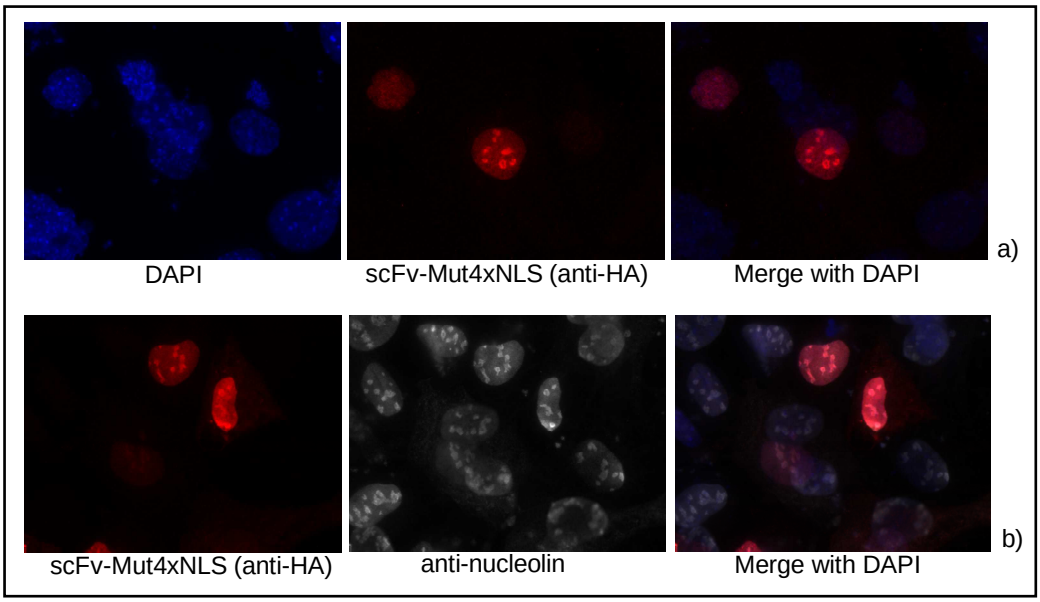

Figure 40. scFv-Mut4xNLS localizes to the nucleus and gives a distinctive nucleolar staining in MEFs NPM1$^{-/-}$p53$^{-/-}$. Panel a) *Immunofluorescence on MEFs NPM1$^{-/-}$p53$^{-/-}$ cells transiently transfected with the scFv-Mut4xNLS expression vector. Cells were stained with a mouse monoclonal antibody anti-HA (diluted 1:200, Covance), followed by an anti-mouse cy3 conjugated secondary antibody.* ***Panel b)*** *Immunofluorescence on MEFs NPM1$^{-/-}$p53$^{-/-}$ cells transiently transfected with scFv-Mut4xNLS expression vector. Antibody was detected by using a mouse monoclonal antibody anti-HA (diluted 1:200, Covance), followed by an anti-mouse cy3 conjugated secondary antibody. Nucleoli were stained with a rabbit anti-nucleolin antibody (diluted 1:800 Abcam), followed by an anti-rabbit cy5 conjugated secondary antibody*

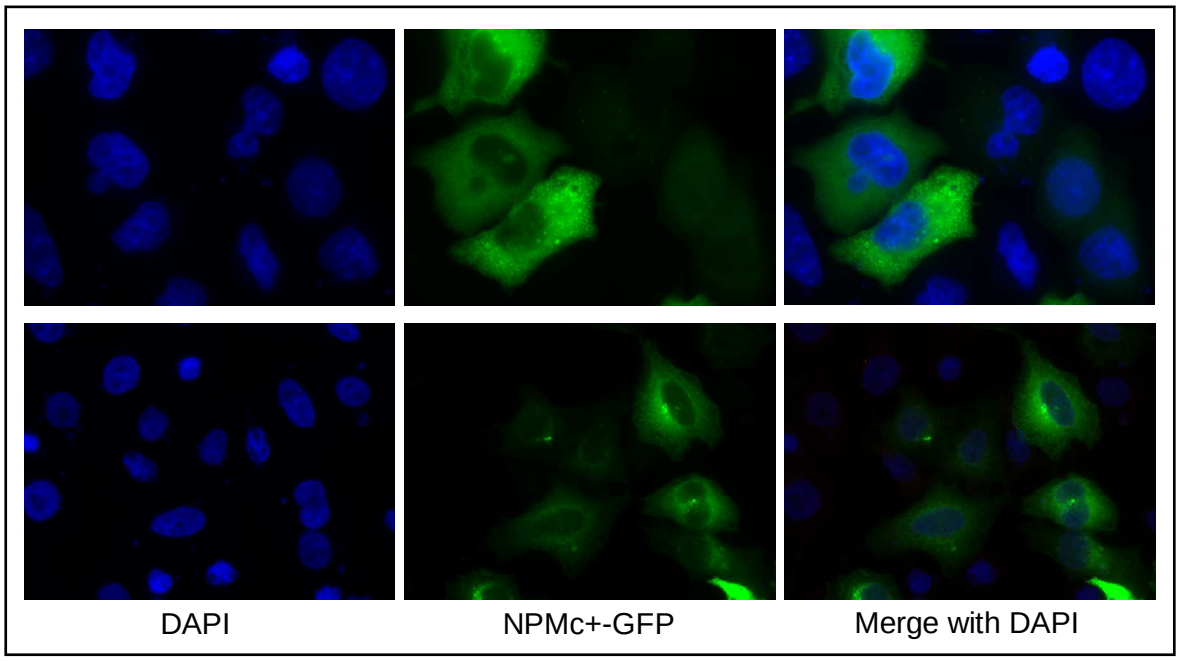

Figure 41. NPMc+-GFP localizes to the cytoplasm in transiently transfected HeLa cells. *Immunofluorescence on HeLa cells transiently transfected with the NPMc+-GFP expression vector.*

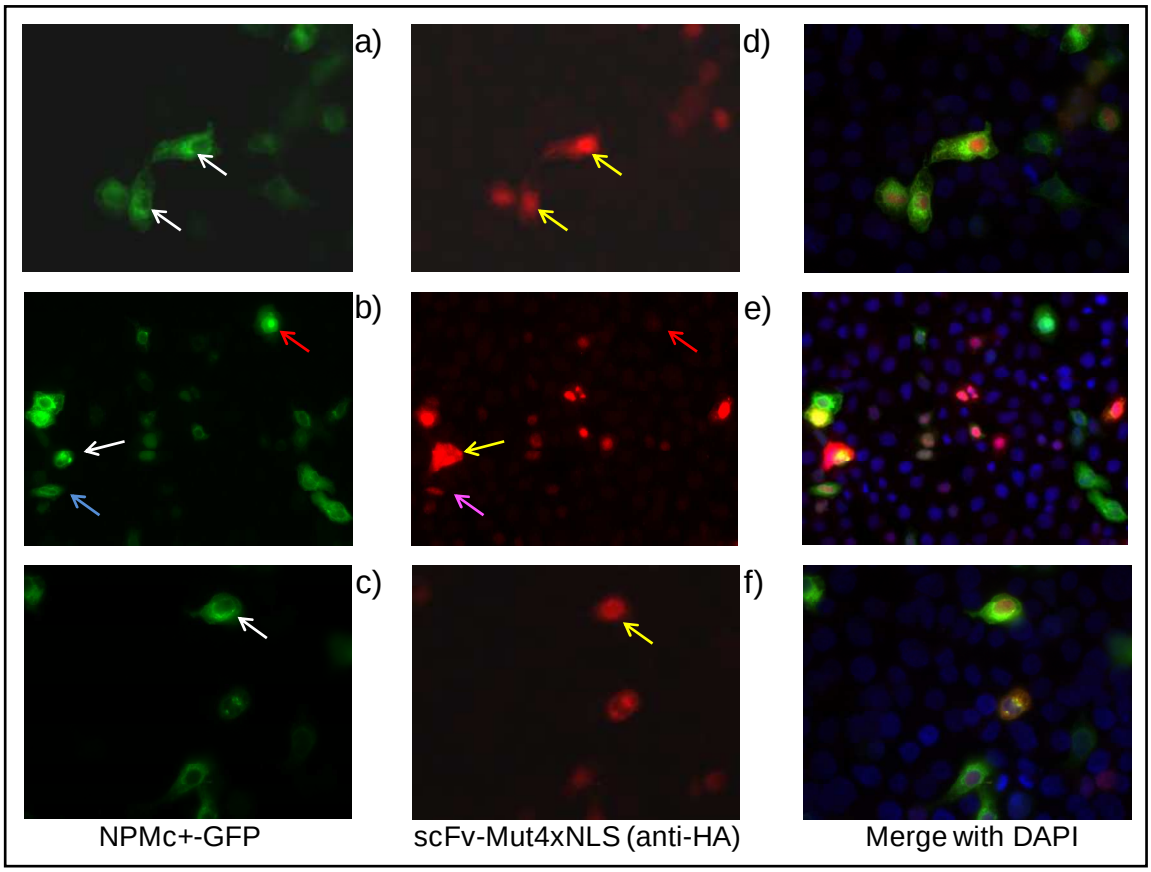

Figure 42. scFv-Mut4xNLS partially co-localizes with the NPMc+-GFP protein in transiently co-transfected HeLa cells. *Immunofluorescence on HeLa cells transiently co-transfected with NPMc+-GFP (**Panels a, b, c**) and scFv-Mut4xNLS (**Panels d, e, f**) expression vectors. The expression of scFv-Mut4xNLS was detected with a mouse antibody anti-HA (diluted 1:200, Covance), followed by an anti-mouse cy3 conjugated secondary antibody*

DISCUSSION

1. Mutated nucleophosmin (NPMc+) is a potential therapeutic target in AML

Mutation of *NPM1* has been demonstrated to be the most frequent genetic alteration present in adult AML patients with normal karyotype (about 35% of the cases, [11]). Different sequence variants have been observed, all characterized by a reading frameshift in the C-terminal portion of NPM1, that leads to the creation of a *de novo* nuclear export signal (NES, [185],[186]) and to the abnormal accumulation of the mutated protein in the cytoplasm. Mutation A (Figure 15) is the most recurrent and it is found in 75-80% of AML patients characterized by mutated *NPM1* (NPMc+, [200]). NPMc+ is responsible for the delocalization of proteins normally localized into the nucleolus thanks to their interaction with wild type NPM1. NPMc+ binds, delocalizes and inactivates the F-box protein Fbw7γ and the tumor suppressor p19/Arf [14, 15]. Based on these data, NPMc+ may be considered a *bona fide* onco-protein whose activity can initiate the tumorigenic program at least through two different, but strictly connected, pathways: 1. Delocalization and destabilization of Fbw7γ (a ubiquitin ligase involved in proteasome-dependent degradation of c-Myc), leading to c-Myc overexpression; 2. Delocalization and destabilization of p19/Arf, thus impairing its ability to activate p53 and induce cell cycle arrest in response to c-Myc overexpression. Even though other molecular mechanisms and biological effects derived by the altered expression of the mutated NPMc+ remain to be further elucidated *in vivo*, the available data strongly support the appealing idea that NPMc+ can be a good target for therapy. Considering that NPMc+ activity depends on the ability to export its intracellular interactors from the nucleus to the cytoplasm inducing their degradation, one option for intervention might be to target downstream of NPMc+, by mimicking p19/Arf activity and trying to reactivate p53. For this purpose, a new class of compounds called nutlins, which act as Mdm2 antagonists inhibiting Mdm2-p53 interaction, have been recently demonstrated to be effective as antitumor molecules both *in vitro* and *in vivo*

[221]. Nevertheless, this approach recovers only one specific NPMc+ function, which may be not the most important in determining tumor development. Moreover, the success of this strategy essentially relies on the functionality of the p53 pathway in human tumors, but the presence of a single cell clone with a new p53 mutation might be sufficient to induce the relapse of the disease. An alternative therapeutic strategy should consider blocking the NPMc+ degradation activity. In this regard, a new anticancer therapy, based on proteasome inhibitors, has been recently introduced [222]. In preclinical and clinical trials, the compound Bortezomib was shown to give significant results in several cancers [223, 224]. Moreover, there are reports of its effectiveness in the treatment of myeloproliferative disorders [225-228] and of anti-proliferative and pro-apoptotic [229-231] effects on human acute myeloid leukemia blasts. Interestingly, it has been shown that all the AML blasts carrying *FLT3* mutations (associated with NPMc+, [11]) are sensitive to Bortezomib, therefore this molecule may be considered a potential therapeutic agent in this type of leukemia. However, the administration of Bortezomib could only block the NPMc+-dependent degradation of p19/Arf and Fbw7γ, but not relocate them into the nucleus where they carry out their physiological functions. Therefore, a better strategy is to directly target the whole NPMc+ molecule with the aim to interfere with its pathological activities i) by re-localizing it to the nucleus, or ii) by preventing NPMc+ binding to its interactors. For this purpose, highly specific molecules able of univocally target NPMc+ in the cells, are necessary. Indeed, one major problem is the high similarity between wild type NPM1 and NPMc+ proteins: they differ only in the last eleven C-terminal amino acids and they are both present in the leukemic cells, since *NPM1* mutations always occur in one of the two *NPM1* alleles [11]. Recently, it has been isolated a monoclonal antibody that specifically recognizes only the mutated form of NPM1 [232], making the antibody-based therapy an attractive possibility. Monoclonal antibodies (mAbs) are amongst the most widely used molecules in both basic research and clinics, and several of them are now currently

employed in cancer therapy (Table 1). Although important results have been achieved in the treatment of solid tumors and hematological malignancies, the application of mAbs presents some drawbacks: their large dimensions prevent efficient tissue penetration and result in dishomogeneous distribution. Furthermore, they can often elicit adverse immunological reactions. In the last years, the introduction of recombinant antibodies, together with phage display technology [32], has opened new frontiers in the field of immunotherapy. The selection of high-affinity and low immunogenicity reagents that can be easily manipulated, has led to the *in vitro* engineering of recombinant antibodies with different formats designed for a wide range of applications. In particular, expression of intrabodies in the cells (intracellular antibodies) was successful i) in inhibiting specific functions of intracellular antigens, ii) in disrupting intracellular protein-protein interactions by competitive inhibition and iii) in diverting antigens from their usual compartment. To date only one monoclonal antibody has been approved for the treatment of patients with relapsed AML [233, 234]. It is a humanized anti-CD33 IgG, chemically coupled to the cytotoxic agent calicheamicin (Gemtuzumab Ozogamicin, GO). CD33 is a surface receptor expressed during myeloid differentiation and present on leukemic blast cells in 90% of AML patients, but neither on normal hematopoietic stem cells nor in non-hematopoietic tissues [235]. However, in June 2010 it was withdrawn from the market because a post-approval clinical trial raised new questions about its safety and effectiveness. Very recently, a scFv isolated against CD33 and fused to soluble tumor necrosis factor-related apoptosis-inducing ligand (sTRAIL) has been demonstrated to perform better than GO in terms of tumor selectivity, activity and stability, opening new possibilities in the treatment of AML [236] and confirming the *in vivo* efficacy of recombinant antibodies.

2. Recombinant mutated NPMc+ can be used as target for specific antibody selection from phage display libraries

In my work I focused on the selection of specific recombinant antibodies targeted against the NPMc+ epitope, starting from two non-immune phage display libraries. In order to perform an efficient selection of specific binders, it is essential that the protein used for bio-panning is properly folded. For this reason, prior to proceeding with my experiments, I investigated the biophysical properties of the purified NPMc+-GST protein. Although the Aggregation Index measure resulted in a significant degree of aggregation (Figure 20A, [205]), Far-UV CD spectra measurement showed that the purified NPMc+-GST conserved at least its secondary structure (Figure 20C). Therefore, I designed a high-throughput selection procedure, starting from the llama naïve phage display library in VHH format. Such library has been developed in our institute and has already demonstrated to be functional, enabling the isolation of several high-affinity antibodies targeted against different recombinant antigens [56, 85]. It is well known that, in spite of their small dimensions, VHHs can have a strong binding activity [81] and display unique molecular and structural features [82-84] which render them suitable for many applications in the therapeutic [89, 237-239] and diagnostic fields [240-242], [102, 243]. The results obtained in the ELISA test performed with the soluble periplasmic extracts of the five selected VHHs showed that they all recognized the N-terminal NPM1 region, common to the wild type NPM1 and the mutated NPMc+ (Figure 23). Even though they were not useful for my initial purpose, however I wanted to evaluate their ability to recognize the native NPMc+ protein. *In vitro* characterization of the selected VHH binders is now in progress: immunofluorescence experiments using clone 23H conjugated to a rabbit Fc domain have shown that it efficiently recognizes both the endogenous wild type NPM1 and NPMc+ in AML-derived cell lines and in patients' samples. When used in combination with the T26

mouse monoclonal antibody specific for NPMc+ [232], a double staining is obtained: nucleolar, corresponding to wild type NPM1 and cytoplasmic, corresponding to NPMc+ (not shown). Experiments performed so far are limited by the fact that all the results obtained are derived from single-antibody staining as, all of antibodies available that work in immunofluorescence are of murine origin. For this reason, it is difficult to design co-staining experiments, necessary for achieving a complete picture of NPM1 cellular distribution. Our preliminary data underline the potential application of the VHH-rabbit Fc antibody as an helpful diagnostic tool. In view of the results obtained from the VHHs selection, I reasoned that the extruding VHH paratope might not be able to target the almost completely unfolded NPMc+ C-terminal domain [203]. Therefore, I decided to perform a new selection by panning the human synthetic ETH2-Gold scFv library [16] against a PCR synthesized small peptide covering the last 45 C-terminal amino acids (NPMc+ mutation-specific epitope). This procedure allowed the selection of a single scFv positive clone (scFv-Mut), which specifically targeted the mutated C-terminal region of NPMc+. Due to its potential therapeutic relevance, I decided to further characterize the antibody using the full length NPMc+ in native conditions.

3. The scFv-Mut antibody univocally targets the C-terminal epitope of NPMc+

The scFv-Mut antibody was purified by affinity chromatography and then subjected to gel-filtration chromatography, in order to separate between the monomeric and the polymeric forms (not shown). Western immuno-blot analysis demonstrated that scFv-Mut specifically recognized both the full length recombinant NPMc+ protein and the C-terminal peptide used for bio-panning. I could also confirm its ability to discriminate between the NPMc+ and the wild type NPM1 proteins overexpressed in Sf9 insect cells (Figure 28A). Successful immunoprecipitation experiments on lysates obtained from HeLa cells transiently transfected with a plasmid for the expression of NPMc+, confirmed that the

selected binder was functional and specifically interacted only with the mutation-specific NPMc+ epitope (Figure 29). Moreover, scFv-Mut was able to immunoprecipitate the endogenous NPMc+ expressed in OCI-AML3 primary cells derived from AML patients (Figure 30), and to bind the overexpressed NPMc+, as shown by immunofluorescence assays (Figure 31 and 32). This set of data clearly showed that my selected scFv-Mut antibody univocally targeted the native NPMc+ protein and, more importantly, it was able to recognize NPMc+ in its native conformation inside the cells. This was a crucial result, because my specific aim was to obtain an antibody able to functionally interact with the endogenous NPMc+ expressed in AML patient's cells. The antibody binding affinity toward its antigen is difficult to determine since NPM forms oligomers of variable complexity and the scFv itself tends to dimerize. However, although antibody specificity and antigen-binding affinity *in vitro* are two key factors for the functional evaluation of a scFv, over the years many studies have pointed out that extended half-life (that is an index of the overall intracellular stability) and elevated steady state expression levels in the cells may be more critical parameters in predicting the effectiveness of an intrabody *in vivo* [244-246]. Furthermore, the affinity of an intrabody for its target in the intracellular milieu depends on several factors, such as the concentrations of the different species present during the expression of the antibody or its folding efficiency [247]. I decided to proceed in the attempt to express the scFv-Mut antibody as an intrabody in order to evaluate whether it was able to target the endogenous NPMc+ *in vivo*. To assess whether the scFv-Mut could be expressed as an intrabody, I prepared different mammalian expression vectors for the transient transfection of Hela cells.

4. The scFv-Mut antibody can be expressed as an intracellular antibody

The limiting step in order to achieve efficient expression of an intrabody is its ability to fold in the mammalian cytoplasmic environment. First attempts to express intrabodies in eukaryotic cells showed that they often failed to bind their target under physiological conditions [248-250]. Normally, immunoglobulins are secreted into the body's extracellular space, where they exploit their functions. The requirement for high stability has kept a selective pressure to retain both the inter- and intra-chain disulfide bridges localized in each domain and formed into the oxidizing endoplasmic reticulum before secretion. In particular, scFvs need their two intra-chain stabilizing disulfide bridges for proper folding, solubility, and stability [251], but they are unlikely to form them in the unfavourable reducing eukaryotic cell cytoplasm [252]. Therefore, it may happen that even though successfully expressed, scFvs may undergo to rapid intracellular degradation. Accordingly, the expression of intrabodies in the eukaryotic cytoplasm often results impaired because of i) reducing environment, which prevents the formation of disulfide bridges, ii) absence of accessory factors, like chaperones, that facilitate their proper folding and iii) intracellular macromolecular crowding. Usually, recombinant antibodies are produced in the bacterial periplasmic space where disulfide bridges are allowed. Very few antibodies, obtained by hybridomas or selected by phage display, have revealed to be functional and soluble when expressed in the eukaryotic cell cytoplasm. However, it has been demonstrated that reduced intracellular stability does not necessarily mean lack of functionality [253, 254]. Some scFvs have been shown to tolerate the absence of these bonds *in vitro* [255-258]. The intracellular behaviour of an intrabody is almost unpredictable and it has been reported that each scFv shows a distinct propensity to aggregate, depending on different factors ranging from the intrinsic stability of its primary sequence to the specific cellular milieu in which it is synthesized [215] and it is not easily

predictable *a priori* [259]. A recent work has compared the cytoplasmic expression of several related scFvs and VHHs in mammalian cells, showing that their solubility is highly influenced by the CDR amino acid content and can be enhanced by overall negative charge at cytoplasmic pH and by reduction of hydrophilicity. The working hypothesis is that ionic repulsion and weak hydrophobic interactions could compensate, to different extent, for impaired disulfide bond formation in the cytoplasm, thereby decreasing the risk for intrabody aggregation [260]. Some efforts have been made to generate functional molecules i) by systematically mutating the framework residues to create an optimized one to be used for the construction of dedicated libraries [261-263], ii) by fusing the antibody coding sequence to a tag protein that can help to enhance its solubility [264] and iii) by trying to isolate functional intrabodies from large phage display libraries using both *in vitro* and *in vivo* suitable selection strategies [265-267]. I started the intrabody characterization by checking for the expression of the scFv-MutGFP in the cell cytoplasm of HeLa cells and I observed a diffused cytoplasmic staining with the occasional presence of visible insoluble granules, indicating a modest propensity of the antibody to aggregate (Figure 33). Considering these positive premises, I co-expressed both scFv-MutGFP and NPMc+ proteins in HeLa cells, showing by immunofluorescence experiments that they localize in the same cell compartment (Figure 34). A confocal microscopy analysis would be necessary to understand whether the two proteins co-localize in the cell cytoplasm. A co-immunoprecipitation assay was then essential to confirm that the intrabody could recognize NPMc+ inside the cells (Figure 35). scFv-MutFlag immunoprecipitated NPMc+ *in vivo*, although the binding efficiency was not elevated. Different problems might have contributed to this result: i) the stoichiometry of the scFv-Mut versus NPMc+ molecules in the cells was apparently too low, ii) only a fraction of the recombinant antibody was properly folded and functional, iii) the affinity of the antibody for its substrate was too low. As I mentioned before regarding this last point, although I did not evaluate the binding

affinity of the recombinant antibody, recent studies have revealed that *in vitro* characteristics, such as affinity, may not be adequate indicators of intrabody activity in the cytoplasm [268, 269] and many scFvs that display high affinity in cell-free systems behave poorly as intracellular antibodies [247, 270, 271]. In any case, the data show the successful binding between at least part of the intrabody and the target NPMc+. Thefore, I asked whether the successfully expressed scFv-Mut would be able not only to interact with NPMc+, but could also interfere with its pathological activities. In particular, I wondered whether I could try exploiting the scFv-Mut antibody to re-locate NPMc+ to the nucleus: I decided to further investigate this possibility.

5. The scFv-Mut intrabody can be targeted to the nucleus

It has been already shown *in vitro* that, using inhibitors of the CRM1/Exportin1-dependent nuclear export machinery (like leptomycin B, that targets CRM1/Exportin1) responsible for the delocalization of NPMc+, it is possible to relocate NPMc+ and its interactors (p19/Arf and Fbw7γ) into the nucleus [272], [14]. However, these molecules cannot be used *in vivo* due to their extreme cellular toxicity [273]. One of the advantages of the intrabody technology is that the intracellular antibodies may be directed and restricted to different cellular compartments, like the endoplasmic reticulum (ER), the Golgi apparatus or the mitochondria, by creating fusions with proper intracellular trafficking sequences. Alternatively, intrabodies can be expressed and targeted to the nucleus, by fusing them to nuclear localization signals (NLSs). It is indeed possible to re-target and sequester cellular proteins into the nucleus by fusing intrabodies with the SV40 NLS (PKKKRKV), which has been demonstrated to direct very efficiently heterologous proteins into the nucleus [121, 217, 218, 244, 245, 274]. Therefore, I prepared a dedicated vector for the fusion of scFv-Mut to the SV40 NLS, and used it to transfect HeLa cells. Immunofluorescence experiments showed that the antibody clearly accumulated into the nucleus (Figure 37,

panel a) but, upon transient co-transfection with the NPMc+ expression plasmid, the two proteins co-localized in the cytoplasm (Figure 37, panel c), where NPMc+-GFP normally localizes. Although these results confirmed that the antibody and NPMc+ bound each other in the cellular environment, unfortunately demonstrated that the NLS that I fused to the scFv-Mut was not enough to counteract the effect of the additional NES present in NPMc+. Indeed, recent findings have demonstrated that such NES motif is more efficient in mediating nuclear export than other physiological NES [220]. Based on these data, I prepared a new construct with the recombinant antibody fused to four NLSs (scFv4xNLS). However, immunofluorescence experiments on HeLa cells co-transfected with the NPMc+ and scFv4xNLS plasmids did not allow to draw any definitive conclusion about its ability to relocate NPMc+ to the nucleus due to the high variability in the levels of expression and in the localization of the two proteins (Figure 42). Moreover, though preliminary, these data suggested that a very high expression level of the scFv might be required, in order to observe an effect on NPMc+ localization. This can be related to the fact that the intrabody was unstable and partially unfolded in the cytoplasmic environment and therefore, only a small fraction was able to bind NPMc+ and exert its biological effect.

6. Conclusions and future remarks

In summary, I reported here the successful selection from the ETH2-Gold library of a scFv antibody specific for the NPMc+ mutation. Furthermore, I demonstrated that the scFv-Mut could be expressed into mammalian cells as an intrabody, retaining its ability to interact with native NPMc+. Importantly, fusion to a NLS led to the antibody nuclear accumulation; however, in the presence of NPMc+, the two proteins co-localized into the cytoplasm. Addition of multiple NLSs to scFv-Mut did not clearly result in re-localization of NPMc+ to the nucleus, likely because of the difficulties linked to co-transfection experiments and problems related to the high variability in the expression levels obtained

with transient transfections. Experiments are now in progress in order to set up a system for stable expression of the antibody, by retrovirally infecting leukemic patients' cell lines. This approach would allow working with a population of cells expressing endogenous NPMc+ and that might be sorted for scFv-Mut expression by FACS analysis. In such a way, it would be possible to standardize the intrabody levels and investigate whether the scFv-Mut4xNLS might compete for the binding between NPMc+ and p19/Arf, contributing to p19/Arf nuclear re-localization or whether it could have any direct effect on NPMc+ localization. In both cases, cell growth and viability will be evaluated. A further possibility that can be explored is the direct delivery of the purified antibody to the cells by encapsulating it into liposomes, avoiding the problems related to the low intracellular expression levels and to the instability due to the unfavourable eukaryotic cell cytoplasm [137, 138, 142, 253]. Lipid-based carriers have attractive biological properties, including general biocompatibility, biodegradability and high versatility. Today, some liposomes have been approved by regulatory agencies as agents employed in targeted therapy of cancer and are employed to carry a range of chemotherapeutics, like Doxorubicin (Doxil®, [275]), Camptothecin and Daunorubicin (Daunoxome®). Furthermore, recent advances in liposome research enabled liposomes to prevent immune reactions, making them very promising tools for targeted therapy.

REFERENCES

1. Okuda, M., et al., *Nucleophosmin/B23 is a target of CDK2/cyclin E in centrosome duplication.* Cell, 2000. **103**(1): p. 127-40.

2. Negi, S.S. and M.O. Olson, *Effects of interphase and mitotic phosphorylation on the mobility and location of nucleolar protein B23.* J Cell Sci, 2006. **119**(Pt 17): p. 3676-85.

3. Rubbi, C.P. and J. Milner, *Disruption of the nucleolus mediates stabilization of p53 in response to DNA damage and other stresses.* EMBO J, 2003. **22**(22): p. 6068-77.

4. Wu, M.H. and B.Y. Yung, *UV stimulation of nucleophosmin/B23 expression is an immediate-early gene response induced by damaged DNA.* J Biol Chem, 2002. **277**(50): p. 48234-40.

5. Li, Y.P., et al., *C23 interacts with B23, a putative nucleolar-localization-signal-binding protein.* Eur J Biochem, 1996. **237**(1): p. 153-8.

6. Valdez, B.C., et al., *Identification of the nuclear and nucleolar localization signals of the protein p120. Interaction with translocation protein B23.* J Biol Chem, 1994. **269**(38): p. 23776-83.

7. Colombo, E., et al., *Nucleophosmin regulates the stability and transcriptional activity of p53.* Nat Cell Biol, 2002. **4**(7): p. 529-33.

8. Kurki, S., et al., *Nucleolar protein NPM interacts with HDM2 and protects tumor suppressor protein p53 from HDM2-mediated degradation.* Cancer Cell, 2004. **5**(5): p. 465-75.

9. Itahana, K., et al., *Tumor suppressor ARF degrades B23, a nucleolar protein involved in ribosome biogenesis and cell proliferation.* Mol Cell, 2003. **12**(5): p. 1151-64.

10. Korgaonkar, C., et al., *Nucleophosmin (B23) targets ARF to nucleoli and inhibits its function.* Mol Cell Biol, 2005. **25**(4): p. 1258-71.

11. Colombo, E., et al., *Nucleophosmin is required for DNA integrity and p19Arf protein stability.* Mol Cell Biol, 2005. **25**(20): p. 8874-86.

12. Schnittger, S., et al., *Nucleophosmin gene mutations are predictors of favorable prognosis in acute myelogenous leukemia with a normal karyotype.* Blood, 2005. **106**(12): p. 3733-9.

13. Mariano, A.R., et al., *Cytoplasmic localization of NPM in myeloid leukemias is dictated by gain-of-function mutations that create a functional nuclear export signal.* Oncogene, 2006. **25**(31): p. 4376-80.

14. Colombo, E., et al., *Delocalization and destabilization of the Arf tumor suppressor by the leukemia-associated NPM mutant.* Cancer Res, 2006. **66**(6): p. 3044-50.

15. Bonetti, P., et al., *Nucleophosmin and its AML-associated mutant regulate c-Myc turnover through Fbw7 gamma.* J Cell Biol, 2008. **182**(1): p. 19-26.

16. Silacci, M., et al., *Design, construction, and characterization of a large synthetic human antibody phage display library.* Proteomics, 2005. **5**(9): p. 2340-50.

17. Peterson, P.A., *[1972 Nobel prize in physiology or medicine. The chemical structure of antibodies].* Lakartidningen, 1972. **69**(44): p. 5069-73.

18. Edelman, G.M. and M.D. Poulik, *Studies on structural units of the gamma-globulins.* J Exp Med, 1961. **113**: p. 861-84.

19. Maynard, J. and G. Georgiou, *Antibody engineering.* Annu Rev Biomed Eng, 2000. **2**: p. 339-76.

20. Honjo, T., et al., *AID to overcome the limitations of genomic information.* Nat Immunol, 2005. **6**(7): p. 655-61.

21. Li, Z., et al., *The generation of antibody diversity through somatic hypermutation and class switch recombination.* Genes Dev, 2004. **18**(1): p. 1-11.

22. Neuberger, M.S., et al., *Immunity through DNA deamination.* Trends Biochem Sci, 2003. **28**(6): p. 305-12.

23. Kohler, G. and C. Milstein, *Continuous cultures of fused cells secreting antibody of predefined specificity.* Nature, 1975. **256**(5517): p. 495-7.

24. Holliger, P. and P.J. Hudson, *Engineered antibody fragments and the rise of single domains.* Nat Biotechnol, 2005. **23**(9): p. 1126-36.

25. Morrison, S.L., et al., *Chimeric human antibody molecules: mouse antigen-binding domains with human constant region domains.* Proc Natl Acad Sci U S A, 1984. **81**(21): p. 6851-5.

26. Boulianne, G.L., N. Hozumi, and M.J. Shulman, *Production of functional chimaeric mouse/human antibody.* Nature, 1984. **312**(5995): p. 643-6.

27. Jones, P.T., et al., *Replacing the complementarity-determining regions in a human antibody with those from a mouse.* Nature, 1986. **321**(6069): p. 522-5.

28. Carter, P., et al., *Humanization of an anti-p185HER2 antibody for human cancer therapy.* Proc Natl Acad Sci U S A, 1992. **89**(10): p. 4285-9.

29. Presta, L.G., et al., *Humanization of an antibody directed against IgE.* J Immunol, 1993. **151**(5): p. 2623-32.

30. Skerra, A. and A. Pluckthun, *Assembly of a functional immunoglobulin Fv fragment in Escherichia coli.* Science, 1988. **240**(4855): p. 1038-41.

31. Better, M., et al., *Escherichia coli secretion of an active chimeric antibody fragment.* Science, 1988. **240**(4855): p. 1041-3.

32. McCafferty, J., et al., *Phage antibodies: filamentous phage displaying antibody variable domains.* Nature, 1990. **348**(6301): p. 552-4.

33. Cragg, M.S., R.R. French, and M.J. Glennie, *Signaling antibodies in cancer therapy.* Curr Opin Immunol, 1999. **11**(5): p. 541-7.

34. Farah, R.A., et al., *The development of monoclonal antibodies for the therapy of cancer.* Crit Rev Eukaryot Gene Expr, 1998. **8**(3-4): p. 321-56.

35. Berard, J.L., et al., *A review of interleukin-2 receptor antagonists in solid organ transplantation.* Pharmacotherapy, 1999. **19**(10): p. 1127-37.

36. Maini, R., et al., *Infliximab (chimeric anti-tumour necrosis factor alpha monoclonal antibody) versus placebo in rheumatoid arthritis patients receiving concomitant methotrexate: a randomised phase III trial. ATTRACT Study Group*. Lancet, 1999. **354**(9194): p. 1932-9.

37. Brekke, O.H. and I. Sandlie, *Therapeutic antibodies for human diseases at the dawn of the twenty-first century.* Nat Rev Drug Discov, 2003. **2**(1): p. 52-62.

38. Mellstedt, H., *Monoclonal antibodies in human cancer*. Drugs Today (Barc), 2003. **39 Suppl C**: p. 1-16.

39. Smith, G.P., *Filamentous fusion phage: novel expression vectors that display cloned antigens on the virion surface.* Science, 1985. **228**(4705): p. 1315-7.

40. Scott, J.K. and G.P. Smith, *Searching for peptide ligands with an epitope library.* Science, 1990. **249**(4967): p. 386-90.

41. Russel, M., *Filamentous phage assembly.* Mol Microbiol, 1991. **5**(7): p. 1607-13.

42. Petrenko, V.A. and V.J. Vodyanoy, *Phage display for detection of biological threat agents.* J Microbiol Methods, 2003. **53**(2): p. 253-62.

43. McLafferty, M.A., et al., *M13 bacteriophage displaying disulfide-constrained microproteins.* Gene, 1993. **128**(1): p. 29-36.

44. Winter, G., et al., *Making antibodies by phage display technology*. Annu Rev Immunol, 1994. **12**: p. 433-55.

45. Krumpe, L.R. and T. Mori, *The Use of Phage-Displayed Peptide Libraries to Develop Tumor-Targeting Drugs.* Int J Pept Res Ther, 2006. **12**(1): p. 79-91.

46. Porter, R.R., *The hydrolysis of rabbit y-globulin and antibodies with crystalline papain.* Biochem J, 1959. **73**: p. 119-26.

47. Tout, N.L., et al., *Synthesis of ligand-specific phage-display ScFv against the herbicide picloram by direct cloning from hyperimmunized mouse.* J Agric Food Chem, 2001. **49**(8): p. 3628-37.

48. Mah, D.C., et al., *Recombinant anti-botulinum neurotoxin A single-chain variable fragment antibody generated using a phage display system.* Hybrid Hybridomics, 2003. **22**(5): p. 277-83.

49. Pelat, T., et al., *High-affinity, human antibody-like antibody fragment (single-chain variable fragment) neutralizing the lethal factor (LF) of Bacillus anthracis by inhibiting protective antigen-LF complex formation.* Antimicrob Agents Chemother, 2007. **51**(8): p. 2758-64.

50. Shaw, I., et al., *Development of a high-affinity anti-domoic acid sheep scFv and its use in detection of the toxin in shellfish.* Anal Chem, 2008. **80**(9): p. 3205-12.

51. Hof, D., M.O. Hoeke, and J.M. Raats, *Multiple-antigen immunization of chickens facilitates the generation of recombinant antibodies to autoantigens.* Clin Exp Immunol, 2008. **151**(2): p. 367-77.

52. Azzazy, H.M. and W.E. Highsmith, Jr., *Phage display technology: clinical applications and recent innovations.* Clin Biochem, 2002. **35**(6): p. 425-45.

53. Tanha, J., et al., *Selection by phage display of llama conventional V(H) fragments with heavy chain antibody V(H)H properties.* J Immunol Methods, 2002. **263**(1-2): p. 97-109.

54. Verheesen, P., et al., *Reliable and controllable antibody fragment selections from Camelid non-immune libraries for target validation.* Biochim Biophys Acta, 2006. **1764**(8): p. 1307-19.

55. Liu, J.L., et al., *Selection of cholera toxin specific IgNAR single-domain antibodies from a naive shark library.* Mol Immunol, 2007. **44**(7): p. 1775-83.

56. Monegal, A., et al., *Immunological applications of single-domain llama recombinant antibodies isolated from a naive library.* Protein Eng Des Sel, 2009. **22**(4): p. 273-80.

57. Pini, A., et al., *Design and use of a phage display library. Human antibodies with subnanomolar affinity against a marker of angiogenesis eluted from a two-dimensional gel.* J Biol Chem, 1998. **273**(34): p. 21769-76.

58. Viti, F., et al., *Design and use of phage display libraries for the selection of antibodies and enzymes.* Methods Enzymol, 2000. **326**: p. 480-505.

59. de Wildt, R.M., et al., *Antibody arrays for high-throughput screening of antibody-antigen interactions.* Nat Biotechnol, 2000. **18**(9): p. 989-94.

60. Goletz, S., et al., *Selection of large diversities of antiidiotypic antibody fragments by phage display.* J Mol Biol, 2002. **315**(5): p. 1087-97.

61. Hoogenboom, H.R., et al., *Building antibodies from their genes.* Immunol Rev, 1992. **130**: p. 41-68.

62. Hoogenboom, H.R. and G. Winter, *By-passing immunisation. Human antibodies from synthetic repertoires of germline VH gene segments rearranged in vitro.* J Mol Biol, 1992. **227**(2): p. 381-8.

63. Soderlind, E., et al., *Recombining germline-derived CDR sequences for creating diverse single-framework antibody libraries.* Nat Biotechnol, 2000. **18**(8): p. 852-6.

64. Hoet, R.M., et al., *Generation of high-affinity human antibodies by combining donor-derived and synthetic complementarity-determining-region diversity.* Nat Biotechnol, 2005. **23**(3): p. 344-8.

65. Bird, R.E., et al., *Single-chain antigen-binding proteins.* Science, 1988. **242**(4877): p. 423-6.

66. Huston, J.S., et al., *Protein engineering of antibody binding sites: recovery of specific activity in an anti-digoxin single-chain Fv analogue produced in Escherichia coli.* Proc Natl Acad Sci U S A, 1988. **85**(16): p. 5879-83.

67. Glockshuber, R., et al., *A comparison of strategies to stabilize immunoglobulin Fv-fragments.* Biochemistry, 1990. **29**(6): p. 1362-7.

68. Huston, J.S., et al., *Protein engineering of single-chain Fv analogs and fusion proteins.* Methods Enzymol, 1991. **203**: p. 46-88.

69. Nakamura, T. and S.J. Russell, *Oncolytic measles viruses for cancer therapy.* Expert Opin Biol Ther, 2004. **4**(10): p. 1685-92.

70. Nakamura, T., et al., *Rescue and propagation of fully retargeted oncolytic measles viruses.* Nat Biotechnol, 2005. **23**(2): p. 209-14.

71. Kortt, A.A., et al., *Dimeric and trimeric antibodies: high avidity scFvs for cancer targeting.* Biomol Eng, 2001. **18**(3): p. 95-108.

72. Kenanova, V., et al., *Tailoring the pharmacokinetics and positron emission tomography imaging properties of anti-carcinoembryonic antigen single-chain Fv-Fc antibody fragments.* Cancer Res, 2005. **65**(2): p. 622-31.

73. Robinson, M.K., et al., *Quantitative immuno-positron emission tomography imaging of HER2-positive tumor xenografts with an iodine-124 labeled anti-HER2 diabody.* Cancer Res, 2005. **65**(4): p. 1471-8.

74. Korn, T., et al., *Recombinant bispecific antibodies for the targeting of adenoviruses to CEA-expressing tumour cells: a comparative analysis of bacterially expressed single-chain diabody and tandem scFv.* J Gene Med, 2004. **6**(6): p. 642-51.

75. Hu, S., et al., *Minibody: A novel engineered anti-carcinoembryonic antigen antibody fragment (single-chain Fv-CH3) which exhibits rapid, high-level targeting of xenografts.* Cancer Res, 1996. **56**(13): p. 3055-61.

76. Li, J., et al., *Influences of amino acid sequences in FR1 region on binding activity of the scFv and Fab of an antibody to human gastric cancer cells.* Immunol Lett, 2000. **71**(3): p. 157-65.

77. Borsi, L., et al., *Selective targeting of tumoral vasculature: comparison of different formats of an antibody (L19) to the ED-B domain of fibronectin.* Int J Cancer, 2002. **102**(1): p. 75-85.

78. Hamers-Casterman, C., et al., *Naturally occurring antibodies devoid of light chains.* Nature, 1993. **363**(6428): p. 446-8.

79. Greenberg, A.S., et al., *A new antigen receptor gene family that undergoes rearrangement and extensive somatic diversification in sharks.* Nature, 1995. **374**(6518): p. 168-73.

80. Harmsen, M.M., et al., *Llama heavy-chain V regions consist of at least four distinct subfamilies revealing novel sequence features.* Mol Immunol, 2000. **37**(10): p. 579-90.

81. Nguyen, V.K., et al., *Camel heavy-chain antibodies: diverse germline V(H)H and specific mechanisms enlarge the antigen-binding repertoire.* EMBO J, 2000. **19**(5): p. 921-30.

82. De Genst, E., et al., *Molecular basis for the preferential cleft recognition by dromedary heavy-chain antibodies.* Proc Natl Acad Sci U S A, 2006. **103**(12): p. 4586-91.

83. Desmyter, A., et al., *Crystal structure of a camel single-domain VH antibody fragment in complex with lysozyme.* Nat Struct Biol, 1996. **3**(9): p. 803-11.

84. Lauwereys, M., et al., *Potent enzyme inhibitors derived from dromedary heavy-chain antibodies.* EMBO J, 1998. **17**(13): p. 3512-20.

85. Muyldermans, S., *Single domain camel antibodies: current status.* J Biotechnol, 2001. **74**(4): p. 277-302.

86. Xu, L., et al., *Systemic tumor-targeted gene delivery by anti-transferrin receptor scFv-immunoliposomes.* Mol Cancer Ther, 2002. **1**(5): p. 337-46.

87. Schrama, D., R.A. Reisfeld, and J.C. Becker, *Antibody targeted drugs as cancer therapeutics.* Nat Rev Drug Discov, 2006. **5**(2): p. 147-59.

88. Newton, D.L. and S.M. Ryback, *Antibody targeted therapeutics for lymphoma: new focus on the CD22 antigen and RNA.* Expert Opin Biol Ther, 2001. **1**(6): p. 995-1003.

89. Baral, T.N., et al., *Experimental therapy of African trypanosomiasis with a nanobody-conjugated human trypanolytic factor.* Nat Med, 2006. **12**(5): p. 580-4.

90. Bagshawe, K.D., S.K. Sharma, and R.H. Begent, *Antibody-directed enzyme prodrug therapy (ADEPT) for cancer.* Expert Opin Biol Ther, 2004. **4**(11): p. 1777-89.

91. Uchino, J., et al., *Tumor targeting carboxylesterase fused with anti-CEA scFv improve the anticancer effect with a less toxic dose of irinotecan.* Cancer Gene Ther, 2008. **15**(2): p. 94-100.

92. Yang, W.P., et al., *CDR walking mutagenesis for the affinity maturation of a potent human anti-HIV-1 antibody into the picomolar range.* J Mol Biol, 1995. **254**(3): p. 392-403.

93. Pini, A., et al., *Hierarchical affinity maturation of a phage library derived antibody for the selective removal of cytomegalovirus from plasma.* J Immunol Methods, 1997. **206**(1-2): p. 171-82.

94. Chowdhury, P.S. and I. Pastan, *Improving antibody affinity by mimicking somatic hypermutation in vitro.* Nat Biotechnol, 1999. **17**(6): p. 568-72.

95. Boder, E.T., K.S. Midelfort, and K.D. Wittrup, *Directed evolution of antibody fragments with monovalent femtomolar antigen-binding affinity.* Proc Natl Acad Sci U S A, 2000. **97**(20): p. 10701-5.

96. Yau, K.Y., et al., *Affinity maturation of a V(H)H by mutational hotspot randomization.* J Immunol Methods, 2005. **297**(1-2): p. 213-24.

97. Fujii, R., M. Kitaoka, and K. Hayashi, *Error-prone rolling circle amplification: the simplest random mutagenesis protocol.* Nat Protoc, 2006. **1**(5): p. 2493-7.

98. Demartis, S., et al., *Selective targeting of tumour neovasculature by a radiohalogenated human antibody fragment specific for the ED-B domain of fibronectin.* Eur J Nucl Med, 2001. **28**(4): p. 534-9.

99. Santimaria, M., et al., *Immunoscintigraphic detection of the ED-B domain of fibronectin, a marker of angiogenesis, in patients with cancer.* Clin Cancer Res, 2003. **9**(2): p. 571-9.

100. Haubner, R. and H.J. Wester, *Radiolabeled tracers for imaging of tumor angiogenesis and evaluation of anti-angiogenic therapies.* Curr Pharm Des, 2004. **10**(13): p. 1439-55.

101. Birchler, M.T., et al., *Immunoscintigraphy of patients with head and neck carcinomas, with an anti-angiogenetic antibody fragment.* Otolaryngol Head Neck Surg, 2007. **136**(4): p. 543-8.

102. Rothbauer, U., et al., *Targeting and tracing antigens in live cells with fluorescent nanobodies.* Nat Methods, 2006. **3**(11): p. 887-9.

103. Biocca, S. and A. Cattaneo, *Intracellular immunization: antibody targeting to subcellular compartments.* Trends Cell Biol, 1995. **5**(6): p. 248-52.

104. Kontermann, R.E., *Intrabodies as therapeutic agents.* Methods, 2004. **34**(2): p. 163-70.

105. Biocca, S., P. Pierandrei-Amaldi, and A. Cattaneo, *Intracellular expression of anti-p21ras single chain Fv fragments inhibits meiotic maturation of xenopus oocytes.* Biochem Biophys Res Commun, 1993. **197**(2): p. 422-7.

106. Cardinale, A., et al., *The mode of action of Y13-259 scFv fragment intracellularly expressed in mammalian cells.* FEBS Lett, 1998. **439**(3): p. 197-202.

107. Jendreyko, N., et al., *Phenotypic knockout of VEGF-R2 and Tie-2 with an intradiabody reduces tumor growth and angiogenesis in vivo.* Proc Natl Acad Sci U S A, 2005. **102**(23): p. 8293-8.

108. Blanco, B., et al., *Induction of human T lymphocyte cytotoxicity and inhibition of tumor growth by tumor-specific diabody-based molecules secreted from gene-modified bystander cells.* J Immunol, 2003. **171**(2): p. 1070-7.

109. Compte, M., et al., *Inhibition of tumor growth in vivo by in situ secretion of bispecific anti-CEA x anti-CD3 diabodies from lentivirally transduced human lymphocytes.* Cancer Gene Ther, 2007. **14**(4): p. 380-8.

110. Beerli, R.R., W. Wels, and N.E. Hynes, *Intracellular expression of single chain antibodies reverts ErbB-2 transformation.* J Biol Chem, 1994. **269**(39): p. 23931-6.

111. Deshane, J., et al., *Intracellular single-chain antibody directed against erbB2 down-regulates cell surface erbB2 and exhibits a selective anti-proliferative effect in erbB2 overexpressing cancer cell lines.* Gene Ther, 1994. **1**(5): p. 332-7.

112. Deshane, J., et al., *Targeted tumor killing via an intracellular antibody against erbB-2.* J Clin Invest, 1995. **96**(6): p. 2980-9.

113. Deshane, J., et al., *Intracellular antibody against erbB-2 mediates targeted tumor cell eradication by apoptosis.* Cancer Gene Ther, 1996. **3**(2): p. 89-98.

114. Jannot, C.B., et al., *Intracellular expression of a single-chain antibody directed to the EGFR leads to growth inhibition of tumor cells.* Oncogene, 1996. **13**(2): p. 275-82.

115. Griffin, H., et al., *Inhibition of papillomavirus protein function in cervical cancer cells by intrabody targeting.* J Mol Biol, 2006. **355**(3): p. 360-78.

116. Corte-Real, S., et al., *Intrabodies targeting the Kaposi sarcoma-associated herpesvirus latency antigen inhibit viral persistence in lymphoma cells.* Blood, 2005. **106**(12): p. 3797-802.

117. Aires da Silva, F., et al., *Camelized rabbit-derived VH single-domain intrabodies against Vif strongly neutralize HIV-1 infectivity.* J Mol Biol, 2004. **340**(3): p. 525-42.

118. Serruys, B., et al., *Production, characterization and in vitro testing of HBcAg-specific VHH intrabodies.* J Gen Virol, 2010. **91**(Pt 3): p. 643-52.

119. Caron de Fromentel, C., et al., *Restoration of transcriptional activity of p53 mutants in human tumour cells by intracellular expression of anti-p53 single chain Fv fragments.* Oncogene, 1999. **18**(2): p. 551-7.

120. Wolfgang, W.J., et al., *Suppression of Huntington's disease pathology in Drosophila by human single-chain Fv antibodies.* Proc Natl Acad Sci U S A, 2005. **102**(32): p. 11563-8.

121. Lynch, S.M., C. Zhou, and A. Messer, *An scFv intrabody against the nonamyloid component of alpha-synuclein reduces intracellular aggregation and toxicity.* J Mol Biol, 2008. **377**(1): p. 136-47.

122. Paganetti, P., et al., *beta-site specific intrabodies to decrease and prevent generation of Alzheimer's Abeta peptide.* J Cell Biol, 2005. **168**(6): p. 863-8.

123. Filesi, I., et al., *Selective re-routing of prion protein to proteasomes and alteration of its vesicular secretion prevent PrP(Sc) formation.* J Neurochem, 2007. **101**(6): p. 1516-26.

124. Lundstrom, K. and T. Boulikas, *Viral and non-viral vectors in gene therapy: technology development and clinical trials.* Technol Cancer Res Treat, 2003. **2**(5): p. 471-86.

125. Zhang, D., et al., *Optimization of ex vivo activation and expansion of macaque primary CD4-enriched peripheral blood mononuclear cells for use in anti-HIV immunotherapy and gene therapy strategies.* J Acquir Immune Defic Syndr, 2003. **32**(3): p. 245-54.

126. Deshane, J., et al., *Transductional efficacy and safety of an intraperitoneally delivered adenovirus encoding an anti-erbB-2 intracellular single-chain antibody for ovarian cancer gene therapy.* Gynecol Oncol, 1997. **64**(3): p. 378-85.

127. Alvarez, R.D., et al., *A cancer gene therapy approach utilizing an anti-erbB-2 single-chain antibody-encoding adenovirus (AD21): a phase I trial.* Clin Cancer Res, 2000. **6**(8): p. 3081-7.

128. Davis, M.E., *Non-viral gene delivery systems.* Curr Opin Biotechnol, 2002. **13**(2): p. 128-31.

129. Aris, A. and A. Villaverde, *Modular protein engineering for non-viral gene therapy.* Trends Biotechnol, 2004. **22**(7): p. 371-7.

130. Dalkara, D., G. Zuber, and J.P. Behr, *Intracytoplasmic delivery of anionic proteins.* Mol Ther, 2004. **9**(6): p. 964-9.

131. Joliot, A. and A. Prochiantz, *Transduction peptides: from technology to physiology.* Nat Cell Biol, 2004. **6**(3): p. 189-96.

132. Matsushita, M. and H. Matsui, *Protein transduction technology.* J Mol Med, 2005. **83**(5): p. 324-8.

133. Arbabi Ghahroudi, M., et al., *Selection and identification of single domain antibody fragments from camel heavy-chain antibodies.* FEBS Lett, 1997. **414**(3): p. 521-6.

134. van der Linden, R., et al., *Induction of immune responses and molecular cloning of the heavy chain antibody repertoire of Lama glama.* J Immunol Methods, 2000. **240**(1-2): p. 185-95.

135. Goldman, E.R., et al., *Facile generation of heat-stable antiviral and antitoxin single domain antibodies from a semisynthetic llama library.* Anal Chem, 2006. **78**(24): p. 8245-55.

136. Liu, J.L., G.P. Anderson, and E.R. Goldman, *Isolation of anti-toxin single domain antibodies from a semi-synthetic spiny dogfish shark display library.* BMC Biotechnol, 2007. **7**: p. 78.

137. Shao, C.Y., C.J. Secombes, and A.J. Porter, *Rapid isolation of IgNAR variable single-domain antibody fragments from a shark synthetic library.* Mol Immunol, 2007. **44**(4): p. 656-65.

138. Tomlinson, I.M., et al., *The imprint of somatic hypermutation on the repertoire of human germline V genes.* J Mol Biol, 1996. **256**(5): p. 813-17.

139. Chothia, C. and A.M. Lesk, *Canonical structures for the hypervariable regions of immunoglobulins.* J Mol Biol, 1987. **196**(4): p. 901-17.

140. Hoogenboom, H.R., et al., *Multi-subunit proteins on the surface of filamentous phage: methodologies for displaying antibody (Fab) heavy and light chains.* Nucleic Acids Res, 1991. **19**(15): p. 4133-7.

141. Tomlinson, I.M., et al., *The structural repertoire of the human V kappa domain.* EMBO J, 1995. **14**(18): p. 4628-38.

142. Wheatley, K., et al., *A simple, robust, validated and highly predictive index for the determination of risk-directed therapy in acute myeloid leukaemia derived from the MRC AML 10 trial. United Kingdom Medical Research Council's Adult and Childhood Leukaemia Working Parties.* Br J Haematol, 1999. **107**(1): p. 69-79.

143. Byrd, J.C., et al., *Pretreatment cytogenetic abnormalities are predictive of induction success, cumulative incidence of relapse, and overall survival in adult patients with de novo acute myeloid leukemia: results from Cancer and Leukemia Group B (CALGB 8461).* Blood, 2002. **100**(13): p. 4325-36.

144. Schnittger, S., et al., *Analysis of FLT3 length mutations in 1003 patients with acute myeloid leukemia: correlation to cytogenetics, FAB subtype, and prognosis in the AMLCG study and usefulness as a marker for the detection of minimal residual disease.* Blood, 2002. **100**(1): p. 59-66.

145. Zhong, S., P. Salomoni, and P.P. Pandolfi, *The transcriptional role of PML and the nuclear body.* Nat Cell Biol, 2000. **2**(5): p. E85-90.

146. Giguere, V., et al., *Identification of a receptor for the morphogen retinoic acid.* Nature, 1987. **330**(6149): p. 624-9.

147. Leroy, H., et al., *CEBPA point mutations in hematological malignancies.* Leukemia, 2005. **19**(3): p. 329-34.

148. Tanner, S.M., et al., *BAALC, the human member of a novel mammalian neuroectoderm gene lineage, is implicated in hematopoiesis and acute leukemia.* Proc Natl Acad Sci U S A, 2001. **98**(24): p. 13901-6.

149. Murakami, K., et al., *Human ERG-2 protein is a phosphorylated DNA-binding protein--a distinct member of the ets family.* Oncogene, 1993. **8**(6): p. 1559-66.

150. Falini, B., et al., *Translocations and mutations involving the nucleophosmin (NPM1) gene in lymphomas and leukemias.* Haematologica, 2007. **92**(4): p. 519-32.

151. Morris, S.W., et al., *Fusion of a kinase gene, ALK, to a nucleolar protein gene, NPM, in non-Hodgkin's lymphoma.* Science, 1994. **263**(5151): p. 1281-4.

152. Redner, R.L., et al., *The t(5;17) variant of acute promyelocytic leukemia expresses a nucleophosmin-retinoic acid receptor fusion.* Blood, 1996. **87**(3): p. 882-6.

153. Redner, R.L., et al., *The t(5;17) acute promyelocytic leukemia fusion protein NPM-RAR interacts with co-repressor and co-activator proteins and exhibits both positive and negative transcriptional properties.* Blood, 2000. **95**(8): p. 2683-90.

154. Okazuka, K., et al., *Successful all-trans retinoic acid treatment of acute promyelocytic leukemia in a patient with NPM/RAR fusion.* Int J Hematol, 2007. **86**(3): p. 246-9.

155. Yoneda-Kato, N., et al., *The t(3;5)(q25.1;q34) of myelodysplastic syndrome and acute myeloid leukemia produces a novel fusion gene, NPM-MLF1.* Oncogene, 1996. **12**(2): p. 265-75.

156. Yoneda-Kato, N. and J.Y. Kato, *Shuttling imbalance of MLF1 results in p53 instability and increases susceptibility to oncogenic transformation.* Mol Cell Biol, 2008. **28**(1): p. 422-34.

157. Vardiman, J.W., et al., *The 2008 revision of the World Health Organization (WHO) classification of myeloid neoplasms and acute leukemia: rationale and important changes.* Blood, 2009. **114**(5): p. 937-51.

158. Ammatuna, E., et al., *Rapid detection of nucleophosmin (NPM1) mutations in acute myeloid leukemia by denaturing HPLC.* Clin Chem, 2005. **51**(11): p. 2165-7.

159. Falini, B., et al., *Immunohistochemistry predicts nucleophosmin (NPM) mutations in acute myeloid leukemia.* Blood, 2006. **108**(6): p. 1999-2005.

160. Gorello, P., et al., *Quantitative assessment of minimal residual disease in acute myeloid leukemia carrying nucleophosmin (NPM1) gene mutations.* Leukemia, 2006. **20**(6): p. 1103-8.

161. Martelli, M.P., et al., *A western blot assay for detecting mutant nucleophosmin (NPM1) proteins in acute myeloid leukaemia.* Leukemia, 2008. **22**(12): p. 2285-8.

162. Noguera, N.I., et al., *Simultaneous detection of NPM1 and FLT3-ITD mutations by capillary electrophoresis in acute myeloid leukemia.* Leukemia, 2005. **19**(8): p. 1479-82.

163. Bacher, U., et al., *Quantitative monitoring of NPM1 mutations provides a valid minimal residual disease parameter following allogeneic stem cell transplantation.* Exp Hematol, 2009. **37**(1): p. 135-42.

164. Ma, W., et al., *Detection of nucleophosmin gene mutations in plasma from patients with acute myeloid leukemia: clinical significance and implications.* Cancer Biomark, 2009. **5**(1): p. 51-8.

165. Papadaki, C., et al., *Monitoring minimal residual disease in acute myeloid leukaemia with NPM1 mutations by quantitative PCR: clonal evolution is a limiting factor.* Br J Haematol, 2009. **144**(4): p. 517-23.

166. Falini, B., et al., *NPM1 mutations and cytoplasmic nucleophosmin are mutually exclusive of recurrent genetic abnormalities: a comparative analysis of 2562 patients with acute myeloid leukemia.* Haematologica, 2008. **93**(3): p. 439-42.

167. Mrozek, K., H. Dohner, and C.D. Bloomfield, *Influence of new molecular prognostic markers in patients with karyotypically normal acute myeloid leukemia: recent advances.* Curr Opin Hematol, 2007. **14**(2): p. 106-14.

168. Schlenk, R.F., et al., *Mutations and treatment outcome in cytogenetically normal acute myeloid leukemia.* N Engl J Med, 2008. **358**(18): p. 1909-18.

169. Suzuki, T., et al., *Clinical characteristics and prognostic implications of NPM1 mutations in acute myeloid leukemia.* Blood, 2005. **106**(8): p. 2854-61.

170. Thiede, C., et al., *Prevalence and prognostic impact of NPM1 mutations in 1485 adult patients with acute myeloid leukemia (AML).* Blood, 2006. **107**(10): p. 4011-20.

171. Dohner, K., et al., *Mutant nucleophosmin (NPM1) predicts favorable prognosis in younger adults with acute myeloid leukemia and normal cytogenetics: interaction with other gene mutations.* Blood, 2005. **106**(12): p. 3740-6.

172. Frelin, C., et al., *Targeting NF-kappaB activation via pharmacologic inhibition of IKK2-induced apoptosis of human acute myeloid leukemia cells.* Blood, 2005. **105**(2): p. 804-11.

173. Guzman, M.L., et al., *Nuclear factor-kappaB is constitutively activated in primitive human acute myelogenous leukemia cells.* Blood, 2001. **98**(8): p. 2301-7.

174. Cilloni, D., et al., *Increase sensitivity to chemotherapeutical agents and cytoplasmatic interaction between NPM leukemic mutant and NF-kappaB in AML carrying NPM1 mutations.* Leukemia, 2008. **22**(6): p. 1234-40.

175. Wang, D., H. Umekawa, and M.O. Olson, *Expression and subcellular locations of two forms of nucleolar protein B23 in rat tissues and cells.* Cell Mol Biol Res, 1993. **39**(1): p. 33-42.

176. Hingorani, K., A. Szebeni, and M.O. Olson, *Mapping the functional domains of nucleolar protein B23.* J Biol Chem, 2000. **275**(32): p. 24451-7.

177. Szebeni, A. and M.O. Olson, *Nucleolar protein B23 has molecular chaperone activities.* Protein Sci, 1999. **8**(4): p. 905-12.

178. Okuwaki, M., et al., *Identification of nucleophosmin/B23, an acidic nucleolar protein, as a stimulatory factor for in vitro replication of adenovirus DNA complexed with viral basic core proteins.* J Mol Biol, 2001. **311**(1): p. 41-55.

179. Okuwaki, M., et al., *Function of nucleophosmin/B23, a nucleolar acidic protein, as a histone chaperone.* FEBS Lett, 2001. **506**(3): p. 272-6.

180. Swaminathan, V., et al., *Human histone chaperone nucleophosmin enhances acetylation-dependent chromatin transcription.* Mol Cell Biol, 2005. **25**(17): p. 7534-45.

181. Wang, D., et al., *The nucleic acid binding activity of nucleolar protein B23.1 resides in its carboxyl-terminal end.* J Biol Chem, 1994. **269**(49): p. 30994-8.

182. Okuwaki, M., M. Tsujimoto, and K. Nagata, *The RNA binding activity of a ribosome biogenesis factor, nucleophosmin/B23, is modulated by phosphorylation with a cell cycle-dependent kinase and by association with its subtype.* Mol Biol Cell, 2002. **13**(6): p. 2016-30.

183. Savkur, R.S. and M.O. Olson, *Preferential cleavage in pre-ribosomal RNA byprotein B23 endoribonuclease.* Nucleic Acids Res, 1998. **26**(19): p. 4508-15.

184. Nishimura, Y., et al., *Tryptophans 286 and 288 in the C-terminal region of protein B23.1 are important for its nucleolar localization.* Biosci Biotechnol Biochem, 2002. **66**(10): p. 2239-42.

185. Yu, Y., et al., *Nucleophosmin is essential for ribosomal protein L5 nuclear export.* Mol Cell Biol, 2006. **26**(10): p. 3798-809.

186. Wang, W., et al., *Temporal and spatial control of nucleophosmin by the Ran-Crm1 complex in centrosome duplication.* Nat Cell Biol, 2005. **7**(8): p. 823-30.

187. Herrera, J.E., et al., *Sedimentation analyses of the salt- and divalent metal ion-induced oligomerization of nucleolar protein B23.* Biochemistry, 1996. **35**(8): p. 2668-73.

188. Namboodiri, V.M., et al., *The structure and function of Xenopus NO38-core, a histone chaperone in the nucleolus.* Structure, 2004. **12**(12): p. 2149-60.

189. Lee, H.H., et al., *Crystal structure of human nucleophosmin-core reveals plasticity of the pentamer-pentamer interface.* Proteins, 2007. **69**(3): p. 672-8.

190. Grisendi, S., et al., *Nucleophosmin and cancer.* Nat Rev Cancer, 2006. **6**(7): p. 493-505.

191. Grisendi, S., et al., *Role of nucleophosmin in embryonic development and tumorigenesis.* Nature, 2005. **437**(7055): p. 147-53.

192. Sportoletti, P., et al., *Npm1 is a haploinsufficient suppressor of myeloid and lymphoid malignancies in the mouse.* Blood, 2008. **111**(7): p. 3859-62.

193. Tanaka, M., et al., *Genes preferentially expressed in embryo stomach are predominantly expressed in gastric cancer.* Cancer Res, 1992. **52**(12): p. 3372-7.

194. Nozawa, Y., et al., *Expression of nucleophosmin/B23 in normal and neoplastic colorectal mucosa.* J Pathol, 1996. **178**(1): p. 48-52.

195. Subong, E.N., et al., *Monoclonal antibody to prostate cancer nuclear matrix protein (PRO:4-216) recognizes nucleophosmin/B23.* Prostate, 1999. **39**(4): p. 298-304.

196. Tsui, K.H., et al., *Association of nucleophosmin/B23 mRNA expression with clinical outcome in patients with bladder carcinoma.* Urology, 2004. **64**(4): p. 839-44.

197. Shields, L.B., et al., *Induction of immune responses to ovarian tumor antigens by multiparity.* J Soc Gynecol Investig, 1997. **4**(6): p. 298-304.

198. Bernard, K., et al., *Functional proteomic analysis of melanoma progression.* Cancer Res, 2003. **63**(20): p. 6716-25.

199. Morris, S.W., et al., *Fusion of a kinase gene, ALK, to a nucleolar protein gene, NPM, in non-Hodgkin's lymphoma.* Science, 1995. **267**(5196): p. 316-7.

200. Falini, B., et al., *Acute myeloid leukemia carrying cytoplasmic/mutated nucleophosmin (NPMc+ AML): biologic and clinical features.* Blood, 2007. **109**(3): p. 874-85.

201. Falini, B., et al., *Both carboxy-terminus NES motif and mutated tryptophan(s) are crucial for aberrant nuclear export of nucleophosmin leukemic mutants in NPMc+ AML.* Blood, 2006. **107**(11): p. 4514-23.

202. Zindy, F., et al., *Myc signaling via the ARF tumor suppressor regulates p53-dependent apoptosis and immortalization.* Genes Dev, 1998. **12**(15): p. 2424-33.

203. Grummitt, C.G., et al., *Structural consequences of nucleophosmin mutations in acute myeloid leukemia.* J Biol Chem, 2008. **283**(34): p. 23326-32.

204. de Marco, A., *Two-step metal affinity purification of double-tagged (NusA-His6) fusion proteins.* Nat Protoc, 2006. **1**(3): p. 1538-43.

205. Nomine, Y., et al., *A strategy for optimizing the monodispersity of fusion proteins: application to purification of recombinant HPV E6 oncoprotein.* Protein Eng, 2001. **14**(4): p. 297-305.

206. Dummler, A., A.M. Lawrence, and A. de Marco, *Simplified screening for the detection of soluble fusion constructs expressed in E. coli using a modular set of vectors.* Microb Cell Fact, 2005. **4**: p. 34.

207. Studier, F.W., et al., *Use of T7 RNA polymerase to direct expression of cloned genes.* Methods Enzymol, 1990. **185**: p. 60-89.

208. Nagai, K. and H.C. Thogersen, *Synthesis and sequence-specific proteolysis of hybrid proteins produced in Escherichia coli.* Methods Enzymol, 1987. **153**: p. 461-81.

209. Stoll, V.S. and J.S. Blanchard, *Buffers: principles and practice.* Methods Enzymol, 1990. **182**: p. 24-38.

210. Eirin-Lopez, J.M., L.J. Frehlick, and J. Ausio, *Long-term evolution and functional diversification in the members of the nucleophosmin/nucleoplasmin family of nuclear chaperones.* Genetics, 2006. **173**(4): p. 1835-50.

211. Kelly, S.M. and N.C. Price, *The application of circular dichroism to studies of protein folding and unfolding.* Biochim Biophys Acta, 1997. **1338**(2): p. 161-85.

212. Lefranc, M.P., et al., *IMGT, the international ImMunoGeneTics database.* Nucleic Acids Res, 1999. **27**(1): p. 209-12, www.imgt.org

213. Gruszka, A.M., et al., *A monoclonal antibody against mutated nucleophosmin1 for the molecular diagnosis of acute myeloid leukemias.* Blood, 2010.

214. Quentmeier, H., et al., *Cell line OCI/AML3 bears exon-12 NPM gene mutation-A and cytoplasmic expression of nucleophosmin.* Leukemia, 2005. **19**(10): p. 1760-7.

215. Cattaneo, A. and S. Biocca, *The selection of intracellular antibodies.* Trends Biotechnol, 1999. **17**(3): p. 115-21.

216. Ohage, E. and B. Steipe, *Intrabody construction and expression. I. The critical role of VL domain stability.* J Mol Biol, 1999. **291**(5): p. 1119-28.

217. Zhou, C., et al., *A human single-chain Fv intrabody blocks aberrant cellular effects of overexpressed alpha-synuclein.* Mol Ther, 2004. **10**(6): p. 1023-31.

218. Lecerf, J.M., et al., *Human single-chain Fv intrabodies counteract in situ huntingtin aggregation in cellular models of Huntington's disease.* Proc Natl Acad Sci U S A, 2001. **98**(8): p. 4764-9.

219. Kalderon, D., et al., *A short amino acid sequence able to specify nuclear location.* Cell, 1984. **39**(3 Pt 2): p. 499-509.

220. Bolli, N., et al., *Born to be exported: COOH-terminal nuclear export signals of different strength ensure cytoplasmic accumulation of nucleophosmin leukemic mutants.* Cancer Res, 2007. **67**(13): p. 6230-7.

221. Vassilev, L.T., *Small-molecule antagonists of p53-MDM2 binding: research tools and potential therapeutics.* Cell Cycle, 2004. **3**(4): p. 419-21.

222. Voorhees, P.M., et al., *The proteasome as a target for cancer therapy.* Clin Cancer Res, 2003. **9**(17): p. 6316-25.

223. Rajkumar, S.V., et al., *Proteasome inhibition as a novel therapeutic target in human cancer.* J Clin Oncol, 2005. **23**(3): p. 630-9.

224. Spano, J.P., et al., *Proteasome inhibition: a new approach for the treatment of malignancies.* Bull Cancer, 2005. **92**(11): p. E61-6, 945-52.

225. Richardson, P.G., T. Hideshima, and K.C. Anderson, *Bortezomib (PS-341): a novel, first-in-class proteasome inhibitor for the treatment of multiple myeloma and other cancers.* Cancer Control, 2003. **10**(5): p. 361-9.

226. Attar, E.C., et al., *Phase I and pharmacokinetic study of bortezomib in combination with idarubicin and cytarabine in patients with acute myelogenous leukemia.* Clin Cancer Res, 2008. **14**(5): p. 1446-54.

227. Conticello, C., et al., *Antitumor activity of bortezomib alone and in combination with TRAIL in human acute myeloid leukemia.* Acta Haematol, 2008. **120**(1): p. 19-30.

228. Szczepanek, J., et al., *Differential ex vivo activity of bortezomib in newly diagnosed paediatric acute lymphoblastic and myeloblastic leukaemia.* Anticancer Res. **30**(6): p. 2119-24.

229. Stapnes, C., et al., *The proteasome inhibitors bortezomib and PR-171 have antiproliferative and proapoptotic effects on primary human acute myeloid leukaemia cells.* Br J Haematol, 2007. **136**(6): p. 814-28.

230. Riccioni, R., et al., *M4 and M5 acute myeloid leukaemias display a high sensitivity to Bortezomib-mediated apoptosis.* Br J Haematol, 2007. **139**(2): p. 194-205.

231. Colado, E., et al., *The effect of the proteasome inhibitor bortezomib on acute myeloid leukemia cells and drug resistance associated with the CD34+ immature phenotype.* Haematologica, 2008. **93**(1): p. 57-66.

232. Gruszka, A.M., et al., *A monoclonal antibody against mutated nucleophosmin1 for the molecular diagnosis of acute myeloid leukemias.* Blood.

233. Sievers, E.L., et al., *Selective ablation of acute myeloid leukemia using antibody-targeted chemotherapy: a phase I study of an anti-CD33 calicheamicin immunoconjugate.* Blood, 1999. **93**(11): p. 3678-84.

234. Bross, P.F., et al., *Approval summary: gemtuzumab ozogamicin in relapsed acute myeloid leukemia.* Clin Cancer Res, 2001. **7**(6): p. 1490-6.

235. Dinndorf, P.A., et al., *Expression of normal myeloid-associated antigens by acute leukemia cells.* Blood, 1986. **67**(4): p. 1048-53.

236. ten Cate, B., et al., *A novel AML-selective TRAIL fusion protein that is superior to Gemtuzumab Ozogamicin in terms of in vitro selectivity, activity and stability.* Leukemia, 2009. **23**(8): p. 1389-97.

237. Cortez-Retamozo, V., et al., *Efficient cancer therapy with a nanobody-based conjugate.* Cancer Res, 2004. **64**(8): p. 2853-7.

238. Roovers, R.C., et al., *Efficient inhibition of EGFR signaling and of tumour growth by antagonistic anti-EFGR Nanobodies.* Cancer Immunol Immunother, 2007. **56**(3): p. 303-317.

239. Forsman, A., et al., *Llama antibody fragments with cross-subtype human immunodeficiency virus type 1 (HIV-1)-neutralizing properties and high affinity for HIV-1 gp120.* J Virol, 2008. **82**(24): p. 12069-81.

240. Saerens, D., et al., *Single domain antibodies derived from dromedary lymph node and peripheral blood lymphocytes sensing conformational variants of prostate-specific antigen.* J Biol Chem, 2004. **279**(50): p. 51965-72.

241. Deckers, N., et al., *Nanobodies, a promising tool for species-specific diagnosis of Taenia solium cysticercosis.* Int J Parasitol, 2009. **39**(5): p. 625-33.

242. Hulstein, J.J., et al., *A novel nanobody that detects the gain-of-function phenotype of von Willebrand factor in ADAMTS13 deficiency and von Willebrand disease type 2B.* Blood, 2005. **106**(9): p. 3035-42.

243. Huang, L., et al., *SPECT imaging with 99mTc-labeled EGFR-specific nanobody for in vivo monitoring of EGFR expression.* Mol Imaging Biol, 2008. **10**(3): p. 167-75.

244. Zhu, Q., et al., *Extended half-life and elevated steady-state level of a single-chain Fv intrabody are critical for specific intracellular retargeting of its antigen, caspase-7.* J Immunol Methods, 1999. **231**(1-2): p. 207-22.

245. Rajpal, A. and T.G. Turi, *Intracellular stability of anti-caspase-3 intrabodies determines efficacy in retargeting the antigen.* J Biol Chem, 2001. **276**(35): p. 33139-46.

246. Strube, R.W. and S.Y. Chen, *Enhanced intracellular stability of sFv-Fc fusion intrabodies.* Methods, 2004. **34**(2): p. 179-83.

247. Arafat, W., et al., *Antineoplastic effect of anti-erbB-2 intrabody is not correlated with scFv affinity for its target.* Cancer Gene Ther, 2000. **7**(9): p. 1250-6.

248. Biocca, S., M.S. Neuberger, and A. Cattaneo, *Expression and targeting of intracellular antibodies in mammalian cells.* EMBO J, 1990. **9**(1): p. 101-8.

249. Carlson, J.R., *A new use for intracellular antibody expression: inactivation of human immunodeficiency virus type 1.* Proc Natl Acad Sci U S A, 1993. **90**(16): p. 7427-8.

250. Marasco, W.A., W.A. Haseltine, and S.Y. Chen, *Design, intracellular expression, and activity of a human anti-human immunodeficiency virus type 1 gp120 single-chain antibody.* Proc Natl Acad Sci U S A, 1993. **90**(16): p. 7889-93.

251. Ramm, K., P. Gehrig, and A. Pluckthun, *Removal of the conserved disulfide bridges from the scFv fragment of an antibody: effects on folding kinetics and aggregation.* J Mol Biol, 1999. **290**(2): p. 535-46.

252. Biocca, S., et al., *Redox state of single chain Fv fragments targeted to the endoplasmic reticulum, cytosol and mitochondria.* Biotechnology (N Y), 1995. **13**(10): p. 1110-5.

253. Lener, M., et al., *Diverting a protein from its cellular location by intracellular antibodies. The case of p21Ras.* Eur J Biochem, 2000. **267**(4): p. 1196-205.

254. Cardinale, A., I. Filesi, and S. Biocca, *Aggresome formation by anti-Ras intracellular scFv fragments. The fate of the antigen-antibody complex.* Eur J Biochem, 2001. **268**(2): p. 268-77.

255. Rudikoff, S. and J.G. Pumphrey, *Functional antibody lacking a variable-region disulfide bridge.* Proc Natl Acad Sci U S A, 1986. **83**(20): p. 7875-8.

256. Proba, K., et al., *Antibody scFv fragments without disulfide bonds made by molecular evolution.* J Mol Biol, 1998. **275**(2): p. 245-53.

257. Martineau, P., P. Jones, and G. Winter, *Expression of an antibody fragment at high levels in the bacterial cytoplasm.* J Mol Biol, 1998. **280**(1): p. 117-27.

258. Worn, A. and A. Pluckthun, *An intrinsically stable antibody scFv fragment can tolerate the loss of both disulfide bonds and fold correctly.* FEBS Lett, 1998. **427**(3): p. 357-61.

259. Cattaneo, A., *Selection of intracellular antibodies.* Bratisl Lek Listy, 1998. **99**(8-9): p. 413-8.

260. Kvam, E., et al., *Physico-chemical determinants of soluble intrabody expression in mammalian cell cytoplasm.* Protein Eng Des Sel, 2010. **23**(6): p. 489-98.

261. Wirtz, P. and B. Steipe, *Intrabody construction and expression III: engineering hyperstable V(H) domains.* Protein Sci, 1999. **8**(11): p. 2245-50.

262. Auf der Maur, A., D. Escher, and A. Barberis, *Antigen-independent selection of stable intracellular single-chain antibodies.* FEBS Lett, 2001. **508**(3): p. 407-12.

263. Auf der Maur, A., K. Tissot, and A. Barberis, *Antigen-independent selection of intracellular stable antibody frameworks.* Methods, 2004. **34**(2): p. 215-24.

264. Bach, H., et al., *Escherichia coli maltose-binding protein as a molecular chaperone for recombinant intracellular cytoplasmic single-chain antibodies.* J Mol Biol, 2001. **312**(1): p. 79-93.

265. Visintin, M., et al., *Selection of antibodies for intracellular function using a two-hybrid in vivo system.* Proc Natl Acad Sci U S A, 1999. **96**(21): p. 11723-8.

266. Tse, E., et al., *Intracellular antibody capture technology: application to selection of intracellular antibodies recognising the BCR-ABL oncogenic protein.* J Mol Biol, 2002. **317**(1): p. 85-94.

267. Philibert, P., et al., *A focused antibody library for selecting scFvs expressed at high levels in the cytoplasm.* BMC Biotechnol, 2007. **7**: p. 81.

268. Gennari, F., et al., *Direct phage to intrabody screening (DPIS): demonstration by isolation of cytosolic intrabodies against the TES1 site of Epstein Barr virus latent membrane protein 1 (LMP1) that block NF-kappaB transactivation.* J Mol Biol, 2004. **335**(1): p. 193-207.

269. Worn, A., et al., *Correlation between in vitro stability and in vivo performance of anti-GCN4 intrabodies as cytoplasmic inhibitors.* J Biol Chem, 2000. **275**(4): p. 2795-803.

270. Tanaka, T. and T.H. Rabbitts, *Intrabodies based on intracellular capture frameworks that bind the RAS protein with high affinity and impair oncogenic transformation.* EMBO J, 2003. **22**(5): p. 1025-35.

271. Mhashilkar, A.M., et al., *Inhibition of HIV-1 Tat-mediated LTR transactivation and HIV-1 infection by anti-Tat single chain intrabodies.* EMBO J, 1995. **14**(7): p. 1542-51.

272. Fukuda, M., et al., *CRM1 is responsible for intracellular transport mediated by the nuclear export signal.* Nature, 1997. **390**(6657): p. 308-11.

273. Kau, T.R. and P.A. Silver, *Nuclear transport as a target for cell growth.* Drug Discov Today, 2003. **8**(2): p. 78-85.

274. Li, L., et al., *Transfection with anti-p65 intrabody suppresses invasion and angiogenesis in glioma cells by blocking nuclear factor-kappaB transcriptional activity.* Clin Cancer Res, 2007. **13**(7): p. 2178-90.

275. Gabizon, A.A., *Pegylated liposomal doxorubicin: metamorphosis of an old drug into a new form of chemotherapy.* Cancer Invest, 2001. **19**(4): p. 424-36.